The Role of Granzymes in Natural Killer Cell Cytotoxicity

Dissertation

submitted to the

Faculty of Chemistry and Biological Chemistry

at the Technische Universität Dortmund

for the degree of

Doctor of Natural Sciences

Thesis by Vivian Bönnemann

(born in Bochum)

Referees Prof. Dr. Carsten Watzl

Prof. Dr. Dr. Philipp Zimmer

Meiner Familie

Table of contents

1 Acknowledgements

First and foremost, I would like to thank Prof. Dr. Carsten Watzl. Thank you very much for allowing me to continue my journey in your research group as a PhD student after my master's thesis. Thank you for your support, motivation and keeping your door always open. I am also grateful and happy that I always had the opportunity to educate myself at various conferences.

I would also like to thank Prof. Dr. Dr. Philipp Zimmer for being my second examiner.

A big thank you goes to all the members of the Watzl lab who accompanied me during my time.

Sarah Abouhegaziah	Mia Juditzki	Naomi Pieris
Peter Bröde	Nicole Klaschik	Arianna Rotili
Nora Bruning	Luca Kröll	Mina Sandusky
Silvia Capellino	Lejla Maksumic	Alexander Schenk
Maren Claus	Sarah Metzler	Elena Schwendich
Jürgen Damaschke	Jens Niemann	Doris Teutsch
Linda Drenkelforth	Martin Obholzer	Doris Urlaub
Anke Flegel	Franziska Petrovic	Karolin Wieber
Leonie Fleige	Lea Picard	Sabine Wingert
Jessica Jankowski		Natalie Wolfsdorff

Thank you so much for welcoming me so sweetly and for being such a great and crazy fun bunch. Thanks to all who have helped me with words and deeds. I had the best time with you.

Finally, I would like to thank my family, who have always supported me and never doubted me. I thank my parents for always making me feel incredibly proud of me and for supporting me no matter what decision I made. A huge thanks to Sebastian Jung who went through this time with me and always motivated and pushed me. I couldn't have done it without you.

2 Abstract

Natural killer (NK) cells are innate immune cells that defend the human body against viral infections and tumor growth. Their “natural cytotoxicity” is tightly regulated by the interplay of several activating and inhibitory receptors. NK cells exhibit two pathways to kill aberrant cells: the granule-mediated pathway and the death-receptor-mediated pathway. Upon target cell contact, NK cells release granules that contain cytotoxic proteins such as granzymes. Although the main contributor granzyme B (GrzB) of the granule-mediated pathway has been investigated extensively, the role of the other four human granzymes A, H, K and M in NK cell cytotoxicity is less understood.

In this thesis, we created fluorescent localization reporters to compare the activity of GrzB to the other four granzymes within single target cells. The reporters not only visualize whether there is granzyme activity within the target cells, they also provide information about the kinetics. In this study, we observed that NK92 cells mainly kill their targets by using GrzB with partial support of GrzA. If GrzB is knocked out, GrzA acts as a backup for GrzB and can induce apoptosis on its own. Although the granzymes H, K and M are expressed by all NK cells investigated in this study, they do not play a role for NK92 cytotoxicity, but rather in target cell killing by primary human NK cells. Here, we found different relevance of granzymes for resting (M > A > K > H) and activated (A > M > K > H) primary NK cells.

In addition, $CD56^{bright}$ primary NK cells exhibit a higher GrzK content compared to $CD56^{dim}$ NK cells. Although $CD56^{bright}$ NK cells also release higher levels of GrzK, target cells are still dominantly killed via GrzB. These findings and additional granzyme release kinetics led to our conclusion, that GrzB is the main player in NK cell cytotoxicity. GrzA plays a greater role for primary activated NK cells in target cell killing than expected and is capable of inducing cytotoxicity without the assistance of other granzymes. Even though the other granzymes are able to cleave apoptosis-inducing substrates in target cells, their activity was mainly found together with GrzB. This could be due to several reasons, which could not yet be conclusively explained in this study. Nevertheless, these results contribute to the understanding of the complexity of NK cell cytotoxicity.

3 Zusammenfassung

Natürliche Killerzellen (NK) sind Zellen des angeborenen Immunsystems, die den menschlichen Körper gegen Virusinfektionen und Tumorwachstum verteidigen. Ihre "natürliche Zytotoxizität" wird durch das Zusammenspiel mehrerer aktivierender und inhibierender Rezeptoren genauestens reguliert. NK-Zellen verfügen über zwei Wege um abnorme Zellen zu bekämpfen: den Granula-vermittelten Weg und den Todesrezeptor-vermittelten Weg. Bei Kontakt mit der Zielzelle setzen NK-Zellen Granula frei, die zytotoxische Proteine wie Granzyme enthalten. Obwohl Granzym B (GrzB), das den Hauptbeitrag zum Granula-vermittelten Weg leistet, umfassend untersucht wurde, ist die Rolle der anderen vier humanen Granzyme A, H, K und M bei der Zytotoxizität von NK-Zellen weniger bekannt. In dieser Arbeit haben wir fluoreszierende Lokalisierungsreporter entwickelt, um die Aktivität von GrzB mit der der anderen vier Granzyme in einzelnen Zielzellen zu vergleichen. Dabei zeigen die Reporter nicht nur an, ob Granzyme in den Zielzellen aktiv sind, sondern geben auch Auskunft über die Kinetik. In dieser Studie haben wir beobachtet, dass NK92-Zellen ihre Zielzellen hauptsächlich mit Hilfe von GrzB und teilweise mit Unterstützung von GrzA töten. Wenn GrzB ausgeschaltet wird, fungiert GrzA als Backup für GrzB und löst Apoptose in den Zielzellen aus. Obwohl die Granzyme H, K und M von allen in dieser Studie untersuchten NK-Zellen exprimiert werden, spielen sie für die Zytotoxizität von NK92, im Gegensatz zu primären NK-Zellen, eine untergeordnete Rolle. In dieser Studie fanden wir eine unterschiedliche Relevanz der Granzyme für ruhende (M > A > K > H) und aktivierte (A > M > K > H) primäre NK-Zellen. Darüber hinaus weisen $CD56^{bright}$ primäre NK-Zellen im Vergleich zu $CD56^{dim}$ NK-Zellen einen höheren GrzK-Gehalt und niedrigere GrzB-Werte auf. Obwohl $CD56^{bright}$ NK-Zellen auch endsprechend höhere Mengen an GrzK freisetzen, konnten wir zeigen, dass die Zielzellen überwiegend durch GrzB getötet werden. Diese Befunde und die analysierte Kinetik der Granzymfreisetzung führten zu der Schlussfolgerung, dass GrzB der Hauptakteur der NK-Zellzytotoxizität ist. GrzA spielt bei der Tötung von Zielzellen durch aktivierte NK-Zellen eine größere Rolle als erwartet und ist in der Lage, selbst Zytotoxizität zu induzieren. Obwohl die anderen Granzyme in der Lage sind, Apoptose-induzierende Substrate in Zielzellen zu spalten, wurde ihre Aktivität hauptsächlich zusammen mit GrzB gefunden. Dies könnte mehrere Gründe haben, die in dieser Studie noch nicht schlüssig erklärt werden konnten. Dennoch tragen diese Ergebnisse zum Verständnis der Komplexität der NK-Zellzytotoxizität bei.

4 Introduktion

4.1 Natural killer cells

Natural killer (NK) cells are peripheral blood cells that belong to the innate immune system. Their “natural cytotoxicity” was first described in 1975 and is very important for early defence against parasites, virus infected and malignant cells (Kiessling et al., 1975, Herberman et al., 1975, Watzl et al., 2014, Terme et al., 2008, Ljunggren and Malmberg, 2007, Jost and Altfeld, 2013). NK cells are not only found in the peripheral blood, but also in several organs such as the spleen, liver, uterus, lungs, bone marrow and to a lesser extend in secondary lymphoid organs, mucosa associated lymphoid tissue and the thymus (Westermann and Pabst, 1992). As the other two lymphocytic linages of T and B lymphocytes, NK cells derive from $CD34^+$ multipotent haematopoietic cells in the bone marrow (Tajer et al., 2019). But in contrast to their siblings, NK cells do not rely on clonotypic antigen receptors. Rather, they are regulated by germline-encoded activating and inhibitory receptors (Watzl et al., 2014). These findings allow a clear separation of NK cells from T and B cells by defining NK cells as $CD3^-$ and $NKp46^+$ (Walzer et al., 2007). Natural killer cells can be further separated in two subpopulations by the surface markers CD16 and CD56. The dominant NK cell subpopulation in human peripheral blood is found to be $CD16^+$ and $CD56^{dim}$, which is highly cytotoxic. The less represented subpopulation of $CD16^-$ but $CD56^{bright}$ NK cells seem to have regulatory functions and are more responsive to cytokines. Furthermore, $CD56^{bright}$ NK cells are the precursors of the more mature $CD56^{dim}$ NK cells (Trinchieri, 1989, Poli et al., 2009, Nagler et al., 1989). These findings highlight the important functions of NK cells, being not only cytotoxic but rather able to interact with other immune cells either by secretion of cytokines and chemokines or by direct contact (Vivier et al., 2008).

As already mentioned, NK cell activation differs from other lymphocytes by being regulated by activating and inhibitory receptors (Watzl and Urlaub, 2012). NK cells express activating receptors such as the natural cytotoxicity receptors (NCR): NKp30, NKp44 and NKp46, as well as receptors of the signalling lymphocytic activation molecule (SLAM)-family like 2B4, NTB-A and CRACC. Furthermore, they express NKG2D, DNAM-1, NKp80, NKp65, the Fcγ receptor

CD16 and activating killer Ig-like receptors (KIR) (Lanier, 2008, Watzl and Long, 2010). Ligands for these receptors are up-regulated on stressed, infected or transformed cells. In moderate numbers they are also found on healthy cells of the haematopoietic system, endothelial cells, epithelial cells and more (Champsaur and Lanier, 2010, Brandt et al., 2009, Claus et al., 2008, Bottino et al., 2003). The activating receptors are opposed by the inhibiting ones, which allows the precise regulation of NK cell functionality. They are not only important to counteract activating signals, but can also affect the adhesion between cell conjugates (Burshtyn et al., 2000). NK cells express two families of inhibitory receptors, inhibitory KIR and receptors that consist of CD94 and the lectin subunit NKG2. Both families are based on the immunoreceptor tyrosine-based inhibition motif (ITIM) (Wagtmann et al., 1995, Long, 2008, Borrego et al., 1998, Colonna et al., 1997). The most important inhibitory ligand is the major histocompatibility complex I (MHC-I), which is ubiquitously expressed on the surface of nucleated healthy cells (Karre et al., 1986, Karre, 2008). Interestingly, NK cells are able to distinguish between healthy and altered cells, even if they have contact with several target cells at the same time (Eriksson et al., 1999). Inhibition occurs in a spatially restricted manner and is therefore able to prevent the activation in an area attached to a healthy cell. Simultaneously, killing of a target cell in contact with another part of the NK cell plasma membrane is possible (Watzl and Long, 2003, Watzl and Urlaub, 2012).

There are two hypotheses which describe the regulation of NK cell activity by receptors: The “induced self” and the “missing self” hypothesis. High numbers of MHC-I molecules on healthy tissue leads to dominant inhibitory signals within the NK cell, which keeps it from killing. Once healthy cells become malignant, they reduce their MHC-I surface expression or lose it completely. Even if the aberrant cell expresses and present a normal number of activating ligands, the activating signal predominates and the NK cell is forced to kill its target. In this case, one speaks of the “missing self” hypothesis. The scenario of “induced self” is given upon strong upregulation of activating ligands triggered by cellular stress, infection or malignant alteration. Here, the activating signal within the NK cell is again stronger than the inhibitory signals, which lead to target cell death (Karre, 2008, Pegram et al., 2011, Watzl and Urlaub, 2012). Interestingly, the activation of resting NK cells through only one activating receptor is not sufficient.

A combination of at least two different receptors is required to trigger a response. Alternatively, NK cells can be primed by cytokines (Lucas et al., 2007, Bryceson et al., 2006, Marcus et al., 2014). The Fc receptor CD16 alone, which mediates antibody dependent cellular cytotoxicity (ADCC), is able to activate resting NK cells without the need of further stimulation (Tarek et al., 2012). Fortunately, NK cells are not exclusively activated by direct cell contact. They also react to cytokines such as IL-2, IL-15, IL-12 and IL-18, as well as chemokines and other soluble activators (Kim et al., 2010). Upon this priming, coactivation is no longer required and NK cells are able to induce cytotoxicity or produce cytokines such as tumour necrosis factor alpha (TNFα) and interferon gamma (IFNγ) when recognizing a target cell.

To prevent NK cells from acting non- or hyporesponsive, the expression of at least one inhibitory receptor specific for self-MHC-I is essential (Valiante et al., 1997). Two models are conceptualized to explain how NK cell functionality is ensured, a process that is called “education”. Due to its ability to receive inhibitory signals, the NK cell is competent to recognize endogenous cells and therefore receives its “license to kill”. Hence, this model is called “licensing”. NK cells that are unable to express inhibitory receptors and thus are not able to recognize MHC-I are disarmed by becoming anergic due to chronic stimulation by activating receptors. To avoid this anergy, the NK cell needs inhibitory signals to counteract the permanent activating signals. Simultaneous stimulation of inhibitory receptors by *trans*-binding the MHC-I ligand is resulting in “arming” the NK cell (Yokoyama and Kim, 2006, Kim et al., 2005, Raulet and Vance, 2006, Watzl, 2014). This model is described as “arming/disarming model”. In educated NK cells, activating receptors are now restricted to nanodomains. With this knowledge, the hyporesponsiveness of noneducated NK cells can be explained (Fernandez et al., 2005). Interestingly, the expression of self-KIR in educated NK cells leads to changes in the secretory lysosome size and higher levels of GrzB, enhancing the cytotoxic potential of these NK cells (Goodridge et al., 2019). Depending on the expression levels and distribution of inhibitory receptors specific for self-MHC-I, the education process can be described as dynamic rather than an on-off system (Brodin et al., 2009).

Following a correct identification of a target cell, the NK cell, like the T lymphocytes, has two possibilities to induce death mechanisms: The granule-mediated or the death receptor-mediated pathway (Ewen et al., 2012, Strasser et al., 2009, Watzl et al., 2014, Prager and Watzl, 2019). The granule-mediated pathway is the main focus of this thesis and will be described in greater detail in the following chapters. Three different pairs of death receptors and their ligands are known: the TNF-related apoptosis-inducing ligand (TRAIL) can bind to TRAIL receptors 1 and 2 (death receptors DR4 and DR5), Fas ligand (FasL/CD95L) engages with the Fas receptor (APO-1/CD95) and tumor necrosis factor alpha (TNFα) can interact with TNF receptor-1 or -2 (Gravestein and Borst, 1998). Starting with the engagement of a death receptor ligand expressed on the NK cell surface and a death receptor on a target cell, the apoptotic signaling cascade is activated. Extrinsic apoptosis starts with the formation of the death-inducing signaling complex (DISC) which is further leading to the cleavage of caspases 8 and 10 within the target cell. The initiated caspase cascade is resulting in a chain reaction including several proteins that lead to damages of mitochondria and DNA and finally to target cell death (Peter and Krammer, 2003, Stennicke et al., 1998, Barnhart et al., 2003).

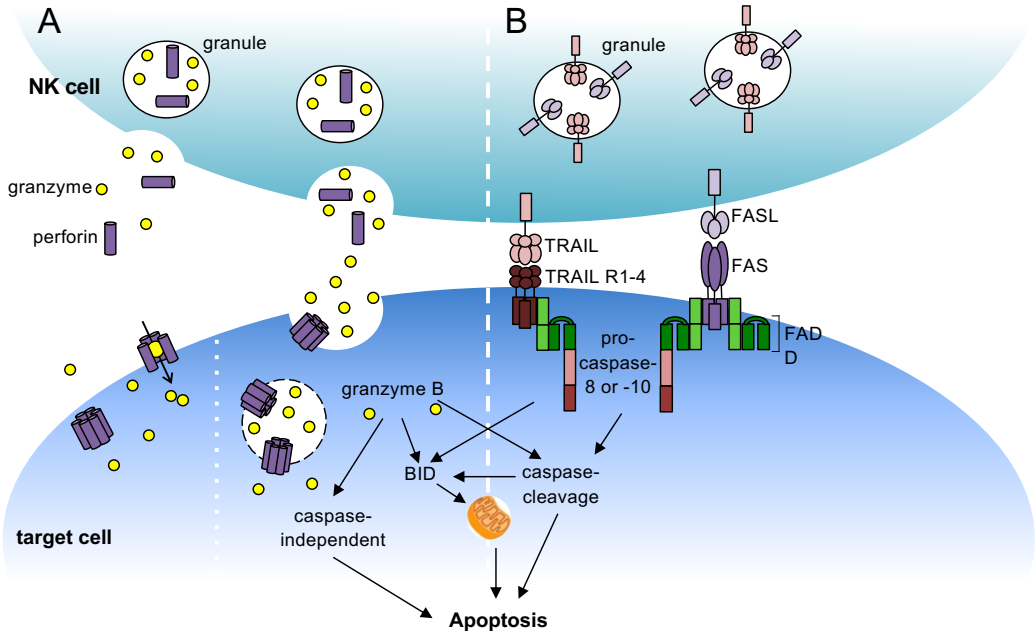

Figure 1: Natural killer cells can use two pathways to induce target cell apoptosis. The granule-mediated pathway (A) or the death receptor-mediated pathway (B). In the granule-mediated pathway the NK releases the content of its lytic granules towards the target cell. These granules mainly contain granzymes and perforin. Granzymes are able to induce apoptosis upon their successful entry into the target cells' cytosol by initiating caspase-dependent or -independent mechanisms. The cytotoxic proteins are either internalized by target cell endocytosis or pore formation by perforin on the target cells' membrane. Death receptor activation on the target cell by respective ligands on the NK cell leads to the initiation of caspase cascades and finally results in apoptosis of the target cell (Prager and Watzl, 2019).

4.2 The five human granzymes

To date, there are five human granzymes known. NK cells express all of them: GrzA and GrzB, as well as GrzH, K and M, of which GrzB is best characterized (Krzewski and Coligan, 2012, Bots and Medema, 2006, Bratke et al., 2005, Grossman et al., 2004). The term "Granzyme" is composed of the words granule and enzyme. Granzymes are serin proteases expressed by three different gene clusters (Chowdhury and Lieberman, 2008). While GrzB can be assigned a clear role in the cytotoxicity of human NK cells, the function of the other four granzymes is described to a lesser extent (Chowdhury and Lieberman, 2008, Lieberman, 2003).

Granzymes exhibit a wide substrate specificity. Although they have some of the substrates in common, cleavage of polypeptides is facilitated between distinct amino acids. GrzB preferentially cleaves c-terminal of aspartic acid (Asp) residues, which are negatively charged under physiological conditions (Fischer

et al., 2003). GrzA and GrzK possess a trypsin-like activity and can cleave c-terminal of the basic residues arginine (Arg) or lysine (Lys), which are positively charged under physiological conditions (Wilharm et al., 1999). In contrast to its siblings, GrzA forms a covalent homodimer, while all other granzymes remain monomeric (Kummer et al., 1996). GrzH cleaves its substrates c-terminal of the hydrophobic amino acids phenylalanine (Phe) or tyrosine (Tyr) and therefore has a chymotrypsin-like activity. GrzM has a rather unusual enzyme specificity: It possesses a Met-ase activity and is preferentially cleaving c-terminal of long aliphatic residues such as methionine (Met) or leucine (Leu) (Edwards et al., 1999, Smyth et al., 1995, 1984, Smyth et al., 1993). Some of these cleavage activities also exhibit a direct influence on the activity of other granzyme relatives. For example, GrzM has the ability to cleave and inactivate serpin B9, a natural inhibitor of GrzB (Kaiserman and Bird, 2010, de Koning et al., 2011).

As already mentioned, the five human granzymes are expressed by three different gene clusters. The genes of GrzA and K are located on chromosome 5, while GrzM is encoded on chromosome 19. GrzB and GrzH are not only both located on chromosome 14, they are also highly structural homologues (Russell and Ley, 2002). Apart from NK cells, granzymes are expressed by a wide range of cells. GrzB for example is found in other immune cells like $CD8^+$ T cells, plasmacytoid dendritic cells (pDC), normal and neoplastic mast cells and basophils, but also in other cell types as myeloid cells, developing spermatocytes, placental trophoblasts and primary human breast carcinomas (Rissoan et al., 2002, Strik et al., 2007, Hochegger et al., 2007, Wagner et al., 2004, Martin et al., 2005, Metkar and Froelich, 2004, Hirst et al., 2001, Horiuchi et al., 2003). The expression of GrzB in so many different cell types shows the importance of granzymes and suggests additional non-cytotoxic functions.

GrzA expression is associated with several infections, sepsis, autoimmune diseases, diabetes, vascular disorders, oncologic diseases and haematological malignancies (Tsubota et al., 1994, Held et al., 1990, Smith et al., 2004, Teo et al., 2013, Muris et al., 2007, Banerjea et al., 2004, Napoli et al., 2012). GrzB is directly linked to neurological and blood disorders, as well as to chronic inflammatory disease (Boivin et al., 2009). GrzH plays an important role in the antiviral response, but is also connected to lymphomas and breast cancer

(Andrade et al., 2007, Tang et al., 2012, Sedelies et al., 2004, Razvi et al., 2008). Elevated levels of GrzK are associated with several inflammatory diseases such as chronic and idiopathic pulmonary diseases, asthma, atherosclerosis, arthritis and sepsis. On the other hand, GrzK appears to be a promising prognostic marker following chemotherapy in pediatric high-risk acute lymphoblastic leukemia patients (Joeckel and Bird, 2014a, Al-Lamki et al., 2005). However, the role of GrzM in pathophysiological conditions is not clarified yet, increased plasma levels are found in context with meningococcal disease. On the other hand, GrzM seems to play an important role in ulcerative colitis by providing innate immune protection (Hollestelle et al., 2011, Souza-Fonseca-Guimaraes et al., 2016).

4.3 Trafficking, storage and activation of Granzymes

In mouse T lymphocytes, the GrzB transcription is regulated by several upstream transcription factor binding-sites that seem to be evolutionary conserved among mice and men (Fregeau and Bleackley, 1991, Wargnier et al., 1995, Haddad et al., 1993). These studies suggested that combinations of the transcription factors, particularly activator protein-1 (AP-1), activating transcription factor/cyclic AMP-responsive element binding protein (ATF/CREB) and core-binding factor (CBF), are required to activate GrzB expression in primary cells (Babichuk et al., 1996, Babichuk and Bleackley, 1997, Wargnier et al., 1995). Two further studies in mice suggest a role for the signal transducer and activator of transcription 1 (STAT1) in the transcriptional regulation of GrzB. Again, only little is known about transcriptional regulation of the other granzymes.

To handle the highly cytotoxic granzymes and to ensure correct delivery to the granules without inducing host cell death, GrzB is synthesized in a pre-pro-form of the protein, the inactive zymogen. The N-terminal pre-sequence (signal peptide) directs it to the endoplasmic reticulum (ER), where pre-sequence cleavage occurs during translocation to obtain the pro-enzyme (Jenne and Tschopp, 1988). From here, pro-granzyme B is transported to the *cis*-Golgi. Within the network, granzymes A and B are modified with mannose-6-phosphate (M6P), directing the transport via mannose-6-phosphate receptor (M6PR) from the *trans*-Golgi apparatus to the early endosomes (Griffiths and Isaaz, 1993).

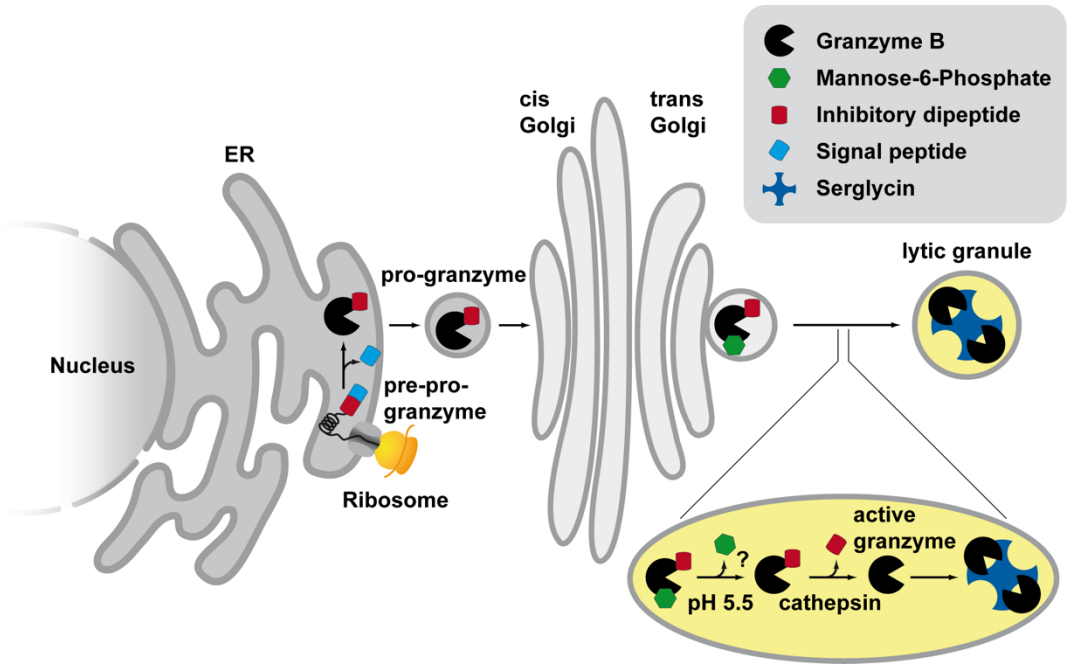

Figure 2: Trafficking, storage and activation of granzyme B. GrzB is expressed as a pre-pro-protein. Upon co-translational translocation into the endoplasmic reticulum (ER) the pre-sequence is cleaved and the pro-protein is transported to the Golgi. Here, GrzB is modified with mannose-6-phosphate which allows the transport to the early endosome. On the way from the early endosome to the lytic granules, the mannose-6-phosphate is removed and cathepsin C cleaves the pro-dipeptide to form the final state of GrzB. To suppress the cytotoxic properties of GrzB it is bound to serglycin to prevent host cell lysis. Figure modified according to (Prager and Watzl, 2019).

The sorting into late endosomes is facilitated by the recruitment of the endosomal sorting complex required for transport (ESCRT) (Williams and Urbe, 2007). The mechanism and role of ESCRT in the biogenesis of cytotoxic granules is not fully understood yet, but its addition to this process is suggested by the consequences of defects in this pathway (Burkhardt et al., 1990, Stinchcombe et al., 2000). Trough the transformation into late endosomes, the acidic pH leads to the release of M6P-modified granzymes from its receptor (Burkhardt et al., 1990). Whether the mannose-6-phosphate modification is removed from granzymes is still debated. However, GrzB is now brought to its cytotoxic form by removing the N-terminal pro-dipeptide by cleavage of cathepsin C (dipeptidyl peptidase I) within the lytic granules (Kummer et al., 1996). To further supress the activity of granzymes and perforin within the granules, the proteins are bound to the acidic serglycin proteoglycan. Additionally, the low pH within the granules keeps the proteolytic activity of the basic granzymes negligible (Grujic et al., 2005). The pathway directing perforin into late endosomes remains unclear (Voskoboinik et al., 2005). Cytotoxic granules are therefore hybrids of lysosomes and late endosomes, which lead to properties of dense core domains for granzyme and

perforin storage, but also hydrolase containing multivesicular bodies (Burkhardt et al., 1990, Peters et al., 1991, Blott and Griffiths, 2002).

4.4 The immunological synapse

Upon target cell contact via integrin-mediated adhesion of a NK cell, the formation of the immunological synapse is initiated (Hoffmann et al., 2011, Bryceson et al., 2009). The directed transport of lytic granules along the microtubules and towards the microtubule organizing center (MTOC) is performed by dynein motor proteins. Together, the granules and the MTOC are polarized near the plasma membrane, which is in contact with the target cell (Mentlik et al., 2010, James et al., 2013). To allow granule-mediated cytotoxicity, the immunological synapse is formed tightly by LFA-1 mediated adhesion of the NK cell to its target cell (Simone and Henkart, 1980). Now the MTOC has direct contact to the plasma membrane, which is dense in signalling molecules and receptors. In cytotoxic T lymphocytes (CTLs) and NK cells this construct is called the central supramolecular activation complex (cSMAC). This specialised area is surrounded by a ring of integrin-rich plasma membrane, the peripheral SMAC (pSMAC) (Beal et al., 2008, Orange, 2008). The contact of MTOC and SMAC allows the direct delivery of granules into the synaptic cleft (Stinchcombe et al., 2006, Davis and Dustin, 2004). Here, members of the Rab GTPase family and mammalian uncoordinated (MUNC) proteins support the fusion of granules and the plasma membrane by regulating vesicle trafficking, compartmentalization and the interaction of soluble N-ethylmaleimide-sensitive-factor attachment receptor (SNARE) complexes (Pereira-Leal and Seabra, 2001, Feldmann et al., 2003, Menager et al., 2007). MUNC proteins and complexin stimulate the vesicle SNARE complex (v-SNARE) to coil into the target membrane SNARE (t-SNARE) to reduce the gap between vesicle and target membrane. This process is important to overcome the repulsion of the polar heads of the membranes and allows fusion to occur (Rizo and Sudhof, 2002, de Wit et al., 2009, Shen et al., 2007). Due to phospholipid flipping, both the vesicle and NK cell plasma membranes are quickly rearranged to one and the content is released into the synaptic cleft. This membrane fusion includes the occurrence of CD107a at the outer membrane, which is used as a degranulation marker (Mace et al., 2014, Krzewski et al., 2013). However, the

forming of the immunological synapse and the release of content may differ among different cytotoxic immune cells.

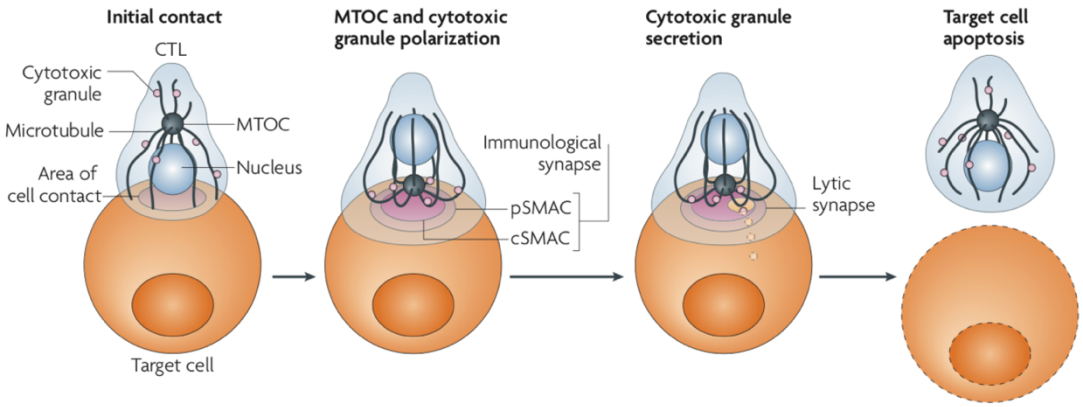

Figure 3: Contact of an effector cell to a target cell forming the immunological synapse. Upon target cell recognition, the effector cell (NK cell or CTL) is reorganizing its microtubule-organizing center (MTOC) towards the contact site. The immunological synapse is organized into a central supramolecular activation complex (cSMAC), where signaling molecules and T cell receptors (TCRs) are localized, surrounded by a peripheral integrin-rich ring, the peripheral SMAC (pSMAC), which defines the boundary of the synapse. The cytotoxic granules are now transported along the microtubules towards the minus end to the synaptic cleft, into which they release their content (de Saint Basile et al., 2010).

Once released into the immunological synapse, the content of lytic granules is proposed to be delivered to the target cell by two distinct mechanisms. The first one describes the perforin-mediated pathway. Due to the neutral pH and the presence of Ca^{2+}, perforin is able to bind to the target cell membrane and forms pores by the accumulation of monomers in close proximity (Simone and Henkart, 1980, Lopez et al., 2013a, Lopez et al., 2013b). These pores (10 – 20 nm) allow the direct entry of granzymes and other cytolytic molecules into the target cell, as the pores' diameter is big enough for passive diffusion (Kurschus et al., 2008, Law et al., 2010, Leung et al., 2017). Granzymes dissociate from serglycin once in the synaptic cleft and bind to the negatively charged target cell membrane, as their net charge is highly positive (pIs ~ 9-11) (Raja et al., 2005, Kurschus et al., 2005, Bird et al., 2005, Shi et al., 2005). Furthermore, this mechanism could lead to an alternative entry of granzymes into the target cell. Since perforin succeeds in damaging the target cell membrane, resulting in increased Ca^{2+} influx, membrane repair processes could lead to the uptake of granzymes via endocytosis (Bird et al., 2005, Keefe et al., 2005). Similarly, granzymes could bind to M6P-receptors, followed by endocytosis, since these receptors are also expressed on the surface of target cells (Froelich et al., 1996, Motyka et al.,

2000). Escape from these endocytosed vesicles is thought to be mediated by the formation of perforin pores, again (Browne et al., 1999, Froelich et al., 1996, Thiery et al., 2010). Interestingly, the heat shock protein hsp70, which is found on the surface of stressed or malignant cells, is described to carry GrzB into cells (Gross et al., 2003). Furthermore, *in vitro* intracellular delivery of GrzB mediated by perforin can be substituted by bacterial and viral endosomolysins, suggesting a potential role *in vivo*, too (Browne et al., 1999).

4.5 Self-protection of effector cells

As already described above, serpin B9 is an efficient GrzB inhibitor. Serpin B9 is expressed in NK cells and T lymphocytes, and also in other cell types like dendritic cells, mast cells, endothelial and mesothelial cells, and cells of immune privileged organs (testis and placenta), to ensure self-protection against misdirected GrzB (Hirst et al., 2003, Buzza et al., 2001, Buzza et al., 2006, Bladergroen et al., 2001, Bladergroen et al., 2005). The expression of Serpin B9 in other cell types underlines its importance in protection from GrzB, as these cells are thereby saved during an immune response in their near environment. GrzB cleaves serpin B9 as a substrate, whereupon a conformational change of serpin B9 results in a stable but resistant complex which efficiently inactivates GrzB (Losasso et al., 2012, Blakely et al., 1987, Bird et al., 1998, Sun et al., 1996, Sun et al., 2001, Huntington et al., 2000). Also, other serpins of the 1500-member superfamily are expressed by CTLs or NK cells (Law et al., 2006, Silverman et al., 2001). To protect the CTLs against further granule contents as for example perforin, roles of CD107a/LAMP-1 as well as tightly packed lipids within the ‘lipid rafts’ are described. During granule exocytosis, CD107a accumulates at the outer plasma membrane of a NK cell within the immunological synapse, thereby inhibiting the binding of perforin and protecting from self-injury (Cohnen et al., 2013). Furthermore, the specialised microdomains formed on the CTL and NK cell membrane within the immunological cleft have additional functions to protect the owner against perforin-mediated lysis. The tightly packed phospholipids prevent perforin binding as well as its intercalation into the host membrane (Antia et al., 1992). On top, another protein that is able to cleave and inactivate perforin reaches the outer membrane during CTL degranulation: cathepsin B (Balaji et al., 2002). Interestingly, the secretion of cathepsin B by

tumor cells allows them to escape T lymphocytes' cytotoxicity (Khazen et al., 2016). Packard et al. was able to show the entrance of GrzB into target cells but not into CTLs or NK cells by using a cell-permeable fluorescent GrzB substrate (Packard et al., 2007).

4.6 Granzyme-mediated cytotoxicity

Once the granzymes enter the target cell, they have a variety of opportunities. Here, they find most of their substrates located in the cytosol or membrane bound to cellular compartments like mitochondria or the nucleus (Jans et al., 1998, Jans et al., 1996). In this field, GrzB is the best characterized granzyme as well. Its extrinsic apoptosis is initiated by cleavage of various caspases, but GrzB also shares substrate specificity of some caspases (Bots and Medema, 2006, Joeckel and Bird, 2014a, Susanto et al., 2012). GrzB is reported to be able to cleave the initiator pro-caspase 8 as well as the effector pro-caspase 3 (Medema et al., 1997, Quan et al., 1996, Yang et al., 1998, Andrade et al., 1998, Atkinson et al., 1998, Goping et al., 2003). Thereby, GrzB is able to induce caspase-dependent or -independent apoptosis, by cleaving caspase 3 either directly or indirectly by initiating the BID (BH3 interacting death domain agonist) cascade (Goping et al., 2003, Quan et al., 1996, Andrade et al., 1998, Pinkoski et al., 2001, Sutton et al., 2000, Atkinson et al., 1998). Furthermore, the cleavage of caspases 3, 7, 8 and 10 in cell-based or cell-free systems by GrzB is reported (Adrain et al., 2005, Andrade et al., 1998, Medema et al., 1997, Martin et al., 1996, Van de Craen et al., 1997). As already mentioned, GrzB shares some substrate specificity close to caspase 6, 8 and 9 and accordingly cleaves their substrates including ICAD, PARP-1, lamin B, NuMa, DNA-PKc, La protein and tubulin (Andrade et al., 1998, Barry et al., 2000, Pinkoski et al., 2001, Sutton et al., 2000, Thornberry et al., 1997). Hence, GrzB plays an important role as both initiator and executioner in death of target cells. The cleavage of these key substrates correspondingly leads to mitochondrial and DNA damage pathways, which further result in target cell death (Casciola-Rosen et al., 2007, Cullen et al., 2007, Heibein et al., 2000, Alimonti et al., 2001, Thomas et al., 2000, Sharif-Askari et al., 2001). Van Damme et al. identified 322 human GrzB substrates in a proteomic approach, of which 14 substrates were identified under physiological conditions (Van Damme et al., 2009). Natural conditions, while searching for protein substrates and being able

to discriminate between authentic and irrelevant substrates, are therefore very important. In addition, important substrates might be disregarded by showing only little efficiency in their cleavage in approaches that are not performed under physiological conditions.

In contrast to GrzB, the granzymes A, H, K and M seem to act exclusively caspase-independent. Beresford et al. has demonstrated that inhibitors of caspase-mediated apoptosis could not protect target cells from dying by GrzA activity (Beresford et al., 1999). Also, GrzK was unaffected by caspase inhibitors (Zhao et al., 2007). Furthermore, overexpression of bcl-2 or bcl-XL, which are inhibitors of the BID induced cascade, was not sufficient to prevent the granzyme A or K initiated apoptosis in target cells, respectively (Beresford et al., 1999, Zhao et al., 2007). Until 2004 it was not clear whether GrzM is able to induce target cell death. In addition, there are conflicting reports in the literature as to whether GrzM causes target cell death via caspases or independently of caspases, but also the type of induced target cell death is controversial (Kelly et al., 2004, Lu et al., 2006, Hua et al., 2007). However, GrzH was found to show clear caspase-independent hallmarks of programmed cell death, but no regular cellular substrates have been identified yet. It is rather reported, that GrzH cleaves the viral proteins DBP (adenovirus DNA-binding protein) and the adenovirus 100K assembly protein. DBP is also described to be a substrate of GrzB and is important for viral DNA replication, while the protein 100K was found to be a GrzB inhibitor. (Fellows et al., 2007, Andrade et al., 2001, Andrade et al., 2007) In addition, GrzH cleaves the cellular phosphoprotein La, which is necessary for hepatitis c virus (HCV) replication (Romero et al., 2009). These findings suggest an anti-viral role for GrzH in infected cells rather than in tumor cells.

Upon BID cleavage in the cytosol, GrzB initiates the same mitochondrial damage pathways as caspases (Casciola-Rosen et al., 2007, Barry et al., 2000, Heibein et al., 2000, Alimonti et al., 2001, Thomas et al., 2000). Cleaved BID causes the activation of the bcl-2 family members Bak and Bax, which lead to the release of pro-apoptotic factors like cytochrome c. Cytochrome c together with the binding of apoptotic protease activating factor 1 (Apaf-1) to pro-caspase 9 results in the mature form of caspase-9. Thereby another circle is closed in which GrzB is able to indirectly activate caspase-3. Furthermore, the mitochondrial damage pathway

includes disruption of mitochondrial membrane integrity, the release of reactive oxygen species (ROS) and more apoptotic factors like smac/DIABOLO, apoptosis-inducing factor (AIF) and Omi/HtrA2 (MacDonald et al., 1999, Heibein et al., 1999, Thomas et al., 2001, Wang et al., 2001, Pinkoski et al., 2001, Sutton et al., 2000).

Martinvalet et al. reported that CTLs expressing all granzymes are unable to induce target cell death when treated with compounds decreasing intracellular ROS concentration (superoxide scavengers), suggesting the importance of mitochondrial damage for all granzyme-mediated pathways (Martinvalet et al., 2005). GrzA mediates mitochondrial damage by trafficking into the mitochondrial matrix. There, it is able to cleave the mitochondrial complex I protein NDUFS3. Additionally, the dysfunction is initiated by the release of ROS and loss of transmembrane potential. In contrast to GrzB, the disruption of mitochondrial morphology is not induced by mitochondrial outer membrane permeabilization (MOMP). As a consequence, cytochrome c, HtrA2/Omi or smac/Diablo are not released upon GrzA activity (Martinvalet et al., 2005, Martinvalet et al., 2008). Analogous to GrzA, recombinant GrzK leads to ROS release and loss of transmembrane potential. The outer membrane remains intact and cytochrome c, HtrA2/Omi or smac/Diablo are not released as well (Zhao et al., 2007, Guo et al., 2008, MacDonald et al., 1999). Also, in this part of the pathway only little is known about GrzH. ROS generation, dissipation of transmembrane potential and mitochondrial depolarization, but not cytochrome c release were described (Fellows et al., 2007). In the case of GrzM, there is some controversy in the literature. While one group cannot find any evidence of mitochondrial depolarization, another group reports mitochondrial disruption including MOMP, mitochondrial swelling, dissipation of transmembrane potential, ROS generation and cytochrome c release. In the latter publication, they found an additional substrate of GrzM, the heat shock protein TRAP75. This protein inhibits ROS generation initiated by GrzM (Kelly et al., 2004, Lu et al., 2006, Hua et al., 2007). Although these research groups base their results on recombinant human GrzM, the expression systems used (insect or yeast cells) are quite different and could therefore influence the activity. This is especially important with respect to glycosylation, which in insect cells is close to human or yeast glycosylation, but not identical and e.g. lacks sialylation (Shi and Jarvis, 2007).

Besides mitochondrial damage, granzymes are as well able to induce DNA damage by cleaving substrates in the cytosol or within the nucleus itself. The primary GrzB mediated way to trigger DNA damage is driven via the cleavage of ICAD. ICAD is the inhibitor molecule of the caspase-activated DNase (CAD). Upon ICAD cleavage, CAD is able to translocate into the nucleus and fragment the DNA. Moreover, GrzB cleaves lamin B and PARP-1, which are DNA stabilization and repair proteins (Blink et al., 2005). First results of granzyme activity within the target cell are shown by membrane blebbing and shrinkage (Beresford et al., 2001, Adrain et al., 2005).

Both GrzA and GrzB are able to translocate into the nucleus. This translocation is suggested to be mediated by importin-α (Jans et al., 1996, Jans et al., 1998, Blink et al., 2005). Inside the nucleus, GrzA cleaves the SET-complex members HMG2, Ape1 and SET, which are involved in DNA repair. The translocation of the ER-associated SET-complex into the nucleus was thereby triggered earlier by the release of ROS, initiated by GrzA induced mitochondrial damage. The remaining parts of the SET complex NM23-H1 and TREX1 now fulfil their task: The endonuclease NM23-H1 induces DNA nicks, which are further expanded by the exonuclease TREX1 (Fan et al., 2003, Chowdhury et al., 2006). Other substrates of GrzA that are involved in DNA repair and stabilization are Ku70, PARP-1, lamins and histones. The cleavage of DNA stabilizing proteins decondenses the chromatin, at the same time making it more accessible for nucleases (Blink et al., 2005, Zhang et al., 2001a, Zhang et al., 2001b). GrzK again mimics GrzA. It is able to cleave the ER-associated SET-complex in the same manner as GrzA, with the same outcome resulting in DNA damage (Zhao et al., 2007, Guo et al., 2008). A unique function of GrzK and GrzM is the cleavage of pre-mRNA binding heterogenous ribonuclear protein k (hnRNP), which leads to splicing errors (Bovenschen et al., 2009, van Domselaar et al., 2013). As for GrzH there are only viral substrates described, no proteins were found that induce DNA damage. The ability to generate ROS alone leads to the usual DNA damages like chromatin decondensation and nuclear fragmentation (Fellows et al., 2007). For GrzM there is a controversy again. On the one hand no evidence for DNA fragmentation was found in one study and on the other hand ICAD cleavage was described in another study. This ICAD cleavage leads to the

release of CAD which further triggers DNA damage as already described for GrzB (Kelly et al., 2004, Lu et al., 2006, Hua et al., 2007).

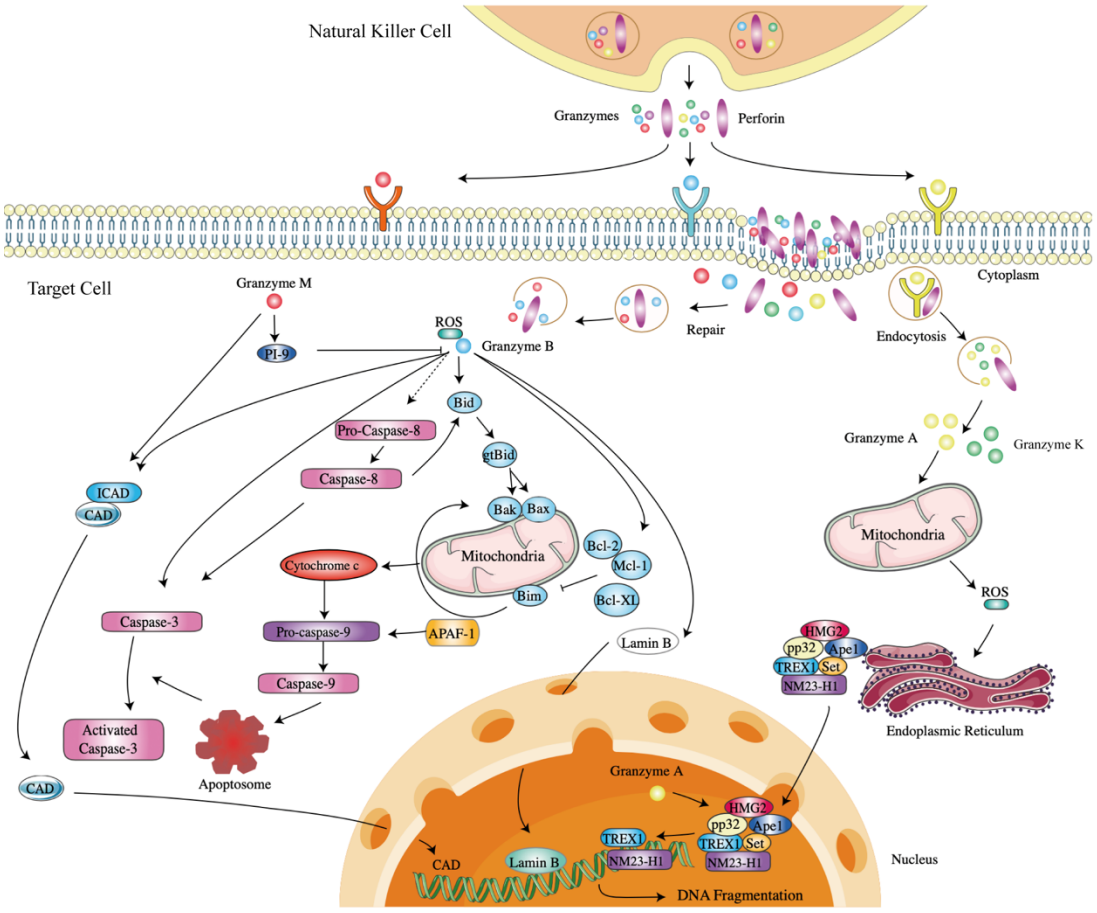

Figure 4: Overview of the granule-mediated apoptotic pathway. Granzymes enter the target cell either by perforin-pores in the target cell membrane or are internalized by endocytosis due to membrane repair mechanisms or receptor recycling. Once the granzymes have entered the cytosol of the target cell, they have a variety of opportunities to induce target cell death. Figure modified according to the Perforin/Granzyme Apoptosis Pathway by Creative Diagnostics®.

4.7 Extracellular roles of granzymes

Since low concentrations of granzyme A, B and K were found in serum of healthy donors and elevated levels during inflammation and infection, there is evidence that granzymes do not only exhibit cytotoxic roles (Bade et al., 2005b, Tschopp et al., 2006, Spaeny-Dekking et al., 2000, Spaeny-Dekking et al., 1998). The fact that not only immune cells produce granzymes indicates that the function of these proteins might be underestimated. The literature predicted extracellular functions of granzymes like the promotion of inflammation and the degradation of the extracellular matrix (Strik et al., 2007, Hochegger et al., 2007, Wagner et al., 2004, Hernandez-Pigeon et al., 2007). GrzA for example seems to act

proinflammatory. It is able to activate IL-1β by cleaving its pro-peptide and furthermore can activate macrophages and monocytes to produce cytokines (Irmler et al., 1995, Sower et al., 1996a, Sower et al., 1996b). GrzB is described to interact or cleave several surface molecules like the RGD integrin-binding domain of vitronectin, proteoglycans, glutamate receptor 3, Notch1 and FGFR1 (Buzza et al., 2005, Choy et al., 2004, Froelich et al., 1993, Ronday et al., 2001, Gahring et al., 2001, Ganor et al., 2007, Loeb et al., 2006).

4.8 Fluorescent localisation reporters

For this thesis, fluorescent protein reporters were expressed in $CD48^+$ HeLa cells to detect the activity of all human granzymes. These reporters were designed as tandem reporters, where GrzB activity is compared to one of the other four human granzymes, respectively. The activity of granzymes within the target cells was observed via live-cell imaging for different NK cell populations on a single cell level. Protease reporters based on luciferase (Li et al., 2014, Vrazo et al., 2015), fluorophore quenching (Packard et al., 2007) and FRET (Choi and Mitchison, 2013, Zhu et al., 2016) have been described previously, but did not allow parallel measurement of two protease activities on a single cell level. The reporters created in this thesis were initially described as single-fluorescent reporters by Liesche et al., 2018 and Beaudouin et al., 2013. These reporters consist of a localisation domain, a protease cleavage site acting as a cleavable linker and a fluorophore (localisation domain – cleavage site – fluorophore). As the respective localisation domain, a nuclear export signal (NES) was used to allow equal distribution of the intact reporter within the cytosol of the target cells. Some of the cleavage sites described in the literature for the individual granzymes were discovered by using positional scanning combinatorial libraries, or granzyme substrates were analysed. The specific amino acid sequences are known for all granzymes and were used to create our reporters. The GrzB cleavage amino sequence VGPD for example was found in DNA-PKc. (Mahrus and Craik, 2005, Guo et al., 2010, Mahrus et al., 2004, Li et al., 2014, Packard et al., 2007, Choi and Mitchison, 2013, Zhu et al., 2016, Backes et al., 2005). If the cleavage sequence is intact, the fluorophore cannot accumulate in the nucleus. Upon its cleavage by granzyme activity in the target cell, the fluorophore is able to diffuse into the nucleus, as it is no longer fused to the nuclear export signal. In this thesis,

the GrzB cleavage site is always coupled to the fluorophore mCherry and the single reporter can be described as: NES-VGPD'FGR-mCherry. The other four granzyme cleavage sites to monitor activity of granzymes A, H, K, M connect the NES domain with the fluorophore GFP. To create tandem reporters, which allow equimolar expression of both protein reporters within the same cell, the single reporters were genetically linked by the self-cleaving peptide T2A of the *Thosea asigna virus* (Liu et al., 2017). The tandem reporter for activity comparison of GrzA and GrzB for example is described as the following: NES-IGNR'S-GFP-T2A-NES-VGPD'FGR-mCherry. To compare the other granzymes' (H, K and M) activity to GrzB, the cleavage site of GrzA was exchanged. Each reporter construct is explained in detail in the method chapter 7.4.

Table 1: Amino acid sequence of the cleavage sites of the respective granzymes used for the fluorescent localization reporters.

Cleavage site	**Amino acid sequence**
Granzyme A	IGNR'S
Granzyme B	VGPD'FGR
Granzyme H	PTSY'G
Granzyme K	YRFK'G
Granzyme M	KVPL'AA

5 Aim of this thesis

The role of granzyme B in NK cell cytotoxicity is well established, but the contribution of the other four human granzymes A, H, K and M is investigated to a lesser extent. Therefore, the aim of the thesis was to classify the role of the other granzymes in NK cell cytotoxicity. We wanted to answer whether NK cells kill their targets exclusively by using granzyme B and how they might compensate a loss of granzyme B. Are the other granzymes able to function as backup and induce cytotoxicity on their own, or do they only have supportive functions? If there is a backup, which granzyme is used and do NK cells with a specific granzyme content exhibit distinct killing strategies? To answer these questions, we created fluorescent localization reporters which allow the tracking of granzyme activity within a target cell in a time-dependent manner. In particular, we want to directly compare each of the other four granzymes to granzyme B within the same target cell, to gather information of the chronological order of granzyme activity and the efficiency in cytotoxicity. A better understanding of each granzymes' contribution to NK cell cytotoxicity might help to identify possible subpopulations of NK cells which preferably express and release specific granzyme content, tailored to certain target cells.

6 Materials

6.1 Equipment

Device	Name and Supplier
Developing machine	CP1000 from AGFA
Centrifuge	Heraeus Multifuge 3 S-R from Thermo Fisher Heraeus Megafuge 40R from Thermo Fisher Heraeus Fresco 21 centrifuge from Thermo Fisher
Clean Bench	HERA Safe 2020 from Thermo Fisher
Flow cytometer	BD LSRFortessa™ Cell Analyzer from BD Biosciences BD FACSAria™ Fusion from BD Biosciences
Gamma counter	Wizard^2 2-Detector Gamma Counter from PerkinElmer
Incubator	HERAcell240i CO2 Incubator from Thermo Fisher
Microscope	EVOS FL auto from life technologies Axio Observer 7 from Carl Zeiss Microscopy GmbH
Nucleofector	4D-Nucleofector X Unit from Lonza
Plate reader	GloMax Explorer from Promega
Power supply	PowerPac™ Basic Power Supply from BioRad
xCELLigence	xCELLigence RTCA DP from Agilent

6.2 Consumables

Consumable	Name and Supplier
Blotting membrane	Polyvinylidene difluoride (PVDF, 0.45 μm) membrane from Millipore
Imaging chamber slides	ibidiTreat μ-Slide 8 well from ibidi
sodium dodecylsulfate (SDS) gel	4 – 12% NuPage Bis-Tris gel from Invitrogen

X-Ray Film	CL-Xposure™ Film from Thermo Scientific
xCELLigence E-Plate	xCELLigence E-Plate 16 PET from Agilent

6.3 Kits

Kit	Supplier
Amaxa SE Cell Line 4D-Nucleofector™ X Kit	Lonza
Dynabeads™ Untouched™ Human NK Cells	Invitrogen
Human Granzyme B DuoSet ELISA	R&D Systems
Human Granzyme K ELISA Kit	BioOcean
SuperSignal™ West Dura Extended Duration Substrate	Thermo Fisher Scientific
Western Bright Chemiluminescence substrate Sirius	Biozym

6.4 Reagents, Buffers and Medium

6.4.1 Reagents

Reagents	Supplier
1 kb / 100 bp DNA Ladder	New England Biolabs
Agarose I	Thermo Fisher Scientific
BD FACS Lysing Solution	BD Biosciences
BD FACS Permeabilizing Solution 2	BD Pharmigen
Chromium Cr^{51}	Hartmann Analytic
Dimethyl sulfoxide (DMSO)	Avantor (J.T.Baker)
EDTA	Carl Roth
EDTA	Carl Roth
Ethidium bromide solution (1% in H_2O)	Carl Roth
Gel loading dye purple (6x)	New England Biolabs

Glycerol	Carl Roth
Lipofectamine 2000	Invitrogen
Methanol	Carl Roth
Paraformaldehyde (PFA)	Sigma-Aldrich
Precision Plus Protein™ All Blue Prestained Protein Standards	BioRad
Sodium chloride	Applichem
Tris-HCl	Carl Roth
Triton X-100	Carl Roth
Tween20	Carl Roth
Z-Lys-SBzl • HCl	BACHEM
Zombie Yellow, Fixable Viability Dye	BioLegend

6.4.2 Cell culture reagents

Reagents	**Supplier**
Donor horse serum	PAN Biotech
Fetal calf serum (FCS)	Gibco®, Thermo Fisher Scientific
G418 / Geneticin	Gibco®, Thermo Fisher Scientific
Penicillin-Streptomycin (P/S)	Gibco®, Thermo Fisher Scientific
Puromycin	Calbiochem/Merck Millipore
TrypLE™ Express	Gibco®, Thermo Fisher Scientific

6.4.3 Bacterial culture reagents

Reagents	**Supplier**
Ampicillin	Sigma-Aldrich
Kanamycin	Sigma-Aldrich
LB Agar	Invitrogen
LB broth base	Invitrogen
SOC Outgrowth Medium	New England Biolabs

6.4.4 Buffer

Buffer	Composition
Blocking buffer (WB)	PBS-T + 5% non-fat dry milk powder
Dynal buffer	PBS, 0,1% BSA, 2 mM EDTA
FACS buffer	PBS + 2% FCS
MOPS (20x)	Invitrogen
Pancoll human (lymphocyte separation medium – LSM)	Density gradient 1.077 g/mL (PAN biotech)
PBS	Gibco®, Thermo Fisher Scientific
PBST	PBS + 0.05% Tween20
PBST-NaCl	PBS-T + 0.5 M NaCl
RSB (5x)	10% (w/v) SDS, 50% (v/v) Glycerol, 25% (v/v) β-Mercaptoethanol 0.1% (w/v) Bromphenol blue, 0.312 mM Tris-HCL, pH 6.8
Transfer buffer (WB)	0.024 M TRIS, 0.129 M Glycine + 20% Methanol
Triton X-100 lysis buffer	150 mM NaCl, 20 mM Tris-HCl, 10% Glyercol, 0.5% Triton X-100, 2 mM EDTA, 10 mM NaF, pH 7.3

6.4.5 Medium

Medium name	Composition
CTL (721.221)	IMDM medium (Gibco®) + 10% FCS + 1% P/S
HeLa	DMEM medium (Gibco®) + 10% FCS + 1% P/S
Jurkat	RPMI medium (Gibco®) + 10% FCS + 1% P/S
NK92	alpha MEM (Gibco®) + 12.5% horse serum + 12.5% FCS + 1% P/S + β-Mercaptoethanol (50 μM)
NKpop	IMDM medium (Gibco®) with GlutaMAX™ (Gibco®) + 10% FCS + 1% P/S
Opti-MEM (+GlutaMAX)	Gibco®

Starving medium	DMEM medium (Gibco®) + 2% FCS + 1% P/S

6.4.6 Recombinant Proteins and Cytokines

Recombinant Protein / Cytokine	Supplier
Cathepsin C/DPPI (active, mouse)	R&D Systems
Granzyme A (NK92, active)	Enzo Life Sciences
Granzyme B (YT, active)	Enzo Life Sciences
Granzyme H (NS0, human)	R&D Systems
Granzyme K (*E. coli*, active, human)	Enzo Life Sciences
Granzyme M (*E. coli*, active, human)	MyBioSource.com
IL-2	NIH Cytokine Repository
IL-12	R&D Systems
IL-15	Pan-Biotech
IL-18	Biozol
IL-21	Miltenyi Biotech
TrueCut™ Cas9 Protein v2	Invitrogen
Universal Type I IFN	PBL assay science

6.5 Synthetic guide RNAs

Invitrogen TrueGuide Synthetic guide RNAs 5' → 3'

Gene of interest	Sequence (Catalogue number)
Granzyme A	TATGACCCAGCCACACGCGA (CRISPR956518_SGM)
Granzyme A	AGACTAAGTAGGACCATGTA (CRISPR956522_SGM)
Granzyme B	GCACGAAGTCGTCTCGTATC (CRISPR801445_SGM)
Granzyme B	GGGATCAGAAGTCTCTGAAG (CRISPR801473_SGM)

6.6 Vectors

Insert	Backbone
NES-C8-GFP-T2A-NES-GrzB-mCherry (Prager, 2020)	pEGFP
NES-C8-GFP-T2A-NES-GrzB-mCherry_BamHI_HindIII	pEGFP
NES-GrzA-GFP-T2A-NES-GrzB-mCherry	pEGFP/pMOWS
NES-GrzH-GFP-T2A-NES-GrzB-mCherry	pEGFP/pMOWS
NES-GrzK-GFP-T2A-NES-GrzB-mCherry	pEGFP/pMOWS
NES-GrzM-GFP-T2A-NES-GrzB-mCherry	pEGFP/pMOWS
NES-GrzA-GFP-T2A-NES-AAAAFGR-mCherry (uncleavable GrzB)	pEGFP/pMOWS
NES-AAAAA-GFP-T2A-NES-GrzB-mCherry (uncleavable GrzA/H/K/M)	pEGFP/pMOWS

6.7 Bacteria

Name	Supplier
NEB® Turbo Competent *E. coli* (High Efficiency)	New England Biolabs

6.8 Cells

Name	Origin	Medium
Primary NK cells	Whole Blood from healthy humans	NKpop
Activated NK cells	Whole Blood from healthy humans	NKpop + IL-2 + IL-15
HeLa	cervical cancer	HeLa
K562	myelogenous leukaemia	CTL
Jurkat (E6.1)	T cell leukemia	Jurkat
NK92	NK cell lymphoma	NK92 + IL2

Phoenix (amphotropic)	Human embryonic kidney	HeLa
721.221	EBV transfected B cell line	CTL

6.8.1 Knock-out cell lines

Name	Knock-out	Parent cell line
NK92 GrzA KO	Granzyme A	NK92 WT
NK92 GrzB KO	Granzyme B	NK92 WT
NK92 GrzA&B KO	Granzyme A & B	NK92 GrzB KO

6.8.2 Reporter cells

Parental cell lines for transfection or transduction: HeLa CD48 or Jurkat (E6.1).

Name	Transfected with
HeLa GrzA-GrzB reporter	pEGFP NES-GrzA-GFP-T2A-NES-GrzB-mCherry
HeLa GrzH-GrzB reporter	pEGFP NES-GrzH-GFP-T2A-NES-GrzB-mCherry
HeLa GrzK-GrzB reporter	pEGFP NES-GrzK-GFP-T2A-NES-GrzB-mCherry
HeLa GrzM-GrzB reporter	pEGFP NES-GrzM-GFP-T2A-NES-GrzB-mCherry

Name	Transduced with
HeLa pMOWS GrzA-GrzB reporter	pMOWS NES-GrzA-GFP-T2A-NES-GrzB-mCherry
HeLa pMOWS GrzH-GrzB reporter	pMOWS NES-GrzH-GFP-T2A-NES-GrzB-mCherry
HeLa pMOWS GrzK-GrzB reporter	pMOWS NES-GrzK-GFP-T2A-NES-GrzB-mCherry
HeLa pMOWS GrzM-GrzB reporter	pMOWS NES-GrzM-GFP-T2A-NES-GrzB-mCherry
HeLa pMOWS GrzA-AAAAFGR reporter	pMOWS NES-GrzA-GFP-T2A-NES-AAAAFGR-mCherry
HeLa pMOWS AAAAA-GrzB reporter	pMOWS NES-AAAAA-GFP-T2A-NES-GrzB-mCherry

Jurkat pMOWS GrzA-GrzB reporter	pMOWS NES-GrzA-GFP-T2A-NES-GrzB-mCherry
Jurkat pMOWS GrzH-GrzB reporter	pMOWS NES-GrzH-GFP-T2A-NES-GrzB-mCherry
Jurkat pMOWS GrzK-GrzB reporter	pMOWS NES-GrzK-GFP-T2A-NES-GrzB-mCherry
Jurkat pMOWS GrzM-GrzB reporter	pMOWS NES-GrzM-GFP-T2A-NES-GrzB-mCherry

6.9 Inhibitors

Inhibitor	Supplier
Cycloheximide (10 mg/mL)	Sigma-Aldrich
3,4-Dichloroisocoumarin (10 mM)	Merck Millipore
Z-VAD-FMK (10 mM)	BD Pharmigen

6.10 Oligonucleotides

Merk Millipore, Sigma-Aldrich (dry, reconstitution to 100 μM)

5' → 3', Restriction site, **annealing**

Oligo / Primer name	Sequence
*Eco*RI_NES F spec.	ATATAGAATTC**TTTAGTGAACCGTCAGATCC**
GrzB *Hin*dIII fwd	**GAGCAGCAG**AAGCTT**GGCGGCGTG**
GrzB *Hin*dIII rev	**CACGCCGCC**AAGCTT**CTGCTGCTC**
GrzB *Bam*HI fwd	**AGGGGAGGA**GGATCC**CGCGTGAGC**
GrzB *Bam*HI rev	**GCTCACGCG**GGATCC**TCCTCCCCT**
GrzA IGNRS fwd	CCGGTGGCGGC**ATTGGTAACAGATCA**GGAGGAGGC
GrzA IGNRS rev	GGCCGCCTCCTCC**TGATCTGTTACCAAT**GCCGCCA
GrzH PTSYG fwd	CCGGTGGCGGC**CCAACATCATATGGT**GGAGGAGGC

GrzH PTSYG rev	GGCCGCCTCCTCC**ACCATATGATGTTGG**GCCGCCA
GrzK YRFKG fwd	CCGGTGGCGGC**TATCGCTTCAAGGGT**GGAGGAGGC
GrzK YRFKG rev	GGCCGCCTCCTCC**ACCCTTGAAGCGATA**GCCGCCA
GrzM KVPLAA fwd	CCGGTGGCGGC**AAGGTTCCACTTGCCGCC**GGAGGAGGC
GrzM KVPLAA rev	GGCCGCCTCCTCC**GGCGGCAAGTGGAACCTT**GCCGCCA
mCherry_NdeI R	TAACATATG**TTATCTAGATCCGGTGGATC**
*Pst*I rev	**CGTC**CTGCAG**GGAGGAGTCC**
*Xho*I fwd	**CCACGAT**CTCGAG**ACTGCTCC**

6.11 Restriction endonucleases and polymerases

Enzyme	Supplier
Q5 High Fidelity DNA Polymerase	New England Biolabs
*Age*I-HF	New England Biolabs
*Bam*HI-HF	New England Biolabs
*Eco*RI-HF	New England Biolabs
*Hin*dIII-HF	New England Biolabs
*Nde*I	New England Biolabs
*Pst*I	New England Biolabs
*Xho*I-HF	New England Biolabs

6.12 Antibodies

6.12.1 Primary monoclonal mouse antibodies for flow cytometry

Antigen	Clone	Conjugate	Dilution	Supplier
CD3	UCHT1	BV510	1:100	BD Biosciences
CD4	multi clone (Leu3a+3b)	FITC	1:200	BD Biosciences
CD8	RPA-T8	AF700	1:100	BD Biosciences

CD11a	HI111	AF647	1:100	BioLegend
CD16	3G8	FITC	1:200	BioLegend
CD16	3G8	PE	1:500	BioLegend
CD18	TS1/18	AF700	1:400	BioLegend
CD19	HIB19	AF700	1:200	BioLegend
CD45	HI30	AF700	1:250	BD Pharmigen
CD56	MEM-188	APC	1:50	BioLegend
CD56	NCAM 16.2	BV421	1:100	BD Biosciences
CD56	MEM-188	PE	1:200	BioLegend
CD56	B159	PerCP-Cy5.5	1:50	BD Pharmigen
CD57	HCD57	AF647	1:300	BioLegend
CD94	N/A	FITC	1:200	BD Pharmigen
CD94	N/A	PE	1:100	BD Pharmigen
CD107a	eBioH4A3	FITC (eBio)	1:100	Invitrogen
CD107a	H4A3	PE	1:200	BioLegend
CD107a	H4A3	PerCP	1:300	BioLegend
CD186 (CXCR6)	K041E5	FITC	1:50	BioLegend
CD226 (DNAM1)	DX11	AF647	1:100	BD Biosciences
CD226 (DNAM1)	N/A	FITC	1:100	BD Biosciences
CD226 (DNAM1)	N/A	PE	1:100	BD Pharmigen
CD244 (2B4)	C1.7	FITC	1:100	BioLegend
CD244 (2B4)	C1.7	PE	1:400	BioLegend
CD253 (TRAIL)	RIK-2	PE	1:100	BioLegend
CD261 (TRAILR1, DR4)	DJR1	PE (eBio)	1:100	Invitrogen
CD262 (TRAIL2, DR5)	DJR-2-4(7-8)	PE (eBio)	1:100	Invitrogen
CD314 (NKG2D)	N/A	AF700	1:100	BD Pharmigen
CD314 (NKG2D)	1D11	PE	1:100	BioLegend

CD335 (NKp46)	9E2	BV421	1:100	BioLegend
CD335 (NKp46)	9E2	PE	1:100	BioLegend
CD335 (NKp46)	9E2	PeCy7	1:100	BD Biosciences
CD336 (NKp44)	P44-8	PE	1:200	BioLegend
CD337 (NKp30)	N/A	AF647	1:100	BD Pharmigen
CD337 (NKp30)	P30-15	PE	1:100	BioLegend
Granulysin	eBioDH2	PE	1:100	Invitrogen
Granzyme A	CB9	PE/Cy7	1:200	BioLegend
Granzyme B	GB11	Pacific blue	1:100	BioLegend
Granzyme B	GB11	AF647	1:200	BioLegend
Granzyme H	Rabbit polyclonal	FITC	1:1600	G-Biosciences
Granzyme K	GM26E7	PE	1:100	BioLegend
Granzyme M	4B2G4	eFluor 660	1:100	Invitrogen
KLRG1	2F1	BV421	1:200	BD Biosciences
Perforin	dG9	FITC	1:200	BioLegend
TNF-α	MAb11	PE	1:100	BioLegend

6.12.2 Primary antibodies for Western Blot

Antigen	Clone	Species of origin	Dilution	Supplier
mCherry	4B3	Mouse monoclonal	1:5000	Invitrogen
mGFP	N/A	Mouse monoclonal	1:1000	N/A

6.12.3 Secondary antibodies

Name	Conjugate	Dilution	Supplier
anti-Mouse IgG	HRP	1:10000 / 1:20000	Cell Signaling Technology
Goat anti Rabbit IgG	HRP	1:10000 / 1:20000	Jackson ImmunoResearch

6.13 Software

Software	Supplier
BD FACS Diva Software 8.0.1	BD Biosciences
FlowJo 10.4.2	*FlowJo*
GraphPad PRISM 9.4.0	GraphPad Software, Inc
ImageJ 1.52q	W. Rasband
Microsoft office 16.54	Microsoft
ZEN 2 (blue version)	Carl Zeiss Microscopy GmbH

7 Methods

7.1 Cell lines

HeLa cells are derived from cervical cancer. HeLa CD48 cells were maintained in DMEM medium supplemented with 10% FCS, 1% P/S and 1 μg/mL Puromycin in an incubator with 5% (v/v) CO_2 at 37 °C. Once the cell density reaches about 70 to 80% confluency, the medium was removed and the cells were washed with PBS. The cells were detached by adding TrypLE™ Express (1x, Gibco®) and split in a ratio of 1:10 or 1:20 with fresh medium. To maintain HeLa CD48 cells transfected with reporter based on pEGFP backbone, 1 mg/mL G418 was additionally added to the medium.

K562 is a human myelogenous leukaemia cell line. The cells were maintained in IMDM medium supplemented with 10% FCS and 1% P/S in an incubator with 5% (v/v) CO_2 at 37 °C. Three times a week the cells were split to an end concentration of 0.3 x 10^6 cells/mL.

721.221 is an Epstein-Barr virus (EBV) transfected B cell line. They were maintained in IMDM medium supplemented with 10% FCS and 1% P/S in an incubator with 5% (v/v) CO_2 at 37 °C. Three times a week the cells were split to an end concentration of 0.3 x 10^6 cells/mL.

Jurkat cells are a T cell leukemia cell line ($CD4^+$). The cells were maintained in RPMI medium supplemented with 10% FCS and 1% P/S in an incubator with 5% (v/v) CO_2 at 37 °C. Three times a week the cells were split to an end concentration of 0.3 x 10^6 cells/mL. To maintain Jurkat cells transduced with reporter base on pMOWS backbone, 1 μg/mL Puromycin was additionally added to the medium.

NK92 is a NK cell lymphoma cell line. The cells were maintained in alpha MEM medium supplemented with 12.5 % horse serum, 12.5% FCS, 1% P/S and 50 μM β-mercaptoethanol in an incubator with 5% (v/v) CO_2 at 37 °C and spilt three times a week to an end concentration of 0.3 x 10^6 cells/mL with fresh media and 100 U/mL IL-2.

7.2 NK cell isolation

In a first step peripheral blood mononuclear cells (PBMC) were purified from the blood of healthy volunteers by density centrifugation with Lymphocyte Separation Medium (LSM). The gradient was set up starting with the LSM, which was covered by twice the volume of blood. After centrifugation (1025 x g for 25 min) the white interface between plasma and buffer layer containing the PBMC, was harvested. Afterwards the NK cells were purified by using the Dynabeads® Untouched™ Human NK Cells Kit (Thermo Fisher) according to the manufacturer's instructions. The purity of isolated NK cells was confirmed by flow cytometry.

7.3 NK cell culture

To maintain the isolated NK cells in culture, the cells were resuspended in NKpop medium (1 x 10^6 – 2 x 10^6 cells/mL) in 96-U-well plates with 200 IU/mL recombinant human IL-2 and 100 ng/mL recombinant human IL-21, mixed with irradiated (30 gray) K562-mb15-41BBL feeder cells (5 x 10^5 cells/mL). After one week of incubation, the NK cells were restimulated with 100 IU/mL IL-2 and 5 x 10^5 – 1 x 10^6 cells/mL irradiated K562-mb15-41BBL feeder cells. At the same time, NK cells were split 1:2 once a density of 2 x 10^6 cells/mL was reached. Again, one week after restimulation the NK cells were maintained by splitting them twice a week in a 1:2 dilution of fresh NKpop medium supplemented with 100 IU/mL IL-2 and 50 IU/mL IL-15.

7.4 Vectors

The tandem reporter consists of two equally structured fluorescent reporters which are linked by a self-cleaving T2A domain. Each reporter consists of a N-terminal nuclear export signal (NES) followed by a specific protease cleavage site and either a green fluorescent protein (GFP) or a red fluorescent protein (mCherry) at the C-terminus. All pEGFP vectors were cloned based on the existing NES-Cas8-GFP-T2A-NES-GrzB-mCherry construct (Prager, 2020). The construct was complemented with the restriction sites for the restriction endonucleases *Age*I / *Not*I or *Hin*dIII / *Bam*HI. Thus, the protease specific cleavage sites for caspase 8 (Cas8) or granzyme B (GrzB) are easily

exchangeable, respectively. To create reporter constructs for every granzyme, Cas8 cleavage side was exchanged for the individual granzyme cleavage site.

The two fluorescent reporters are genetically fused by a “self-cleaving” T2A (Thosea asigna virus capsid) domain to allow equimolar expression of both proteins from a common promoter and to achieve a co-translational separation into two individual proteins. The following amino acids sequence was utilized for the T2A peptide: EGRGSLLTCGDVEENPG’P (cleavage site marked by ’). The T2A domain is flanked by six non-coding amino acids.

The constructs were cloned into the pEGFP vector carrying a human cytomegalovirus (CMV) promoter and enhancer to ensure strong protein expression in a broad range of cell types. For plasmid replication in bacteria the aph(3')-II gene (or nptII) driven by the bla promotor is content of the plasmid to provide kanamycin resistance. The very same gene driven by the SV40 promotor enables the positive selection of transfected cells by neomycin / G418. To enable viral transduction of the reporter constructs, they were cloned into the pMOWS backbone.

Motive / Cleavage site	**Amino acid sequence**
NES	MNLVDLQKKLEELELDEQQ
T2A	EGRGSLLTCGDVEENPG’P
Granzyme A	IGNR’S
Granzyme B	VGPD’FGR
Granzyme H	PTSY’G
Granzyme K	YRFK’G
Granzyme M	KVPL’AA
Uncleavable Granzyme A/H/K/M	AAAAA
Uncleavable Granzyme B	AAAA’FGR

7.5 Transient transfection

One day prior to transfection 3.2 x 10^5 HeLa CD48 cells per well were seeded in a 6-well plate. Two hours before transfection the media was changed to 1.5 mL

starving medium. Per well 250 μL OPTIMEM medium were incubated with 10 μL Lipofectamine 2000 as well as 250 μL OPTIMEM medium together with 4 μg DNA for 5 minutes at RT. The two solutions were then combined and incubated for another 20 minutes at RT. The mixture was added to the cells and gently mixed. The cells were incubated for 24 h before changing the medium to fresh growth medium (HeLa medium). The following day 1 μg/mL Puromycin and 1 mg/mL G418 was added to the cell culture.

7.6 Transduction

For the generation of stable transfectants the Phoenix ampho system was used. On the first day 2 x 10^6 Phoenix ampho cells were seeded in a T25 tissue culture flask in 3 - 4 mL HeLa medium. The following day the cells were transfected by incubating first 237.5 μL OPTIMEM medium with 12.5 μL Lipofectamine 2000 as well as 240 μL OPTIMEM medium with 10 μg DNA separately for 5 minutes at RT. Then these mixtures were combined and incubated for another 20 minutes at RT and gently added to the Phoenix ampho cells. On the third day the medium was exchanged to fresh growth medium of the cells to be transduced. A spinfection was performed the day after. Therefore, the supernatant of the Phoenix ampho cells was harvested and centrifuged for 5 min at 1500 rpm to remove all cells. The supernatant was used to resuspend 0.5 x 10^6 cells to be transfected and plated in a 12-well plate, supplemented with 5 μg/mL polybrene. The plate was centrifuged for 1.5 h at 2500 rpm and 30 °C. After 24 h the medium was changed to the appropriate growth medium for the individual cell line. To ensure selective cell growth, 0.5 μg/mL puromycin was added to the cell culture one day after medium exchange.

7.7 Knock-out generation by using CRISPR/Cas9

To generate granzyme deficient NK92, the CRISPR/Cas9 system was used. For each condition 4 x 10^6 NK92 cells were harvested, centrifuged at 100 xg for 10 min, washed with PBS and again centrifuged at 100 xg for 5 min. Meanwhile, 20 μg Cas9 nuclease together with two different sgRNAs (200 pmol each gRNA) were incubated for 10 min at RT. After centrifugation the NK92 cell pellet was

resuspended in 100 µL SE solution (AMAXA SE cell line 4D Nucleofector X Kit) including Cas9 and gRNA and transferred to a cuvette. The program CA-139 of the 4D-Nucleofector™ X Unit (Lonza) was used for electroporation. 500 µL of warm RPMI medium + 10% FCS was gently and slowly added to the cuvette and cells were transferred to a 12-well. The cuvette was rinsed with 500 µL warm NK92 medium including 100 U/mL IL-2 and added to the 12-well. NK92 granzyme KO cells were maintained as described in chapter 6.8, success of granzyme knock-out was verified by flow cytometry.

7.8 Staining protocol for flow cytometry

In a first step, cells were stained with Zombie Yellow in 50 µL PBS per well in a 96-V-well plate for 20 min at RT in the dark. All further incubation steps were also performed at RT in the dark. The cells were washed by adding 150 µL PBS and centrifuged at 1500 rpm for 5 min. For surface staining, respective amounts of antibodies were diluted in FACS buffer and incubated for 20 min and washed afterwards with FACS buffer.

For intracellular staining the cells were fixed with 2 % PFA in FACS buffer for 10 min, washed and then permeabilized with BD FACS Permeabilizing Solution 2 (1:10 in H_2O) for 10 min at. The cells were washed again and then intracellularly stained with antibodies diluted in FACS buffer for 20 min. After a final washing step, the cells were resuspended in FACS buffer and analyzed by flow cytometry.

7.9 Whole blood staining protocol

Staining of cell surface antigens was performed by directly adding the respective amounts of antibodies to whole blood samples. After 20 minutes incubation at RT, the BD FACS Lysing Solution was added in a 1:10 dilution to the sample and incubated for 10 minutes. Beforehand, the BD FACS Lysing Solution itself was 1:10 diluted with water. The cells were washed with FACS buffer and centrifuged for 5 minutes at 1500 rpm. Afterwards, the cells were permeabilized with BD FACS Permeabilizing Solution 2 (1:10 in H_2O) for 10 minutes. Following another washing step, the intracellular staining was performed by the incubation with

respective antibodies for 20 minutes. Finally, the cells were washed and resuspended in FACS buffer.

7.10 Degranulation assay

2.5 x 10^5 target cells were seeded in a 96-U-well plate in 50 µL CTL medium per well. For control conditions 50 µL CTL per well was added to the plate with or without additional Ionomycin (1 µg/mL) / PMA (10 µM). 2.5 x 10^5 NK92 cells in 50 µL CTL per well were added to the culture. In the presence of an α-CD107a antibody the cells were incubated for 3 h at 37 °C.

Afterwards the cells were harvested, transferred to a 96-V-well plate and stained with Zombie Yellow, α-CD56 antibody, fixed, permeabilized and intracellularly stained for granzymes as already described in method chapter 7.8. Cells were analyzed by flow cytometry.

7.11 Granula kinetic

One day before the experiment 1 x 10^5 HeLa cells were seeded in a 6-well plate in HeLa medium. On the day of the experiment, HeLa medium was changed to 500 µL CTL and 3 x 10^5 NK cells in 500 µL CTL including an α-CD107a antibody were added to the culture. The kinetic was done by adding NK cells in reverse time line to ensure simultaneous sample collection. To exclude dead cells, samples were stained with Zombie Yellow. For distinction of target and NK cells a CD45 or CD56 staining was done. Granzymes were stained after fixation and permeabilization as described in method chapter 7.8.

7.12 PBMC stimulation

Peripheral blood mononuclear cells (PBMC) were purified from the blood of healthy volunteers by density centrifugation with Lymphocyte Separation Medium (LSM). 2 x 10^6 PBMC per condition were resuspended in NKpop medium and the respective stimulus was added (final concentration): low dose IL-15 as negative control (10 IU/mL), interleukin-cocktail of IL-12, IL-15 and IL-18 (1 µg/mL, 50 IU/mL, 5 µg/mL), lipopolysaccharide (LPS) (1 µg/mL), universal

type I interferon (uIFNα) (1000 U/mL), irradiated (30 gray) K562-mb15-41BBL feeder cells (K562 feeder) (5 x 10^5, E:T 4:1). Together with the respective stimulus, the PBMC were incubated for 2 h, 24 h, 48 h or 120 h. As a negative control PBMC were incubated without any stimulus.

7.13 ^{51}Cr-release assay

For a ^{51}Cr-release assay, 721.221, Jurkat or HeLa CD48 cells were used as target cells. 5 x 10^5 cells (per 96-well plate) were harvested and resuspended in 100 µL CTL medium, labeled with 100 µCi ^{51}Cr (3.7 MBq) for 1 h at 37 °C. In the meanwhile, NK cells were harvested and plated in a serial dilution (log2) of E:T 10:1, 5:1, 2.5:1 and 1.25:1. The samples were prepared in triplicates. After washing the target cells twice with fresh CTL medium 5 x 10^4 target cells/well were seeded for the experiment and incubated for 4 h at 37 °C. The maximum ^{51}Cr-release was examined by incubating target cells in CTL + 1% Triton X-100. To determine the spontaneous release, target cells were incubated alone without effector cells. Samples were centrifuged and the supernatant was analyzed by a gamma-counter.

7.14 Sample preparation for ELISA

PBMC of healthy donors were stained for sorting of CD56 dim and bright NK cells as described in chapter 7.15. 10^5 CD56 dim or bright NK cells were separately incubated in 200 µL CTL medium with the respective stimulus or lysed in 30 µL lysis buffer as described in chapter 7.18 (chemical lysis). To measure spontaneous granzyme release, the NK cells were incubated in CTL medium only. NK cells were stimulated with 10 µM PMA and 1 µg/mL ionomycin, or 2 µg/mL plate-bound MOPC21 or αNKp30, or 10^5 HeLa CD48 cells. The stimulation was performed for 4 hours at 37 °C. Then the cells were centrifuged for 5 min at 1500 rpm to collect the supernatant. The supernatant was stored at -80 °C until immediately prior to ELISA preparation, diluted 1:5 and further processed according to the manufactures' instructions.

7.15 Cell sorting

Double positive ($mGFP^+mCherry^+$) transfected or transduced target cells were sorted by using a BD FACSAria™ Fusion (BD Biosciences) to a purity of 70 to 90%.

To separate $CD56^{dim}$ and $CD56^{bright}$ NK cells, PBMC were stained for CD3, CD56 as well as for CD57. CD57 is used to identify terminally differentiated cells and is clearly expressed on $CD56^{dim}$ NK cells compared to $CD56^{bright}$. CD57 staining facilitates therefore the gating on the respective populations and ensures a more accurate sorting result.

7.16 xCELLigence impedance-based measurement

3 x 10^4 HeLa cells were seeded in 100 µL CTL medium per well in a xCELLigence E-Plate 16 PET (Agilent) and incubated in the xCELLigence machine for 6 h at 37 °C to let them adhere, while already measuring the impedance. Then 10 µM Z-VAD-FMK or DMSO in 50 µL CTL medium per well were added to the plate and incubated for 30 min at 37 °C. In a last step, 6 x 10^4 NK cells in 50 µL CTL medium per well were added to the plate and incubated overnight at 37 °C in the xCELLigence machine to continue the measurement.

7.17 Microscopy

The day before the experiment 3 x 10^4 HeLa cells in 200 µL HeLa medium per well were seeded in an ibidiTreat µ-Slide 8 well and incubated overnight at 37 °C. The next day, the medium was changed to 200 µL CTL medium and 3 x 10^4 to 6 x 10^4 NK cells in 50 µL CTL were added per well right before image acquisition.

For experiments with Z-VAD-FMK, HeLa cells were pre-incubated for 30 min in CTL including the inhibitor, then washed and fresh CTL medium was added.

Live cell imaging was performed in a preheated and humidified (37 °C and 5% CO_2) incubation chamber with the Axio Observer 7 microscope (Zeiss) equipped with a 20×/0.8 Plan-Apochromat objective. HeLa reporter target cell fluorescence was excited by the Colibri 7 LED-module 561 (filter set 64 HE LED) for mCherry and the LED-module 488 (filter set 38 HE LED) for GFP. Bright-field

recording was performed by using the TL LED module. Images were acquired every 2.5 min for 5 h using an Axiocam 506 mono camera.

7.18 Cell lysis

Chemical lysis of cells was performed by incubating the cells in Triton X-100 lysis buffer for 20 min at 4 °C. The samples were then centrifuged at 14800 rpm for 20 min at 4 °C. The supernatant was transferred in a new tube and either stored at -20 °C/-80 °C or further processed for the experiments.

Physical cell lysis was performed by using nitrogen caviation. The pressure vessel was cooled down to 4 °C one day or at least 6 h prior to the experiment. Cells were harvested and washed with PBS. The cells were resuspended in PBS to an end concentration of 5 x 10^6 cells/mL and incubated within the pressure vessel on ice for 5 min at 1000 psi. Samples were collected in 15 mL falcons and further processed for the experiments.

7.19 SDS-PAGE and Western Blot

Cell lysates were mixed with reducing sample buffer (5x RSB) to a final volume of 20 μL and incubated for 5 min at 95 °C. Then the samples were either stored at – 20 °C or cooled down on ice to load them onto a 4 – 12 % NuPage Bis-Tris gel (Invitrogen). The Precision Plus Protein Standard (BioRad) was used as a marker. The samples were separated for 1 h 15 min at 150 V in 1x MOPS buffer.

After separation, the samples were transferred to a polyvinylidene difluoride (PVDF, 0.45 μm) membrane (Millipore), which was pre-activated in methanol and transfer buffer. The transfer was carried out for 1.5 h at 200 mA in transfer buffer. After a successful transfer, unspecific binding sites were blocked by incubating the membrane in blocking buffer for 1 h at RT. Blocking buffer was removed by three washing steps with fresh PBS-T. Then the primary antibody (in 5% BSA in PBS-T + 0.1% Azid) was added to the membrane and incubated overnight at 4 °C. Hereafter, the membrane was washed in PBS-T + NaCl and then incubated with a horseradish peroxidase (HRP)-conjugated secondary antibody in blocking buffer (dilution 1:10000) for 1 h at RT. In a last step the membrane was washed

again with PBS-T and then developed by using the DURA or Sirius kit. Results were visualized by using X-Ray films and a developing machine.

7.20 Data analysis

7.20.1 ^{51}Cr-release assay

The specific lysis of target cells by NK cells triggered in the ^{51}Cr-release experiments was calculated with the following equation:

$$\text{specific lysis} = \frac{(\text{experimental release} - \text{spontanous release})}{(\text{maximum release} - \text{spontanous release})} \cdot 100$$

7.20.2 Microscopy

Data analysis of live cell imaging experiments was performed with the ImageJ software and the RGB (red, green, blue) measure plug-in. GFP and mCherry channels were stacked. Upon a target cell killing was observed for a single NK cell, the RGB signals of the target cells' nucleus, cytosol as well as the background were measured. The measurement was started three frames before the NK cell made contact to its target cell (offset), to capture the "alive" status of the target cell. The measurement of all three points of the target cell was stopped upon the target cell death was observed. The collected values were then processed in a calculation:

$$\text{Rel. fluor. of nucleus} = \frac{\text{MFI (R or G Nucleus)} - \text{MFI(R or G Backgound)}}{\text{MFI (R or G Cytosol)} - \text{MFI(R or G Backgound)}} - \text{Offset}$$

To calculate the relative fluorescence of the target cell nucleus (Rel. fluor. of nucleus) the mean fluorescence intensity (MFI) of the RGB measurement of the background was subtracted from the nucleus and the cytosol for every frame, respectively. This was done for the red and green measurement (R or G). Then the calculation outcome for the nucleus was divided by the cytosol, again for every frame, to normalize the data. In a last step the mean of the three offset measurements was subtracted from the result of the division. The calculated data for all frames was plotted for every single reporter cell.

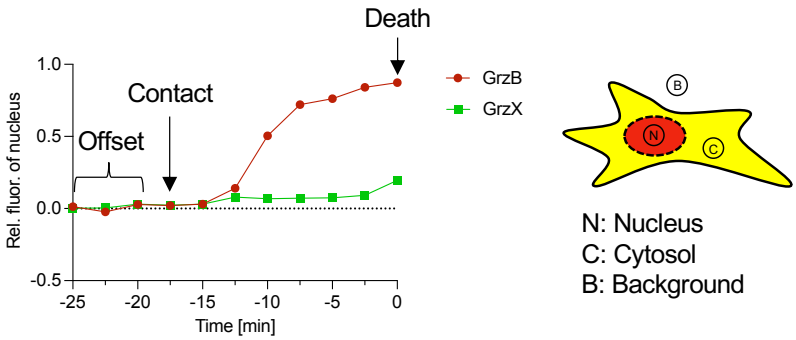

Figure 5: Data analysis of live cell imaging experiments. Granzyme activity within reporter cells is measured three frames before effector to target cell contact (offset) until target cell death was observed (timepoint 0). Each frame was taken every 2.5 minutes. For every frame the RGB signal was measured for the nucleus and the cytosol of the target cell as well as the background.

7.20.3 Flow cytometry

Flow cytometry data was analyzed with FlowJo. The program allows to calculate the mean fluorescence intensity of a measurement as well as the calculation of the percentage of a subpopulation. In all experiments, a negative control was used for background subtraction.

7.20.4 Statistical analysis

Statistical analysis was performed by using GraphPad Pism9 software. One-way ANOVA and unpaired *t* test were performed to calculate possible differences among the data. In most analyses we assume that the data points are normally distributed but we cannot prove that for n ≤ 3. Therefore, the statistically analysis was performed with logarhytmized data points, to correct possible variances. Following this, the Fisher's LSD test was applied. P values lower than P > 0.05 were considered to be not significantly different. Values were considered significantly different when P ≤ 0.0001 (****), P ≤ 0.001 (***), P ≤ 0.01 (**) or P ≤ 0.05 (*) was determined.

8 Results

8.1 Design principles for fluorescent tandem reporters to measure granzyme activity

Being a robust tool for measuring enzyme activity, a variety of fluorescent reporters are commonly used for analyzing both activity and specificity of a wide range of target enzymes *in vivo*. They are thus, in a sense, a modern continuation of classic biochemical approaches to analyze enzyme activity *in vitro* via bait-prey systems. For this study, a system based on subcellular localization of fluorescent proteins was used. An established set of fluorescent reporters was genetically modified for easy exchange of cleavage site, localization domain or fluorescent protein and adopted to a wider range of target enzymes (Prager, 2020). Those targets were granzyme A, B, H, K and M. For simplicity, the fluorescence tandem reporters will be referred to as granzyme reporters in the following text. In order to directly compare each of the granzyme A, H, K or M to GrzB, individual reporters were created, resulting in a set of four (**figure 6**). The reporter's DNA was delivered into HeLa CD48 target cells either by transient transfection or by an amphotropic retrovirus transduction system (methods chapter 7.5 and 7.6). Since this work based mainly on microscopy experiments, the choice of cell line to express the granzyme reporter fell on adherent HeLa cells. These cells are epithelial-like cells growing in monolayers and exhibit an appropriate relation of cytosol to nucleus size, which is advantageous for our requirements in microscopy experiments. Most importantly, these cells are responsive to granzymes, as well as death receptor ligands-initiated pathways (Beaudouin et al., 2013, Albeck et al., 2008, Medema et al., 1997, Pinkoski et al., 2001). For this purpose, we used HeLa cells transfected with the 2B4 (CD244) ligand CD48 to make them more sensitive to killing by NK cells (Hoffmann et al., 2011).

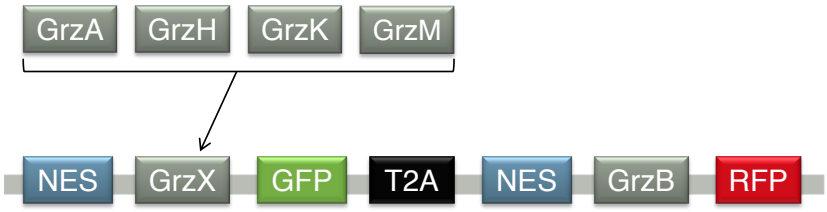

Figure 6: Structure of the fluorescent localization reporters. Each reporter construct consists of two single reporters that are genetically fused by a T2A domain to allow equimolar expression levels. A single reporter consists of a nuclear export signal (localization domain) which is linked to a fluorescent protein by a granzyme cleavage site. Granzyme activity triggered by A, H, K or M can be directly compared to granzyme B activity.

The fluorescence of each reporter was verified by flow cytometry (data not shown). Subcellular localization of the respective reporter was analyzed by fluorescence microscopy (**figure 7**). For reporter expression, double positive ($mCherry^{+}GFP^{+}$) HeLa CD48 cells were sorted two to three times. During this research project, the reporter's expression was reviewed regularly and sufficiently high expression of the reporter by at least 70% of the cells was secured by repeated sorting of the HeLa reporter cells. As previously described, the equimolar expression of the reporters coupled to the fluorophores mCherry and GFP results in a homogeneous distribution of yellowish fluorescence throughout the cytosol (**figure 7**, upper rows). Due to the nuclear export signal (NES), the intact form of the reporter is rapidly and actively exported from the cell's nucleus. In co-incubation experiments with NK cells, the functionality of the reporters was tested and resulted in three different outcomes (**figure 7A - C**). Reporter cleavage resulted either in the diffusion of mCherry (**figure 7A**) or GFP (**figure 7B**) into the nucleus. As there was additionally a third option observed where "yellow" fluorescence was detected within the target cell's nucleus (**figure 7C**), the simultaneous activity of two granzymes was suggested. This resulted in both mCherry and GFP to be present in the nucleus. NK cell contact with target cell was observed in bright field channel (**figure 7**, lower rows) and served as orientation to determine the starting point of the measurement.

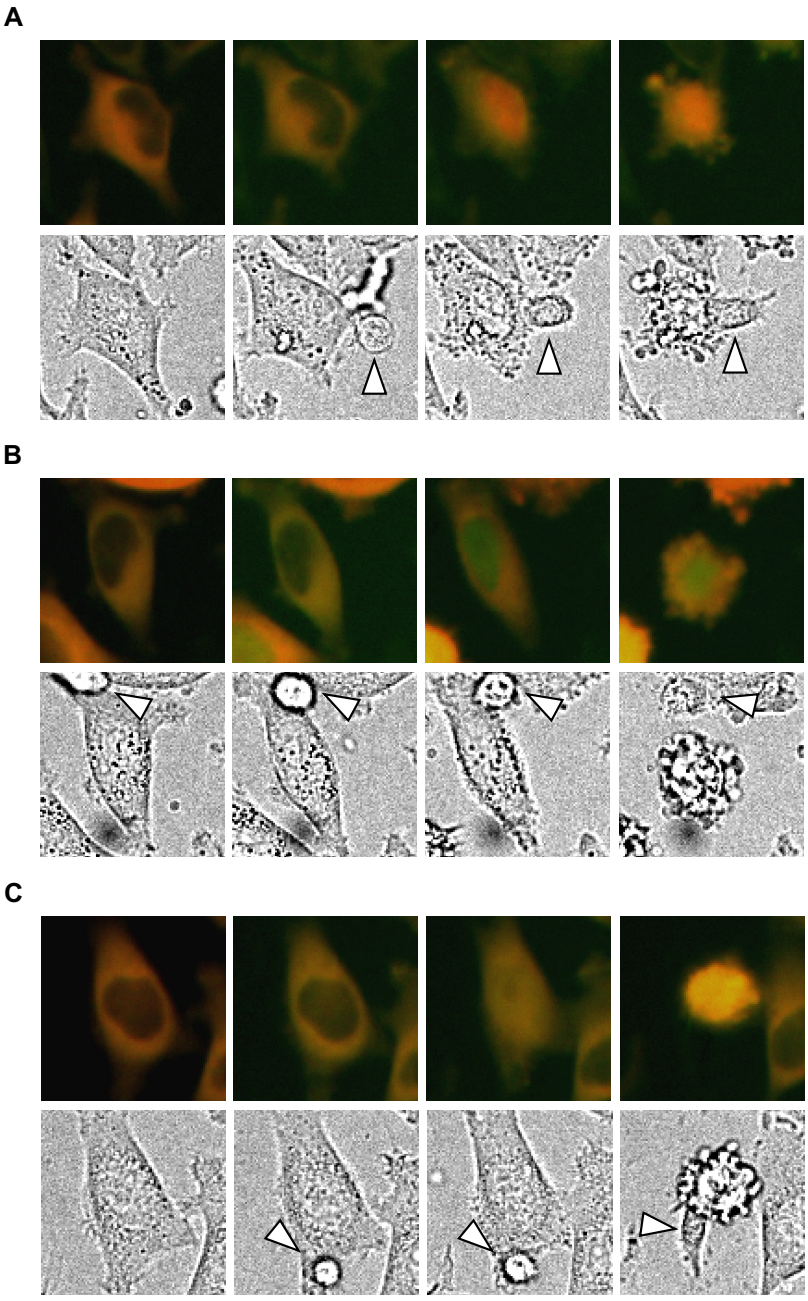

Figure 7: Subcellular localization of the granzyme reporters in HeLa target cells. Target cell killing events triggered by NK cells display the activity of granzymes within the target cells by cleaving the fluorescence localization reporters. Upper rows show an overlay of the red and green fluorescent channel, the lower rows show the respective brightfield image in which the NK cells are marked by a white arrow. Three different cases were observed: **A** GrzB activity leads to the diffusion of mCherry into the nucleus, which results in a red nucleus. **B** GrzX (X = A/H/K/M) activity leads to the diffusion of GFP into the nucleus, which results in a green nucleus. **C** Both cleavage sites were equally cleaved and both mCherry and GFP diffuse into the nucleus, resulting in a yellow nucleus.

8.2 Confirmation of granzyme reporter specificity

Despite being a fluorescent reporter system used in microscopy and flow cytometry experiments, the status of the reporters additionally was analyzed by

Western blot. For this purpose, HeLa reporter cells were incubated with or without recombinant human granzymes. Two different methods were used to deliver these granzymes to the cytosol of target cells. Electroporation of target reporter cells was sufficient to deliver GrzB but not GrzA into the target cells' cytosol (data not shown). Thus, whole cell lysates were produced by using nitrogen cavitation, which successfully resulted in reporter cleavage by both GrzA and GrzB (**figure 8**). The reporters' cleavage status was detected by the primary antibodies anti-mCherry or anti-GFP. Signals were observed between the marker bands of 25 kDa and 37 kDa. The single reporters consist of 294 amino acids (GFP reporter) or 287 amino acids (mCherry reporter) which result in calculated protein weight of 32.5 kDa and 32.1 kDa, respectively. In addition to the uncleaved reporters' signal, an approximately 3 kDa smaller cleavage product is expected upon any granzyme activity, due to the loss of NES. In **figure 8** the results of these experiments are shown. In **figure 8A** all HeLa reporters were incubated with or without 2.5 μg/mL of recombinant human GrzB, **figure 8B** shows the equivalent results after incubation with or without 1 μg/mL GrzA. The working concentration of the respective granzyme was titrated and defined in preliminary experiments (data not shown). For simplification, the reporter description was abbreviated. Thus, as an example the abbreviation GrzA-GrzB stands for the reporter NES-GrzA-GFP-T2A-NES-GrzB-mCherry. Furthermore, two uncleavable reporters were designed as negative controls: NES-GrzA-GFP-T2A-NES-AAAAFGR-mCherry (GrzA-AAAAFGR) which is uncleavable for GrzB and NES-AAAAA-GFP-T2A-NES-GrzB-mCherry (AAAAA-GrzB) which is uncleavable for the other four granzymes.

In **figure 8A** the intact granzyme reporter can be observed in every lane. When incubating the mCherry-coupled GrzB reporter with recombinant GrzB, a cleavage product with lower molecular mass occurs (blot αmCherry). For every HeLa reporter cell line that was incubated with recombinant GrzB, except for GrzK-GrzB and the uncleavable control (GrzA-AAAAFGR), this cleavage product can be recognized. This finding suggests, that the recombinant GrzB was able to cleave the reporter in two parts, which can be interpreted as a partially cleavage of the available reporter expressed in target cells. HeLa reporter cell lines incubated without GrzB show only a single band which is interpreted as intact reporters. In the lower row, the results of GFP detection are shown (blot αGFP).

Here, only one band per condition can be found, concluding that GrzB is not able to cleave the peptide sequences specific for the other granzymes A, H, K or M. The expression of the GrzK-GrzB reporter seems to be lower, compared to the other reporters' signal strength. As mentioned above, the reporter expression was regularly checked by flow cytometry. In case that less than 70% of the reporter cells were double positive ($mCherry^+GFP^+$) the cells were sorted again. Nevertheless, the flow cytometry measurements show heterogeneous reporter expression among the individual cells (data not shown). More than 70% of the GrzK-GrzB reporter cells do express the reporter proteins, but the amount of protein expression per individual cell seems to be lower compared to the other reporter cell lines.

In **figure 8B** the same order of HeLa reporter cell line lysates was analyzed. The samples were incubated together with or without 1 μg/mL GrzA. The single signals of the mCherry staining in the upper row show no obvious reporter cleavage, suggesting that GrzA is not able to cleave them (blot αmCherry). In this blot, the band intensity for the GrzH-GrzB reporter is lower compared to the bands of the other reporters, showing a heterogeneity in the reporter expression, despite the preceding cell sorting. For the GFP reporter in the lower row of **figure 8B**, a smaller cleavage product than the intact reporter was observed for the GrzA-GrzB reporter as well as for the GrzA-AAAAFGR. No cleavage products were observed for the other reporter cell lysates which were incubated with recombinant GrzA. In conclusion, GrzA is not able to cleave the specific sites of other granzymes, as well as the uncleavable reporter AAAAA-GrzB. Again, the bands of the GrzK-GrzB reporter show a lower intensity for the GFP staining, as already observed in **figure 8A**. The same digestion experiments were performed with the recombinant human granzymes H, K and M, but no cleavage products were detected and the results are therefore not shown. An examination of the enzyme activity was only possible for GrzK with a designated activity test. Due to the fact, that two distinct methods were tested to induce reporter cleavage by recombinant granzymes and only one method was successful for GrzA, we cannot exclude that the recombinant granzymes H, K and M were prevented to fulfill their task by yet unknown disturbing factors. Finally, our reporter cells show sufficient expression and correct localization of reporter proteins. GrzA and GrzB

specifically cleave the designated cleavage sites, but not those of the other granzymes.

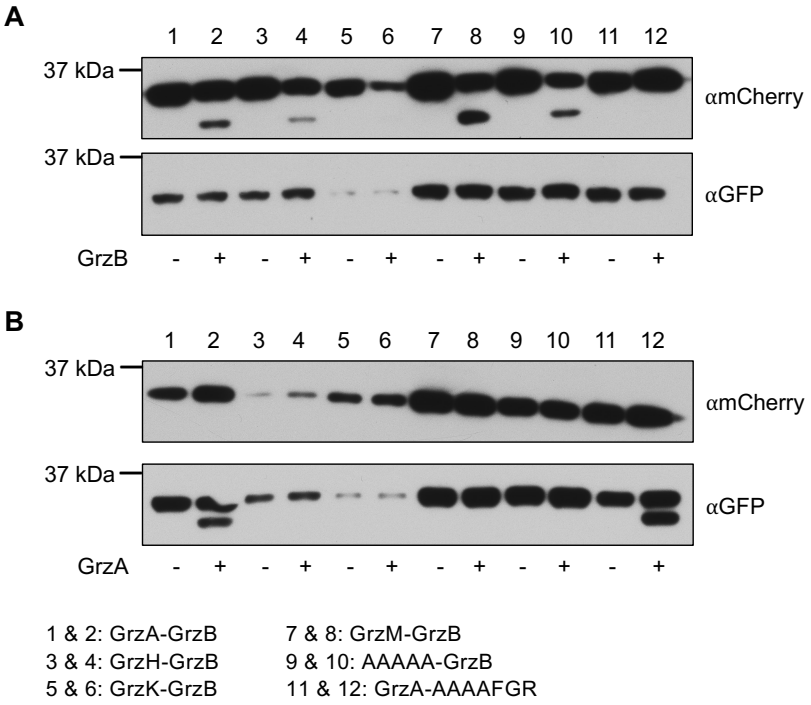

Figure 8: Confirmation of reporter specificity by granzyme digestion and subsequent Western blotting. Western blots of all HeLa reporter cell lines lysed by nitrogen cavitation. Cell lysates were incubated with **A** 2.5 μg/mL human recombinant, active GrzB or **B** 1 μg/mL human recombinant, active GrzA. Reporter cleavage by the individual granzyme was detected by immunostaining with an anti-GFP or anti-mCherry antibody, respectively.

8.3 NK92 cell line characterization

Following the functional verification of the fluorescent reporters we generated NK92 granzyme knockout (KO) cell lines to be able to further prove the reporter specificity, as well as to analyze NK92 killing behavior when granzymes are not available. In brief, granzyme gene-specific guide RNAs were used with CRISPR/Cas9 method to silence the gene of interest. The NK92 WT cell line shows reliable ability to kill cancer cells, including our HeLa cell lines. Once the granzyme KO cell lines were created, we wanted to characterize these cell lines in terms of several cytotoxic proteins, surface markers and functionality.

In **figure 9** the characterization of the different NK92 cell lines' granzyme content is shown. It illustrates the granzyme content of NK92 WT cell line in comparison to the content of the CRISPR/Cas9 generated GrzA KO, GrzB KO and GrzA&B KO cell lines. In **figure 9A**, a representative flow cytometry staining of the

granzyme content of the NK92 WT cell line and their granzyme KO relatives is shown to verify the success of the KOs. Compared to the WT cell line, all NK92 KO cell lines show a clear loss of the respective granzyme, while having no effect on expression levels of GrzH, GrzK and GrzM. These findings are underlined by the quantification in **figure 9B**, where no significant change could be observed among the different cell lines for the latter three granzymes. NK92 WT carries a high load of GrzA and GrzB. The absence of GrzA can be noticed when comparing the expression levels of GrzA KO or GrzA&B KO cell lines to NK92 WT levels. Furthermore, the loss of GrzB can be observed when comparing NK92 WT levels to NK92 GrzB KO or GrzA&B KO cell lines (**figure 9A & B**). Importantly, the KO of GrzA had no influence on GrzB levels and vice versa. In conclusion, it was possible to generate specific NK92 KO cell lines deficient of a subset of granzymes, while leaving the remaining granzyme content unaltered.

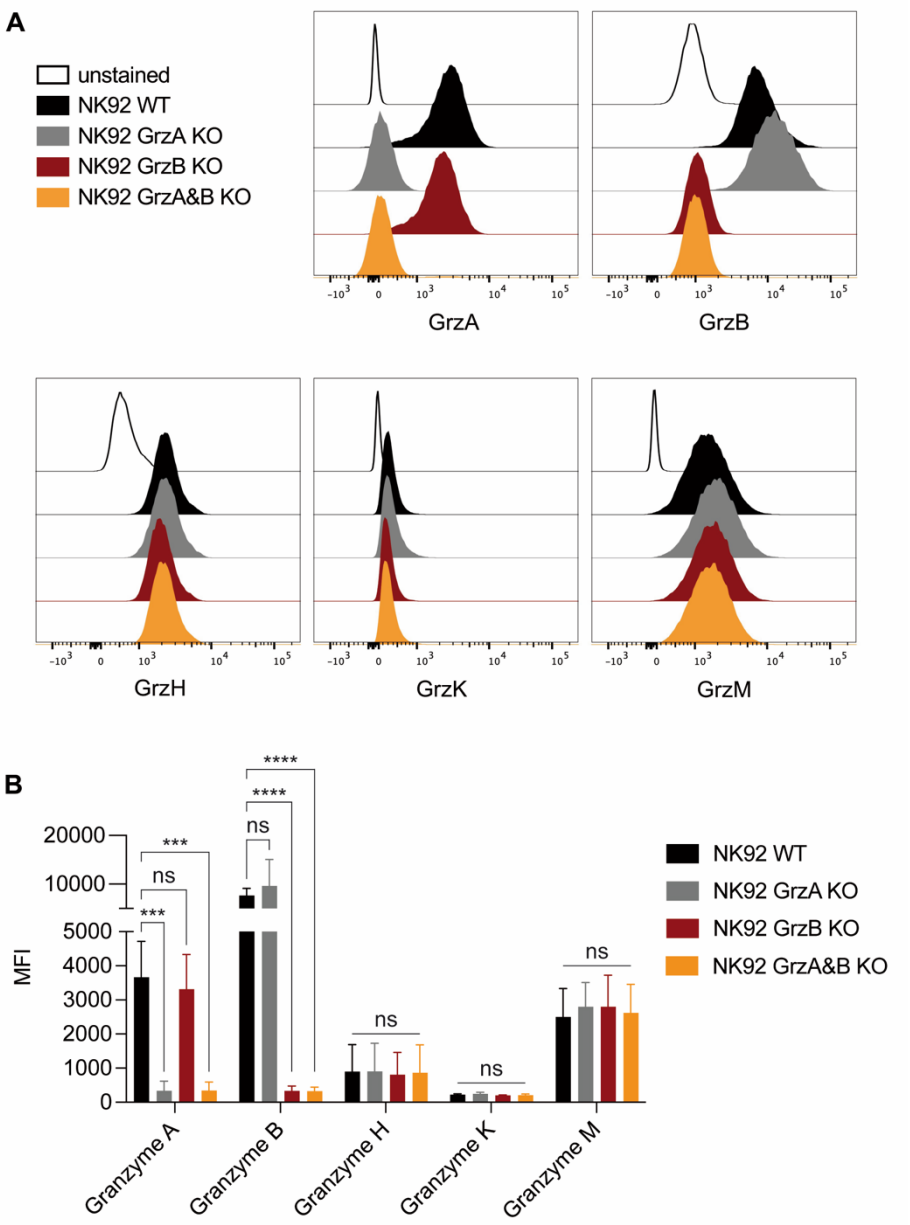

Figure 9: Quantitative analysis of granzyme content of NK92 WT, NK92 GrzA KO, NK92 GrzB KO and NK92 GrzA&B KO cell lines. A Representative flow cytometry measurement of granzyme expression levels in NK92 cell lines and confirmation of GrzA/GrzB/GrzA&B KO in NK92. **B** Quantification of the mean fluorescence intensity (MFI) signal of n = 3 granzyme stainings of the individual NK92 cell line. Statistical analysis was performed with log(Y) data points and one-way ANOVA test. P values: *** $P \leq 0.001$, **** $P \leq 0.0001$.

Additionally, the expression of further effector molecules such as perforin, granulysin and TRAIL of NK92 cell lines was analyzed and compared to activated primary NK cells to assess the potential cytotoxicity. In **figure 10A** representative stainings of perforin and granulysin are shown. Compared to activated NK cells, the expression levels of perforin and granulysin are more homogenous in the NK92 cell lines analyzed, while the activated NK cells exhibit two populations, respectively. Representative stainings of both surface and intracellular levels of TRAIL are shown in **figure 10B**. There is a higher intracellular TRAIL storage found for NK92 cell lines in comparison to activated NK cells, while the surface expression of TRAIL seems to be rather similar. Depicted by the quantification in **figure 10C**, the levels of the respective cytotoxic proteins are comparable between NK92 WT and knockout cell lines. Interestingly, the effector molecules perforin and granulysin are significantly increased in activated primary NK cells in comparison to the NK92 cell lines. In case of intracellular TRAIL expression, the NK92 cell lines exhibit a greater potential of intracellular TRAIL in comparison to primary NK cells. The low TRAIL surface expression levels can be explained by the fact that this molecule is brought to the NK cells' surface only upon stimulation (Johnsen et al., 1999).

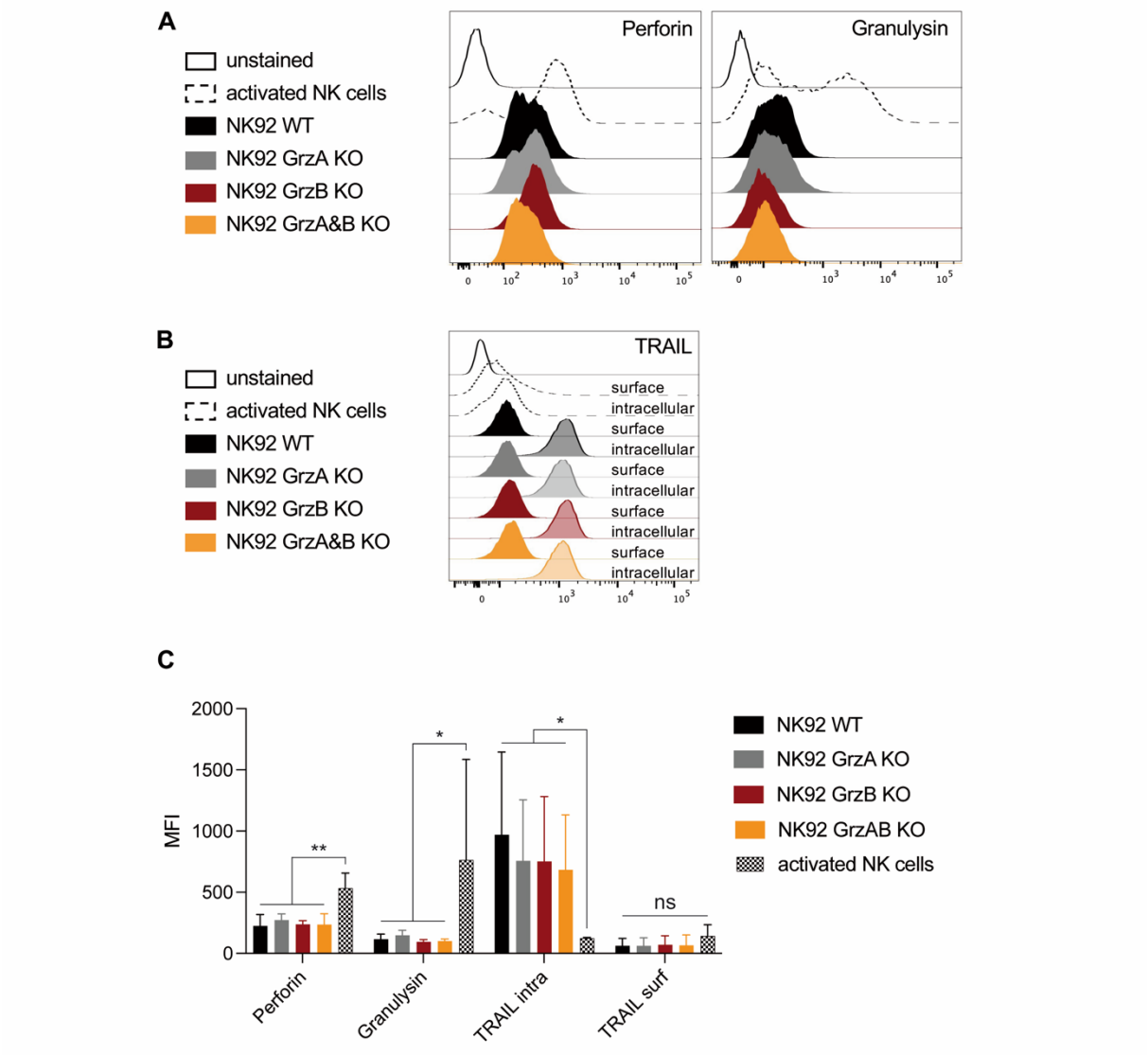

Figure 10: Quantitative analysis of cytotoxically active molecules of NK cells. **A** Representative perforin and granulysin stainings. Unstained NK92 WT (black outline), activated primary NK cells as control (dotted black line), NK92 WT (black), NK92 GrzA KO (gray), NK92 GrzB KO (red) and NK92 GrzA&B KO (orange). **B** Representative TRAIL staining, intracellular (light colors) or surface staining (dark colors). **C** Quantification of the mean fluorescence intensity (MFI) signal of the n = 3 stainings of the individual NK cell lines. Statistical analysis was performed with log(Y) data points and one-way ANOVA test. P values: * $P \leq 0.05$, ** $P \leq 0.01$.

In order to test whether the NK92 cell lines are equally capable to respond to stimuli, eleven NK cell relevant surface molecules were compared between WT and KO cells (**figure 11**). Here the activated primary NK cells served again as positive control. In **figure 11A** representative histograms of the stainings are shown. The surface staining included the following molecules: CD11a, CD16, CD18, CD56, CD94, DNAM-1 (CD226), NKG2D (CD314), NKp30 (CD337), NKp44 (CD336), NKp46 (CD335) and 2B4 (CD244). The comparability of the surface molecules among the NK92 cell lines can already be observed in these graphs, but is more meaningful in the quantification shown in **figure 11B**. The only significant differences among NK92 cell lines were found for the expression of NKp30 and NKp44. These differences were detected for NK92 GrzA KO to GrzB KO and GrzA&B KO respectively, which can be explained by the order in which these KO cell lines were generated. NK92 GrzA&B KO was built from GrzB KO clones and is therefore more related than the independently generated NK92 GrzA KO cell line. Nevertheless, this staining shows that the NK92 cell lines are comparable for adhesion molecules as well as for activating receptors, among others. As already known by the literature, the NK92 cell lines do not express CD16 compared to primary NK cells.

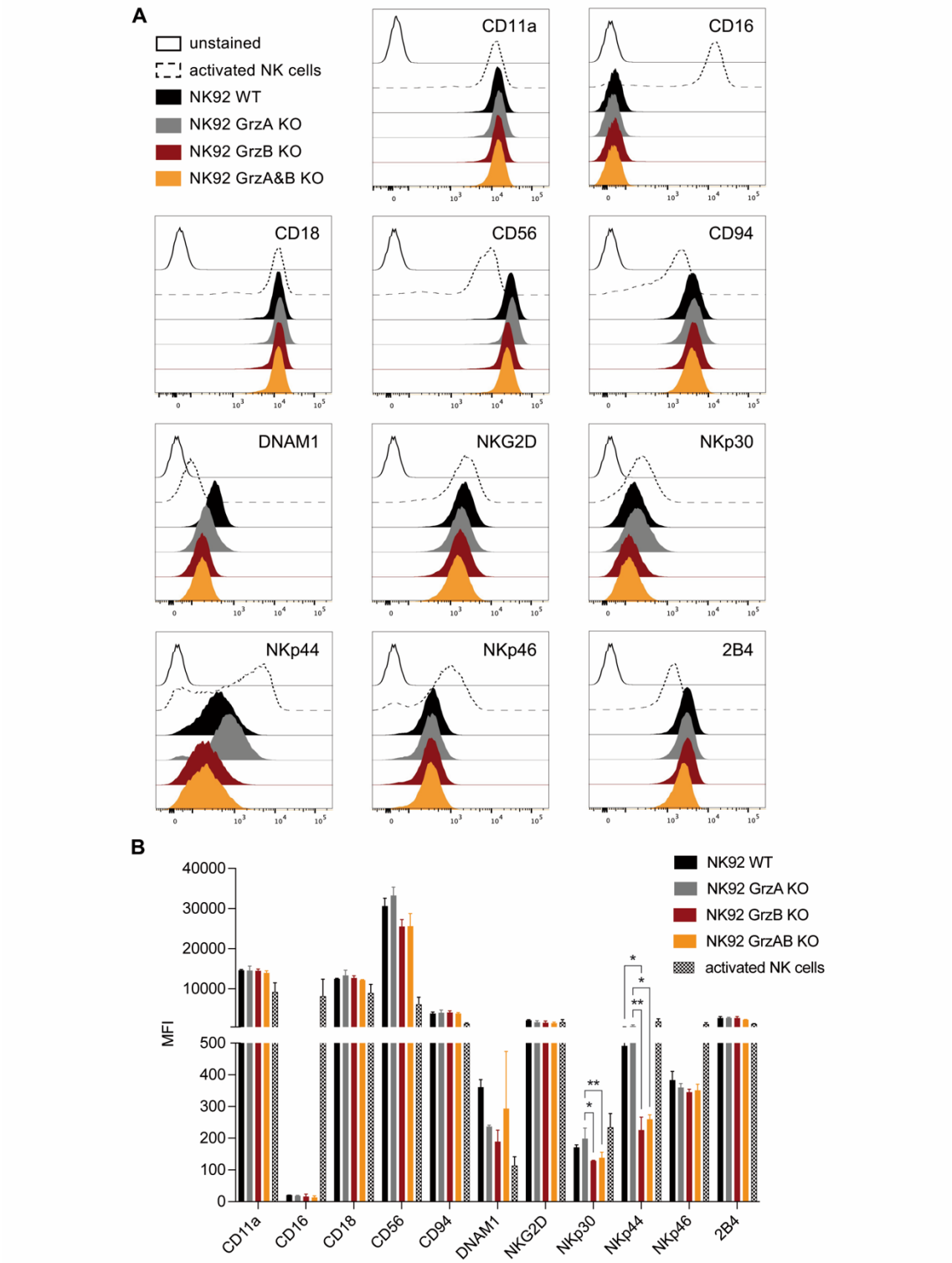

Figure 11: Quantitative analysis of surface expression of relevant NK cell receptors. **A** Representative staining of the surface molecules CD11a, CD16, CD18, CD56, CD94, DNAM1, NKG2D, NKp30, NKp44, NKp46 and 2B4. Unstained NK92 WT (black line), activated primary NK cells as control (dotted black line), NK92 WT (black), NK92 GrzA KO (gray), NK92 GrzB KO (red) and NK92 GrzA&B KO (orange). **B** Quantification of the mean fluorescence intensity (MFI) signal of the n = 3 stainings of the individual NK cell lines. Statistical analysis was performed with log(Y) data points and one-way ANOVA test. P values: * $P \leq 0.05$, ** $P \leq 0.01$.

8.4 Functional NK92 characterization

As a next step, we were interested if the functionality of the NK92 granzyme KO cell lines was still comparable to WT properties. For this purpose, a degranulation assay was performed (**figure 12**) with five different stimulatory conditions: Ionomycin combined with PMA as positive control, and further the cell lines K562, 721.221, HeLa CD48 and Jurkat as target cells. CTL medium served as negative control. Ionomycin and PMA stimulate immune cells in an unspecific manner, while the target cells cause a more specific stimulus. Overall, all NK92 cell lines respond to the stimuli. The strongest degranulation of all NK92 cell lines was triggered by the unspecific stimulation with ionomycin and PMA ($P \leq 0.0001$), followed by the stimulation with HeLa CD48 or 721.221 cells ($P = 0.004 – P \leq 0.0001$). The degranulation upon NK92 contact to K562 resulted in heterogenous results. While K562 triggered significant degranulation of NK92 WT ($P = 0.0354$ - 0.0121), there was no significant difference for NK92 granzyme KOs. Jurkat cells seem to be the weakest stimulus for NK92 degranulation. These results demonstrate the functional comparability of the NK92 KO cell lines with the WT form, especially under nonspecific stimulation. The heterogenous response to different cell lines could be explained by minor phenotypical differences among KO clones. Thus, our results show that the expression of cytotoxic proteins and surface molecules as well as the degranulation of Grz KO cell lines is comparable to that of WT cells. The small differences that were observed can be attributed to the generation process of the clones and cannot be completely avoided.

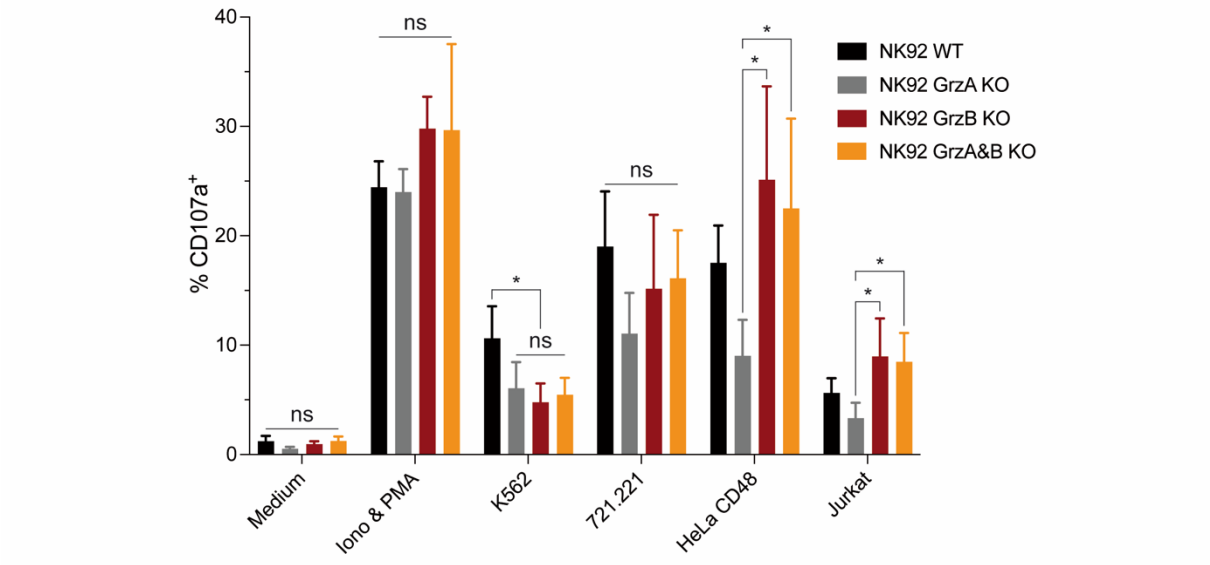

Figure 12: Functional characterization of NK92 cell lines. Degranulation assay of NK92 WT and granzyme KO cell lines incubated for 3 h with different target cell lines in an E:T of 2:1 (K562, 721.221, HeLa CD48 or Jurkat). NK92 in medium served as negative control, while the incubation with Ionomycin (1 μg/mL) and PMA (10 μM) served as positive control (n = 3). Statistical analysis was performed with log(Y) data points and one-way ANOVA test. P values: * P ≤ 0.05.

8.5 NK92 WT mainly use granzyme B in their killing strategy

Once the NK92 cell lines used in this study were characterized, we were interested in their killing strategy. Therefore, we started measurements of reporter cleavage by co-incubating NK92 WT cells with HeLa reporter cells in live cell imaging experiments. In **figure 13** the relative fluorescence of the nucleus (rel. fluor. of nucleus) was monitored over the time of target cell killing triggered by a single NK92 WT cell. The reporter cleavage of 20 to 27 killing events for each granzyme reporter is shown. The measurement of the normalized mean fluorescence intensity starts three frames (one frame = 2.5 minutes) before effector-target cell contact. Upon reporter cleavage within the HeLa target cells, the fluorophores are able to enter the target cell nucleus and the fluorescence intensity is increasing accordingly. The monitoring of the nuclear fluorescence signal was stopped as the target cell died, which was indicated by membrane blebbing and cell shrinkage (timepoint 0). The fluorescence signal depicting GrzB activity (red) within the HeLa reporter cells' nuclei shows a greater increase (**figure 13A**) compared to the signals triggered by all other granzymes tested (green) (**figures 13B – D**). Relative to the signal intensities of the granzymes GrzH, GrzK and GrzM, the activity of GrzA seems to be higher, as shown by higher nuclear fluorescence intensities. These results correlate with our findings

that granzyme A and B are dominantly expressed by NK92 WT cells. As the graphs are summaries of individual killing events, the detailed killing strategies are further illustrated in the **figures 13E - H**. Here, the increase in relative nuclear fluorescence of the respective granzyme reporter is shown in relation to GrzB activity. The relative increase of fluorescent signals triggered by one of the other granzymes A, H, K or M was divided into three categories to provide a more detailed insight into the killing strategies. Fluorescence signals representing 0% to 30% of GrzB signal intensity were considered as "weak", 30% to 70% were categorized as "medium", and signals representing over 70% of the GrzB signal intensity were considered "strong". For the GrzA-GrzB reporter (**figure 13E**) the majority (77%) of all killing events showed a medium GrzA signal compared to the relative nuclear fluorescence of the GrzB reporter. Only a small number of killing events (11%) reached a strong GrzA-related reporter cleavage activity. Roughly the same amount of NK92 WT cells triggered weak GrzA reporter cleavage. For the other granzymes tested, based on the marginally increased fluorescence levels relative to fluorescence increased by GrzB activity, the majority seem to be less important for death induction. For example, only a single killing event was found to trigger a strong GrzH cleavage (**figure 13F**). Three NK92 cells induced a medium GrzH signal and the remaining GrzH-related killing events were weak compared to GrzB-related fluorescence increase. In case of granzyme K or M (**figures 13G or H**), the proteases were not able to induce such high reporter cleavage levels. Compared to GrzB activity, the majority of target cell deaths showed only weak reporter cleavage of GrzK or GrzM reporters. Around 35% of GrzK-related and 25% of GrzM-related reporter activity showed medium fluorescence increase relative to the respective fluorescence increase caused by GrzB activity. This analysis allows a classification of the contribution of the individual granzymes to the final result. Thus, NK92 cells appear to kill their targets predominantly by GrzB supported by GrzA. The contribution of the other granzymes is weak and cannot yet be definitively confirmed by this experiment.

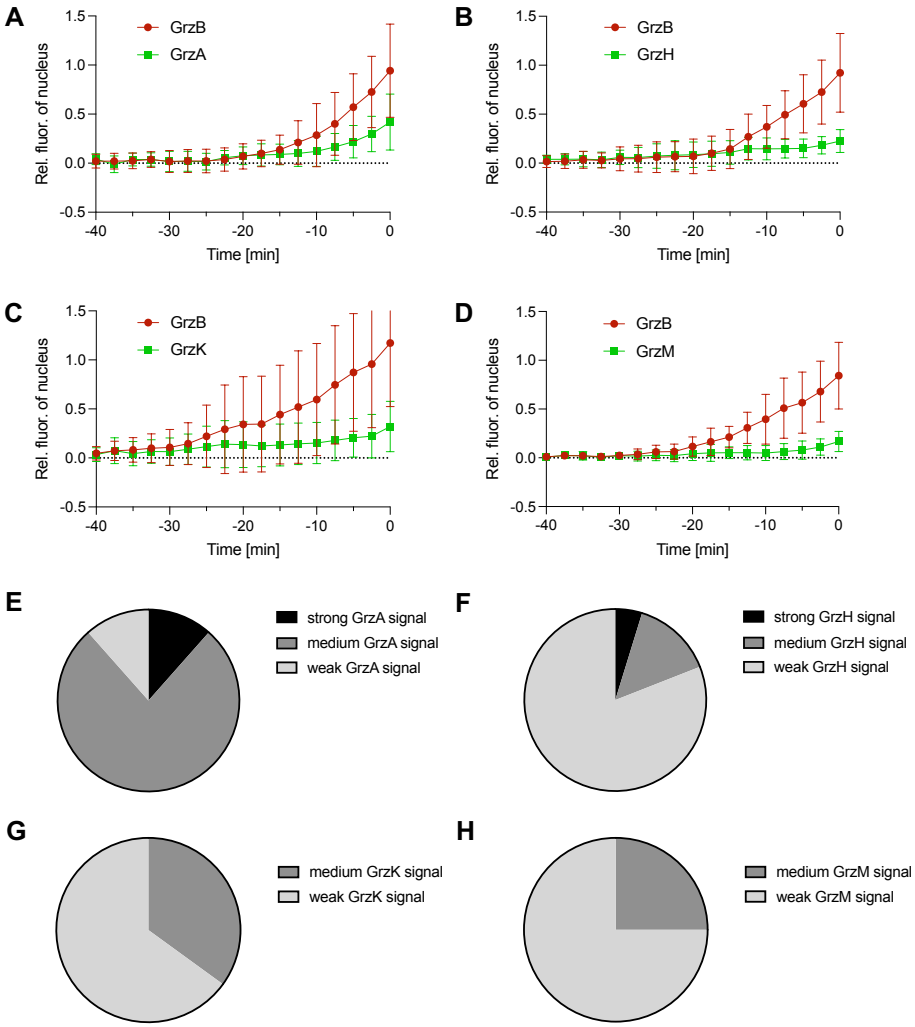

Figure 13: Live cell imaging of NK92 WT cells in co-culture with HeLa CD48 granzyme reporter cells. HeLa cells were seeded one day prior the experiment in an ibidiTreat µ-slide 8 well in CTL medium. The cells were co-cultured in an E:T of 2:1 for 5 h. Three experimental replicates were performed and a total cell number of 20 - 27 was analyzed. **A** NK92 WT cells incubated with HeLa CD48 NES-GrzA-mGFP-T2A-NES-GrzB-mCherry reporter cells, **B** with HeLa CD48 NES-GrzH-mGFP-T2A-NES-GrzB-mCherry reporter cells, **C** with HeLa CD48 NES-GrzK-mGFP-T2A-NES-GrzB-mCherry reporter cells or **D** with HeLa CD48 NES-GrzM-mGFP-T2A-NES-GrzB-mCherry reporter cells. **E – H** Pie charts of the killing strategies of the individual single cell measurements. Strong signal: GrzX (X = A, H, K or M) signal is more or makes up to 70% of GrzB signal intensity, medium signal: GrzX (X = A, H, K or M) makes 30% to 70% of the GrzB signal intensity, weak signal: GrzX (X = A, H, K or M) signal is maximum 30% of the GrzB signal intensity.

8.6 Granzyme B knockout in NK92 cell line reveals granzyme A activity

Following the results of the killing strategy analysis, which revealed GrzB release to be the dominant killing strategy, we wondered if NK92 cells are still able to efficiently kill HeLa reporter cells in the absence of GrzB. For this purpose, the NK92 GrzB KO cell line was co-incubated with HeLa reporter cells under the same conditions as for the experiments with NK92 WT. In **figure 14A and B** the results of live cell imaging of HeLa GrzA-GrzB reporter cells co-incubated with

either NK92 WT (**A**) or NK92 GrzB KO (**B**) are shown for a direct comparison. In contrast to the high GrzB activity of NK92 WT, NK92 GrzB KO cells only showed basal levels of GrzB-related reporter cleavage (**figure 14B**). This underlines the success of GrzB KO in the NK92 cell line and verifies the reporter specificity. For NK92 GrzB KO cells the fluorescence increase caused by cleavage of the GrzA reporter is now clearly dominant. Moreover, the target cell killing triggered via GrzA takes much longer, on average 100 minutes, compared to about 40 minutes when NK92 WT cells were able to use both granzymes (comp. **figures 14A and B**). In **figures 14C – E** NK92 GrzB KO cells were co-cultured with HeLa reporter cells GrzH-GrzB, GrzK-GrzB or GrzM-GrzB, respectively. Here, only basal levels of the reporter cleavage can be observed for all granzymes, concluding that NK92 killing strategy relays mainly on the granzymes A and B. The live cell imaging experiment in which the NK92 A&B KO cell line was incubated with HeLa GrzA-GrzB reporter cells is shown in **figure 14F**. Neither GrzA nor GrzB activity was detected in the reporter cells, supporting the high reporter cleavage specificity for these granzymes. Since the measurement does not indicate any involvement of granzymes, it is assumed that the target cells are killed by death receptor-mediated apoptosis.

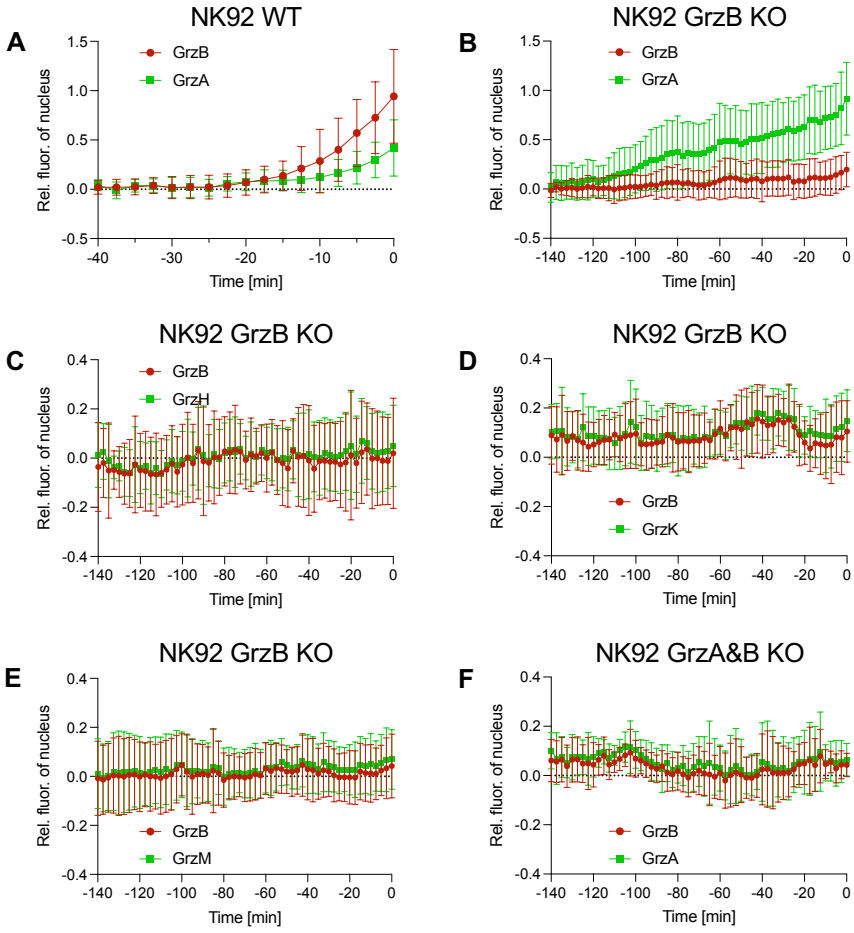

Figure 14: Live cell imaging of NK92 WT or NK92 Grz KO cells in co-culture with HeLa CD48 granzyme reporter cells. HeLa cells were seeded one day prior the experiment in an ibidiTreat µ-slide 8 well in CTL medium. The cells were co-cultured in an E:T of 2:1 for 5 h (n = 3 experimental replicates). **A** NK92 WT cells incubated with HeLa CD48 NES-GrzA-mGFP-T2A-NES-GrzB-mCherry reporter cells (n = 27 cells), **B** NK92 GrzB KO cells incubated with HeLa CD48 NES-GrzA-mGFP-T2A-NES-GrzB-mCherry reporter cells (n = 20 cells), **C – E** NK92 GrzB KO with HeLa CD48 GrzH-GrzB, GrzK-GrzB, or GrzM-GrzB reporter cells, respectively (n = 7 – 19 cells). **F** NK92 GrzA&B KO cells in co-culture with HeLa CD48 NES-GrzA-mGFP-T2A-NES-GrzB-mCherry reporter cells (n = 8 cells).

8.7 Uncleavable reporters reveal background noise of granzyme reporters

The killing strategy analysis depicted in **figure 13** revealed an obvious preference for a GrzB-related cytotoxicity of NK92 WT cells. While the granzymes H, K and M showed an overall low level of involvement, they did show a recurring pattern in the form that the detected fluorescence on average suddenly increased in the last five minutes of the respective experiment. To probe the causes of the rising GFP fluorescence within target cell nuclei in **figure 13** we designed two uncleavable reporters by exchanging specific granzyme cleavage sites by short alanine-based peptide sequences. The NES-AAAAA-GFP-T2A-NES-GrzB-mCherry (AAAAA-GrzB) can still be cleaved by GrzB, but GrzA, H, K and M are

no longer able to do so. NES-GrzA-GFP-T2A-NES-AAAAFGR-mCherry (GrzA-AAAAFGR) is uncleavable for GrzB while still being cleavable for GrzA. **Figure 15A** shows fluorescence measurements within target cell nuclei of the uncleavable reporters upon effector cell contact. In HeLa AAAAA-GrzB reporter cells, GrzB activity can still be detected, but also baseline levels of GFP fluorescence were observed in the nucleus. Following the initial question, signals barely above the baseline can be explained by target cell shrinkage rather than granzyme activity. Target cell death leads to the concentration of proteins within the nucleus due to the shrinkage of the cell membrane, causing an increased signal intensity of both fluorescent reporters shortly before cell death. In addition, the membrane integrity of the nucleus is lost during cell death and the fluorescent reporters can enter the nucleus without the need for NES cleavage. The killing of HeLa GrzA-AAAAFGR reporter cells by NK92 WT leads to baseline fluorescence of nuclear mCherry, including the late sudden rise in measured fluorescence. Here, GrzB is no longer able to cleave the peptide coupled to mCherry and the signal most likely occurs due to target cell shrinkage, too. GrzA activity reaches comparable levels in these fluorescent target cells as in cells with GrzA-GrzB reporters (comp. **figure 13A**). In **figure 15B** the quantification of the granzyme activity compared to the uncleavable reporters, normalized to the GrzB activity, is shown. The last measurements' (timepoint 0) signal intensity of GrzB specific cleavage was set to 100%. The granzyme activity signals measured with the reporters for the granzymes A, H, K and M (**figure 13**), as well as the uncleavable reporters (**figure 15A**) were relatively arranged to the GrzB signal. By arranging the uncleavable reporter signal intensities relative to GrzB, we were able to set a threshold for the granzyme activity measured for A, H, K and M in **figure 13**. It was found that the uncleavable GFP reporter (AAAAA) accounted for 19% and the uncleavable mCherry reporter (AAAAFGR) accounted for 21% of the corresponding GrzB signal. Thus, only GrzA activity is clearly above the GFP background noise of the AAAAA reporter whereas the mean granzyme H, K and M activity is only slightly above the threshold. This underlines our initial assumption that NK92 kill their target cells primarily via GrzB and GrzA.

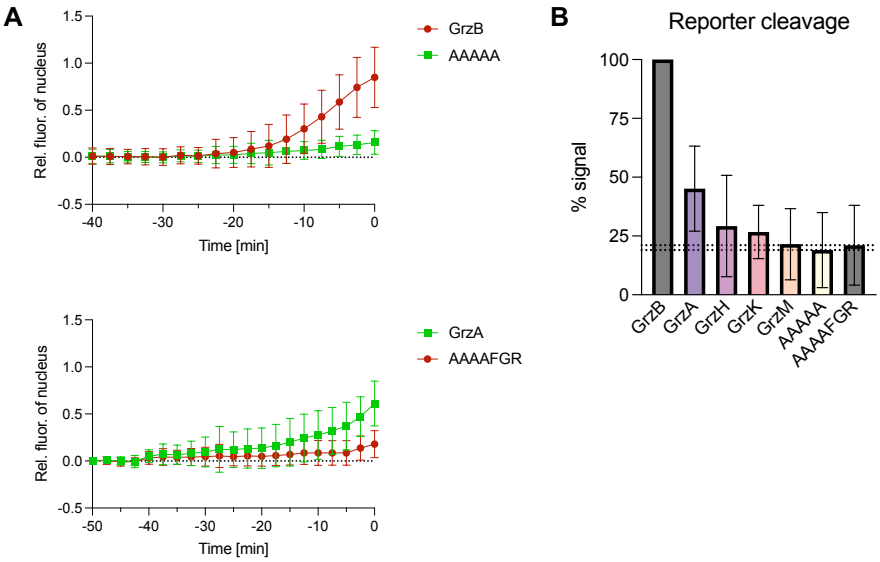

Figure 15: Analysis of fluorescence reporter background noise. Live cell imaging of NK92 WT co-cultured (E:T 2:1) with HeLa CD48 uncleavable reporter cells. Four experimental replicates were performed and a total number of 44 - 50 cells was analyzed. **A** Relative fluorescence of the nucleus of HeLa CD48 NES-AAAAA-mGFP-T2A-NES-GrzB-mCherry reporter cells (top) or of HeLa CD48 NES-GrzA-mGFP-T2A-NES-AAAFGR-mCherry reporter cells (bottom). **B** Normalization of endpoint measurements (timepoint 0) of the fluorescent signal upon reporter cleavage for all granzyme and uncleavable reporters in percentage, relative to the signal of GrzB.

8.8 Loss of granzymes reduces cytotoxicity of NK92 knockout cells

Since the live cell imaging investigates the killing strategy of NK92 cells at single cell level, we wanted to examine whether the granzyme knockouts influence the bulk cytotoxicity. Therefore, we performed xCELLigence experiments, which is an impedance-based measurement. The cell index reflects the cell confluency of adherend target cells (HeLa) on the e-plates. A high HeLa cell confluency interrupts the electron flow, which results in a higher cell index. Decrease in the cell index indicates a better electron flow due to less target cell confluency. For the experiment, we co-incubated HeLa CD48 cells in an effector to target ratio of 2:1 with NK92 WT cells or the granzyme KO cell lines (**figure 16**). Additionally, the HeLa CD48 cells were pre-incubated for 30 minutes with either DMSO (**figure 16A**) or 10 μM of the pan-caspase inhibitor Z-VAD-FMK (zVAD) (**figure 16B**). Z-VAD-FMK is an inhibitor that irreversibly binds to the catalytic site of caspase proteases and is therefore able to block death receptor signaling. Inhibition of the death receptor-induced apoptosis pathway reveals the contribution of granzymes to target cell death. On the left side of **figure 16A**, a representative graph of the xCELLigence killing assay is shown. Without any

influence of effector cells, HeLa cells (+ symbols) are able to grow over the entire measuring time of 24 hours. In a parallel set, NK92 WT cells were added to the HeLa cell culture after 6 hours (black line). Here, the cell index rapidly decreased and reached a plateau just above baseline after around 6 additional hours of incubation. The conclusion is that the addition of NK92 WT cells leads to the detachment of HeLa cells by cell death. When incubated with the respective NK92 granzyme KO cell lines (gray, red & orange lines), the HeLa cell indices decreased less and remained stable about halfway within the range of HeLa only and NK92 WT conditions. This suggests that these knockout cell lines are still able to kill, but to a lesser extent than NK92 WT cells. Furthermore, there are only slight differences in killing efficiency among NK92 granzyme KOs. On the right-hand side of **figure 16A**, the area under the curve (AUC) of all five performed experiments was calculated. In comparison to uninfluenced HeLa growth, significant reduction of the HeLa cell confluency was observed for all added effector cell lines, of which NK92 WT induced the highest cytotoxicity ($P = 0.0007 – P < 0.0001$).

In **figure 16B** HeLa target cells were pre-incubated with 10 μM zVAD. The representative graph on the left side displays HeLa cell indices with and without the influence of the different NK92 effector cell lines. While the growth of HeLa cells without any effector cell influence (+ symbols) seems to be unaltered under zVAD conditions compared to DMSO control (comp. **figure 16A**), the indices of HeLa cells that were co-incubated with NK92 effector cells showed increased values, compared to cells without zVAD pre-treatment. As the incubation with NK92 WT and GrzA KO still leads to target cell killing compared to medium control (+ symbols), the cytotoxic effect of NK92 GrzB KO and GrzA&B KO on target cells is suppressed under zVAD influence. These observations are reflected in the quantification on the right-hand side. The HeLa cell index is still significantly reduced in the presence of NK92 WT and GrzA KO, although not to the same extent as in the DMSO solvent control condition (**figure 16A**). Compared to the medium control, no killing by NK92 GrzB KO and GrzA&B KO can be observed. Increased HeLa cell indices of the NK92 GrzB KO and GrzA&B KO conditions in the representative figure on the left-hand side could have a simple cause, where the NK92 cells contribute to the electron flow resistance by attaching to their target cells but can no longer kill them.

These results show that the loss of granzymes has a strong impact on the cytotoxicity of NK92, however this loss seems to be compensated by death receptors. If the cells are denied this alternative mechanism by inhibiting the death receptors, it becomes clear that the loss of GrzB is more severe for their cytotoxicity than that of GrzA.

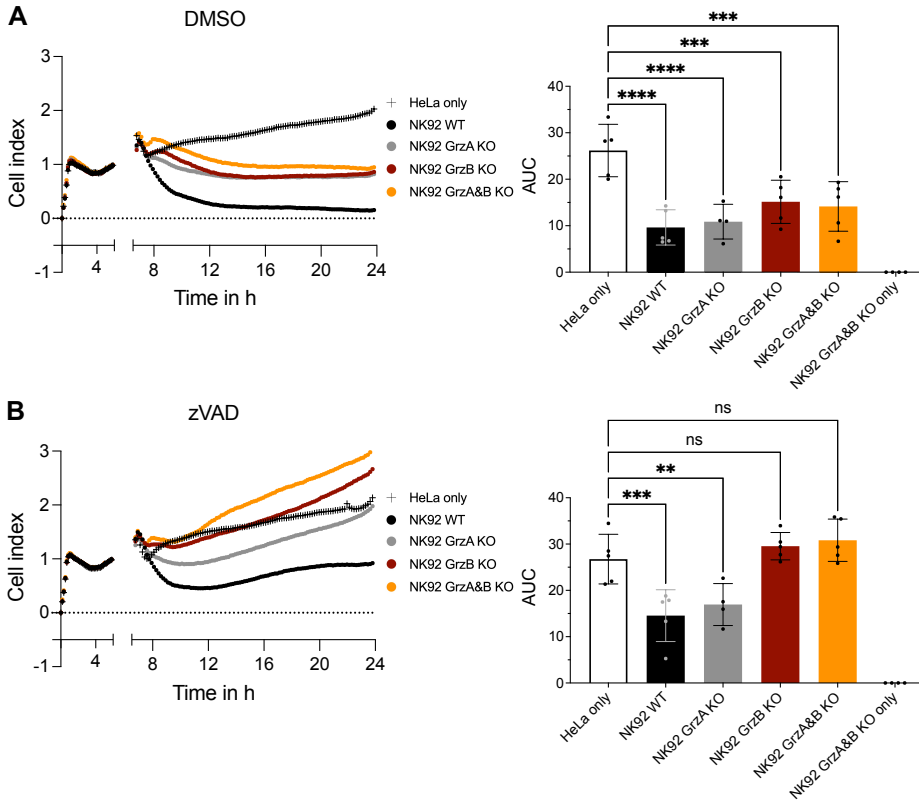

Figure 16: Bulk NK92 cytotoxicity experiments (xCELLigence) of NK92 WT and granzyme knockout cell lines. HeLa cells were seeded in e-plates and incubated for 6 h. After target cell adhesion, the effector cells were added and co-incubated for another 18 h (E:T 2:1). On the left-hand side representative graphs show target cell growth in co-culture with the individual NK92 effector cell line or HeLa CD48 alone. Quantification of all performed experiments (n = 5 - 6) was executed by calculating the area under the curve (AUC) (right-hand side). **B** HeLa cells were pre-incubated with pan-caspase inhibitor Z-VAD-FMK (10 μM) for 30 minutes, DMSO served as a negative control in **A**. Z-VAD-FMK concentration was maintained throughout incubation time. Statistical analysis was performed with log(Y) data points and one-way ANOVA test. P values: ** P ≤ 0.01, *** P ≤ 0.001, **** P ≤ 0.0001.

8.9 Jurkat target cells exhibit distinct sensitivity to NK92 WT and granzyme KO cell lines

Bulk cytotoxicity assays performed with the xCELLigence method allow real-time measurements but are more or less limited to adherent cells. Since the granzyme substrate expression could be various for distinct target cells, we were interested if we can detect differential cytotoxic capacity of our NK92 cell lines against

specific target cells. Thus, we used among HeLa CD48 cells, the lymphoma cell lines Jurkat, which is a $CD4^+$ T cell line, and 721.221, which is a B cell line. We performed a chromium-release assay (**figure 17**) in which the NK92 cell lines were co-cultured for 4 h with these target cell lines. The target cells were pre-incubated with either zVAD (HeLa & 721.221 with 10 μM, Jurkat with 20 μM) or DMSO as solvent control. Furthermore, various effector to target cell ratios were implemented. In **figure 17A** representative graphs of the specific lysis of the different target cells by the NK92 cell lines are shown. Herein, the specific lysis of HeLa CD48 and 721.221 cells caused by the NK92 cell lines shows to be effector to target cell dependent, while the specific lysis of Jurkat cells decreases less at the different ratios. Moreover, the efficiency of NK92 cells to kill target cells is reduced for granzyme knockout cell lines. This is true for HeLa CD48 and 721.221, but not for Jurkat cells. To get a better overview, the area under the curve (AUC) was calculated for each condition (**figure 17B**). For both HeLa and 721.221 cells a similar cytotoxicity pattern can be observed. The highest cytotoxicity is caused by NK92 WT in the DMSO control condition, followed by NK92 GrzA KO, NK92 GrzB KO and NK92 GrzA&B KO. The additional death receptor inhibition via zVAD leads to a further reduction of the killing capacity by the individual NK92 cell lines. For NK92 GrzA&B KO zVAD conditions, no significant lysis of the target cells HeLa and 721.221 is observed. However, there is an entirely different picture for Jurkat target cells in contrast to the other target cell lines. Death receptor inhibition by zVAD has a recognizable influence on cytotoxicity for all NK92 cell lines compared to DMSO control. Nevertheless, the NK92 GrzA&B KO cell line in co-incubation with HeLa or 721.221 is not able to kill the target cells under the influence of zVAD, while high cytotoxicity is still achieved by these effector cells under similar conditions in co-culture with Jurkat cells. The fact that no significant reduction in cytotoxicity can be calculated for the killing of Jurkat cells supports this observation. Therefore, phenotypic differences of the target cells could lead to these contrasting outcomes.

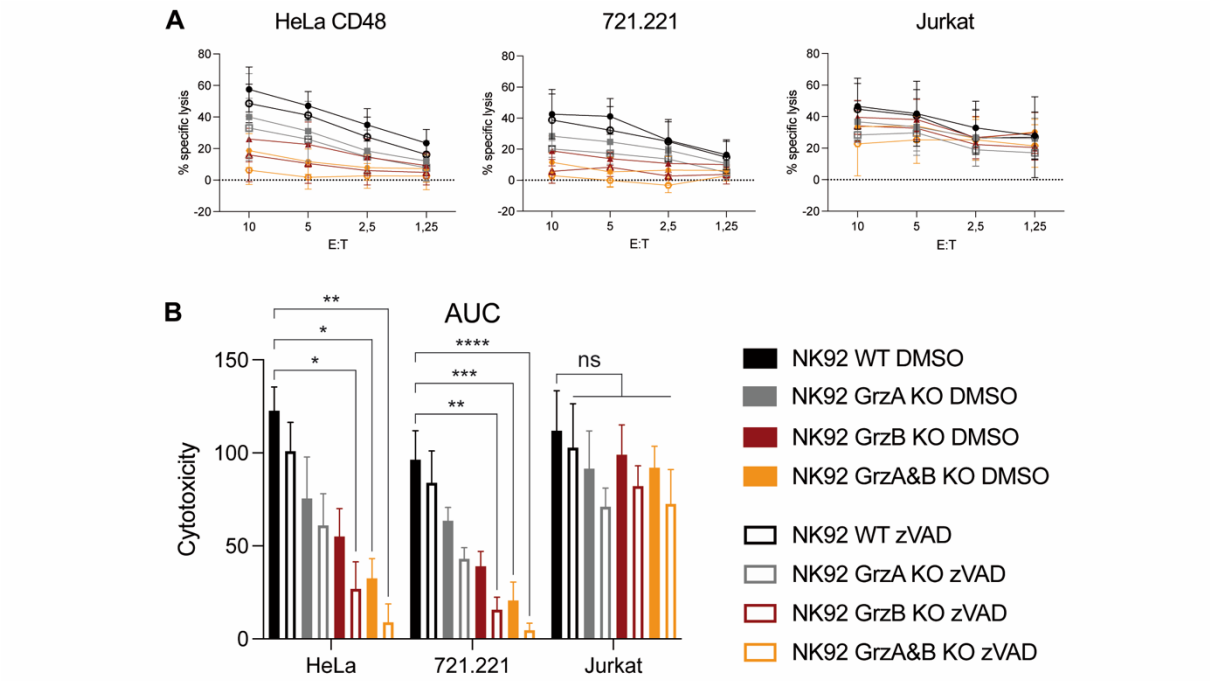

Figure 17: Chromium-release assay of NK92 cell lines (WT, GrzA KO, GrzB KO, GrzA&B KO) in co-incubation with different target cell lines (HeLa CD48, 721.221, Jurkat). 3 individual replicates with E:T of 10:1, 5:1, 2.5:1 and 1.25:1. In **A** representative graphs of the specific lysis are shown. For better comparison the calculated area under the curve (AUC) is shown in **B**. Full bars show the total AUC of specific lysis with DMSO as a solvent control, empty bars represent the target cell killing with additional 30 minutes pre-incubation with the pan-caspase inhibitor Z-VAD-FMK (10 μM, or 20 μM for Jurkat cells). Statistical analysis was performed with log(Y) data points and one-way ANOVA test. P values: * P ≤ 0.05, ** P ≤ 0.01, *** P ≤ 0.001, **** P ≤ 0.0001.

8.10 Phenotyping of different target cell lines

To clarify if the variable killing capacity of NK92 cell lines, especially NK92 GrzA&B KO, is due to different sensitivity of death receptors of Jurkat and other target cell lines, we aimed to investigate the expression of the death receptors on these cell lines. The death receptors DR4 and DR5 engaging with TRAIL, as well as CD95 (Fas) coupling to CD95L (FasL), are stained intracellularly and on the target cell surface. **Figure 18A** shows representative graphs of surface and intracellular death receptor stainings by flow cytometry measurement. All target cell stainings, except for DR4 surface expression on Jurkat cells, are clearly positive compared to the unstained control. The quantification in **figure 18B** reveals that, additionally to DR4 surface expression, DR5 surface and intracellular expression is significantly decreased in Jurkat cells in comparison to the other target cell lines. Only intracellular DR4 levels are equivalent for all target cells. Significant differences are found between 721.221 and HeLa or Jurkat cells

for both CD95 on the surface of the target cells and intracellular levels. Contrary to our expectations, no common features can be found for 721.221 and HeLa cells that distinguish them equally from Jurkat cells. These results suggest that the ability of NK92 cells to kill the target cell lines is not due to death receptor expression. Therefore, we predict that another granzyme or protease is responsible for killing the Jurkat cell line, which has no effect on the other target cells HeLa or 721.221.

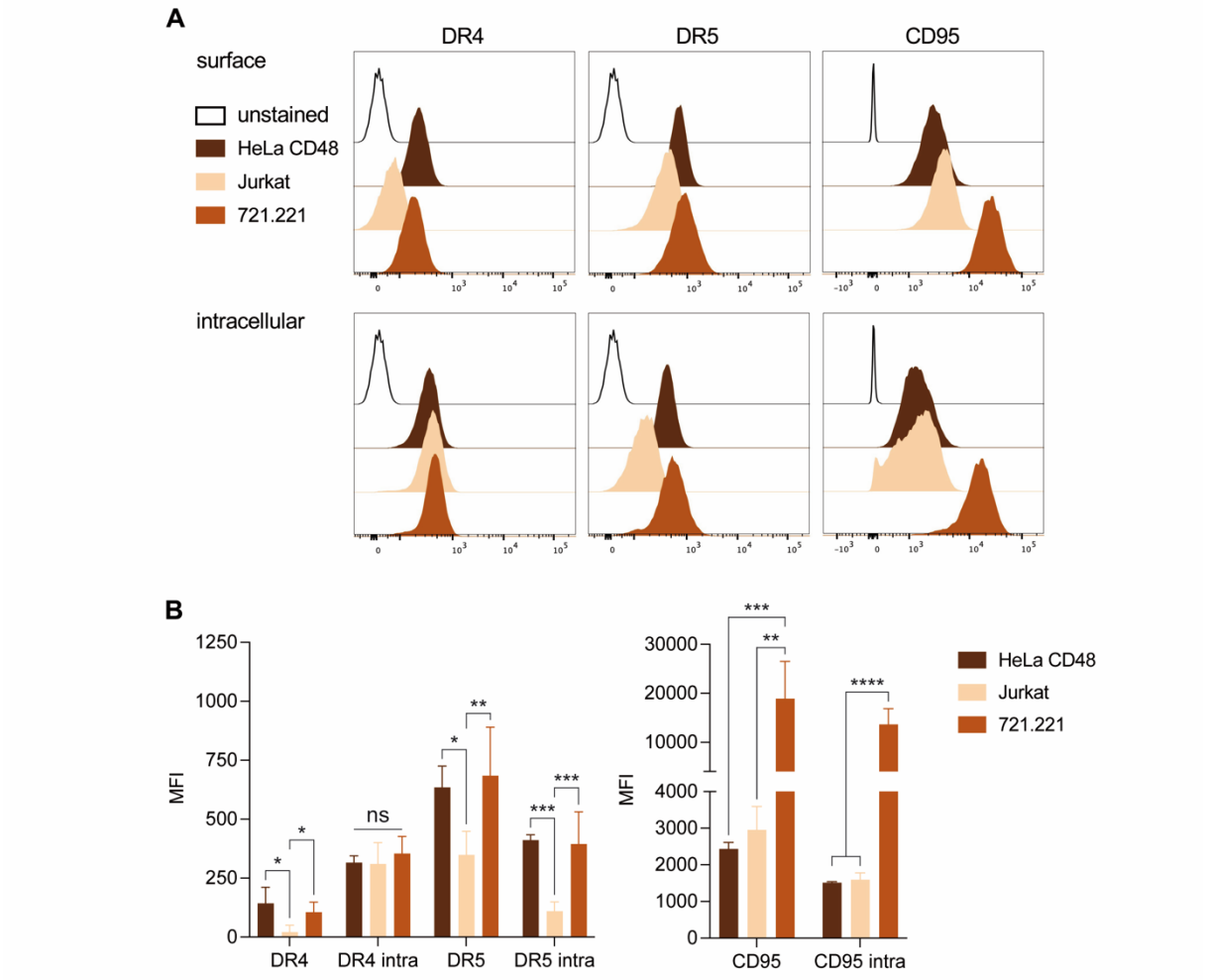

Figure 18: Death receptor staining of several target cell lines. A Representative graphs of stainings for the death receptors DR4, DR5 or CD95 on the surface or intracellular of the target cell lines HeLa CD48, Jurkat and 721.221. **B** Quantification of the mean fluorescent intensity of the individual stainings (n = 3). Statistical analysis was performed with log(Y) data points and one-way ANOVA test. P values: * P ≤ 0.05, ** P ≤ 0.01, *** P ≤ 0.001, **** P ≤ 0.0001.

8.11 High NK92 cytotoxicity towards Jurkat cells is induced by proteases

Since NK92 GrzA&B KO cells are still able to efficiently kill Jurkat cells under the influence of death receptor inhibition by zVAD, we wanted to examine whether

remaining granzymes could play a role. Therefore, another chromium release assay was performed with the results shown in **figure 19A and B**. Again, Jurkat target cells were incubated with NK92 WT, GrzB KO or GrzA&B KO cells. The target cells were pre-incubated with zVAD (20 μM) or DMSO, while NK92 cells were pre-incubated with 3,4-Dichloroisocoumarin (DCI, 25 μM) or DMSO as solvent control. DCI is a potent and irreversible inhibitor of serine proteases. In **figure 19A** a representative graph of the specific lysis of Jurkat cells by the different NK92 cell lines and inhibitor conditions is pictured. As already described in **figure 17A** the killing capacity of NK92 granzyme KO cell lines is only slightly decreased compared to NK92 WT in the DMSO control condition (black lines). The inhibition of death receptor signaling by zVAD already reduces the killing efficiency of NK92 cells, but is surpassed by the inhibition of serine proteases or a combination of both inhibitors. For better comparability, the quantification of the specific lysis is depicted as area under the curve (AUC) in **figure 19B**. The cytotoxicity among NK92 cell lines is comparable (ns) for DMSO control, DCI and DCI plus zVAD conditions. The incubation with DCI or both inhibitors significantly and equally reduces the cytotoxicity for all effector cell lines. Inhibiting only the granzyme activity by DCI, there is comparable death receptor cytotoxicity among the effector cell lines. Inhibition of the death receptor by zVAD reveals the effects of granzyme loss of the NK92 granzyme KO cells on their cytotoxicity compared to NK92 WT. Additionally, this shows the greater importance of GrzB in Jurkat cell killing compared to GrzA, since the cytotoxicity of NK92 GrzB KO and GrzA&B KO is similar. When treaded with both inhibitors, almost no cytotoxicity can be detected for all NK92 cell lines, supporting the hypothesis that remaining serine proteases of NK92 GrzA&B KO are still able to induce Jurkat cell death. In addition, death of Jurkat by the cytotoxic proteins perforin and granulysin can be excluded, since DCI is not able to inhibit their functionality.

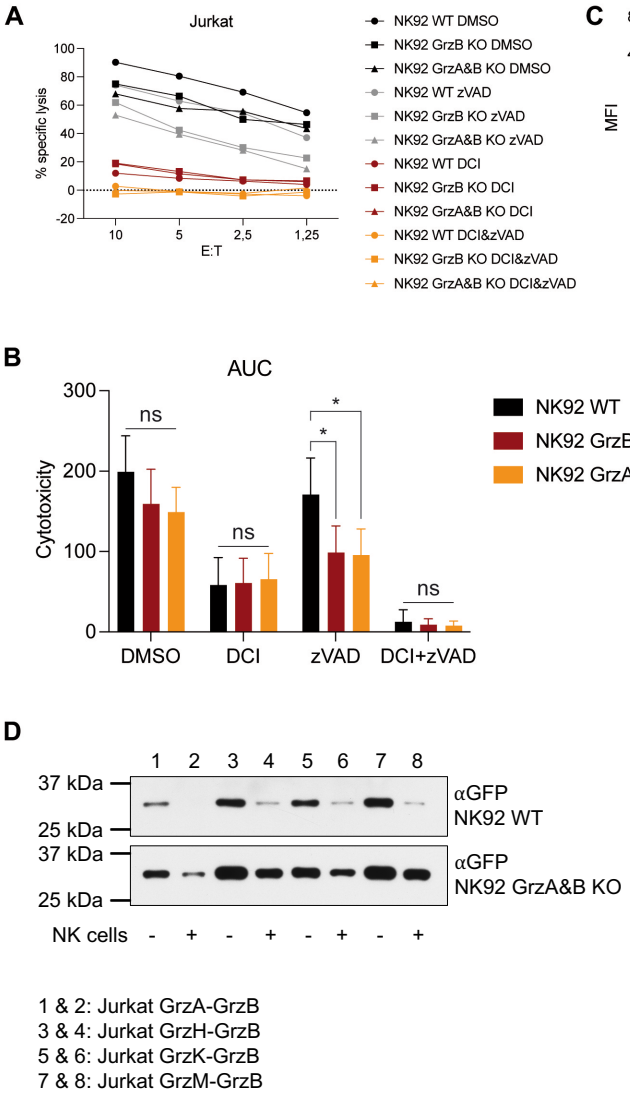

Figure 19: Jurkat cells are more sensitive to protease induced cytotoxicity. **A & B** Chromium-release assay of NK92 cells (WT, GrzB KO, GrzA&B KO) in co-incubation with Jurkat cells (n = 3) with E:T of 10:1, 5:1, 2.5:1 and 1.25:1. In **A** representative graphs of the specific lysis are shown. For better comparison the calculated area under the curve (AUC) is shown in **B**. DMSO serves as a solvent control, target cells were 30 min pre-incubated with the pan caspase inhibitor Z-VAD-FMK (20 μM), while the effector cells were pre-incubated with DMSO or 3,4-Dichloroisocoumarin (DCI, 25 μM). **C** Flow cytometry staining of important cytotoxic proteins expressed by Jurkat cells. **D** Western blot of Jurkat reporter cells incubated with or without NK92 WT cells (upper row) or NK92 GrzA&B KO cells (lower row). The reporter cleavage is shown by the detection with an anti-GFP antibody. Statistical analysis was performed with log(Y) data points and one-way ANOVA test. P values: * P ≤ 0.05.

Another hypothesis is that Jurkat cells inadvertently cause their own death. Jurkat cells are aberrant $CD4^+$ T cells and might express some cytotoxic proteins that induce cell death upon the influence of e.g. NK92 perforin on their membrane. To prove this theory, we stained granzymes as well as the cytotoxic proteins perforin and granulysin within Jurkat cells. In **figure 19C** the result of this staining is displayed. At first glance, granzymes and granulysin are expressed by Jurkat cells in negligible amounts. Perforin expression is comparable to expression

levels of NK cells (comp. **figure 10**). As discussed earlier, the cytotoxicity of NK92 cells towards Jurkat cells is reduced by inhibition with DCI and zVAD and is therefore independent of the influence of perforin. We thus conclude that Jurkat cells do not harm themselves in these experiments.

To find out if any of the other granzymes H, K, or M was responsible for killing the Jurkat cells, we generated Jurkat reporter cells for all granzymes as well. Microscopy of Jurkat reporter cells turned out to be impossible. In these cells, the ratio of nucleus to cytosol is quite different from that in adherent HeLa cells, which is why the measurement of the cytosol was therefore not possible. Hence, we wanted to visualize the reporter cleavage by using Western blotting. **Figure 19D** shows the results of the incubation of Jurkat reporter cells with either NK92 WT cells or the A&B KO cell line. The activity of the granzyme A, H, K or M was monitored by anti-GFP detection. In the upper panel, the Jurkat reporter cells were incubated together with NK92 WT cells. The samples were loaded as described in the figure. Each sample contained the same amount of Jurkat target cells. The signals in lanes with effector cell incubation show a clear reduction in their intensity, compared to signals in lanes without NK92 WT influence. Unlike the cleavage of the GFP reporters in **figure 8**, no cleavage product can be observed for the GFP reporters in this Western blot (**figure 19D**). In the lower panel, Jurkat reporter cells were incubated with the NK92 GrzA&B KO cell line. Here, a slight reduction of signal intensity can be observed when reporter cells were incubated with effector cells, but the effect is less prominent than in the upper panel of the figure. Jurkat GrzA reporter cells incubated with NK92 GrzA&B KO cells showed a reduction in signal intensity compared to the signal from untreated reporter cells, but GrzA activity should not be possible in this case. Therefore, it cannot be clearly determined whether the reporters were actually cleaved. It can be assumed that the mere addition of NK92 cells seems to have an influence on the readout of the Western blot. Alternatively, another method must be found to demonstrate the possible activity of the granzymes or another (unknown) protease and thus the responsibility for the death of the Jurkat cells. These results indicate that NK92 cytotoxicity may depend not only on the phenotype of the effector cell itself, but also on the phenotype of the target cell.

8.12 Granzyme content in primary resting effector cells

Consistent with our results with NK92 cell lines, we were interested in granzyme expression and possible differential cytotoxic effects of primary NK cells. In **figure 20** the granzyme content of primary resting NK cells is shown in representative flow cytometry plots. To determine both the expression levels of the granzymes and possible correlations between them, the granzymes A, H, K and M (y-axis) were plotted against GrzB on the x-axis (**figure 20A**). Resting NK cells seem to express all granzymes, although not to the same extend. Here, a positive correlation of granzyme A, H and M with GrzB can be noticed, but it seems to be stronger for GrzH and GrzM compared to GrzA. For granzyme K and B, no correlation can be recognized. In **figure 20B** a positive correlation of granzyme expression levels was found for the granzymes A and H (y-axis) to granzyme M (x-axis), respectively. This suggests that NK cells with higher combined granzyme expression levels might fulfill different tasks than NK cells with low granzyme expression levels.

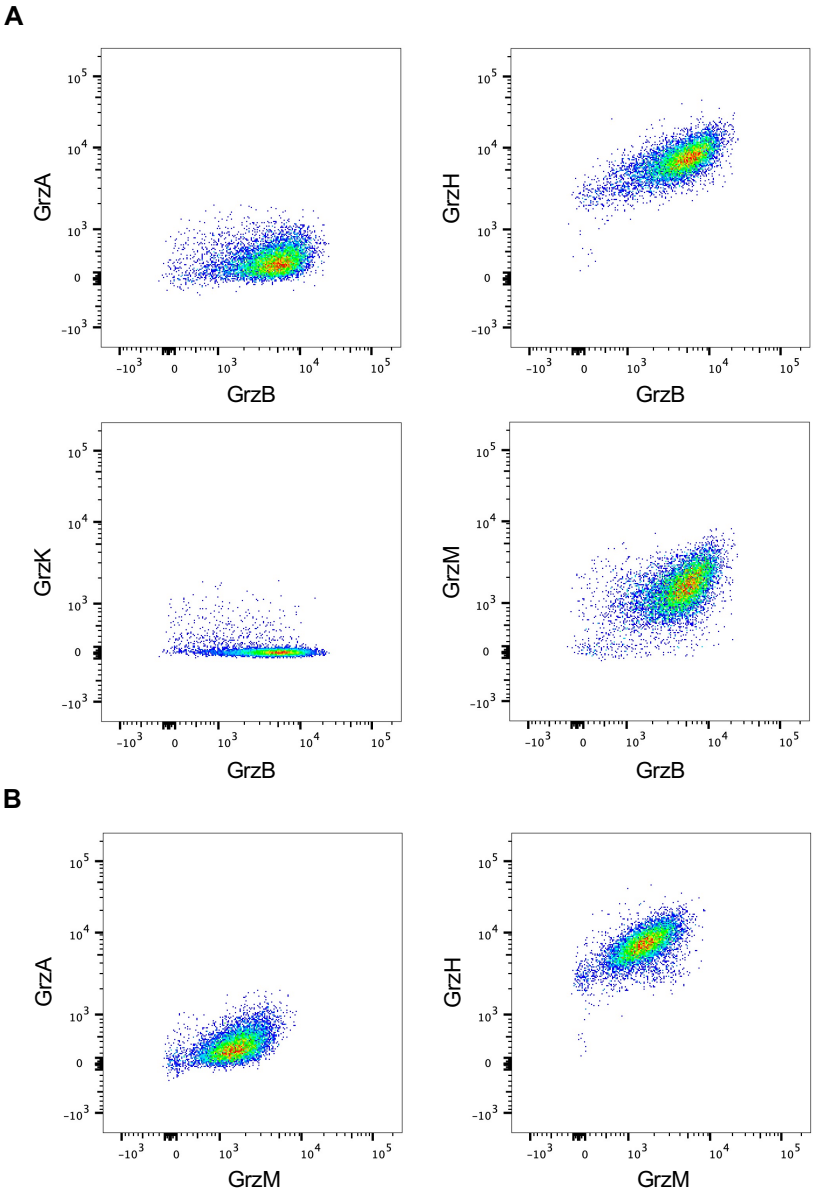

Figure 20: Granzyme content of freshly isolated resting NK cells. A Granzyme expression levels of every human granzyme (y-axis) correlated to granzyme B (x-axis). **B** Correlating expression levels of GrzA and GrzH (y-axis) to GrzM (x-axis).

8.13 Partial activity of all granzymes in primary resting NK cells

Since all granzymes are expressed in human primary resting NK cells, we wanted to know whether these granzymes will be used and have the capability to kill target cells. For this purpose, we incubated resting NK cells with the different HeLa reporter cell lines and set up live cell imaging experiments (**figure 21**). In the **figures 21A – D** the results of the co-incubation with the individual HeLa reporter cell lines are shown. The results were sorted by the fluorescence signal outcome within the nucleus. On the left-hand side, NK cells that used GrzB as a

dominant killing strategy are presented, whereas on the right-hand side an equal usage of GrzB and the respective compared granzyme was detected. In all cases, GrzB is the dominant actor in the killing strategies, with more or less support from the other granzymes A, H, K and M. In **figure 21E** the composition of these killing strategies is summarized to allow a deeper insight to all events. Again, GrzB can be identified as the main contributor responsible for 58% to 85% of the killing events. This is followed by GrzM with 42%, GrzA with 34%, GrzK with 24% and GrzH with the lowest involvement in killing events with 15%. With this knowledge, we wondered whether the granzyme influence in killing strategies by NK cells changes when they possess different content of distinct granzymes.

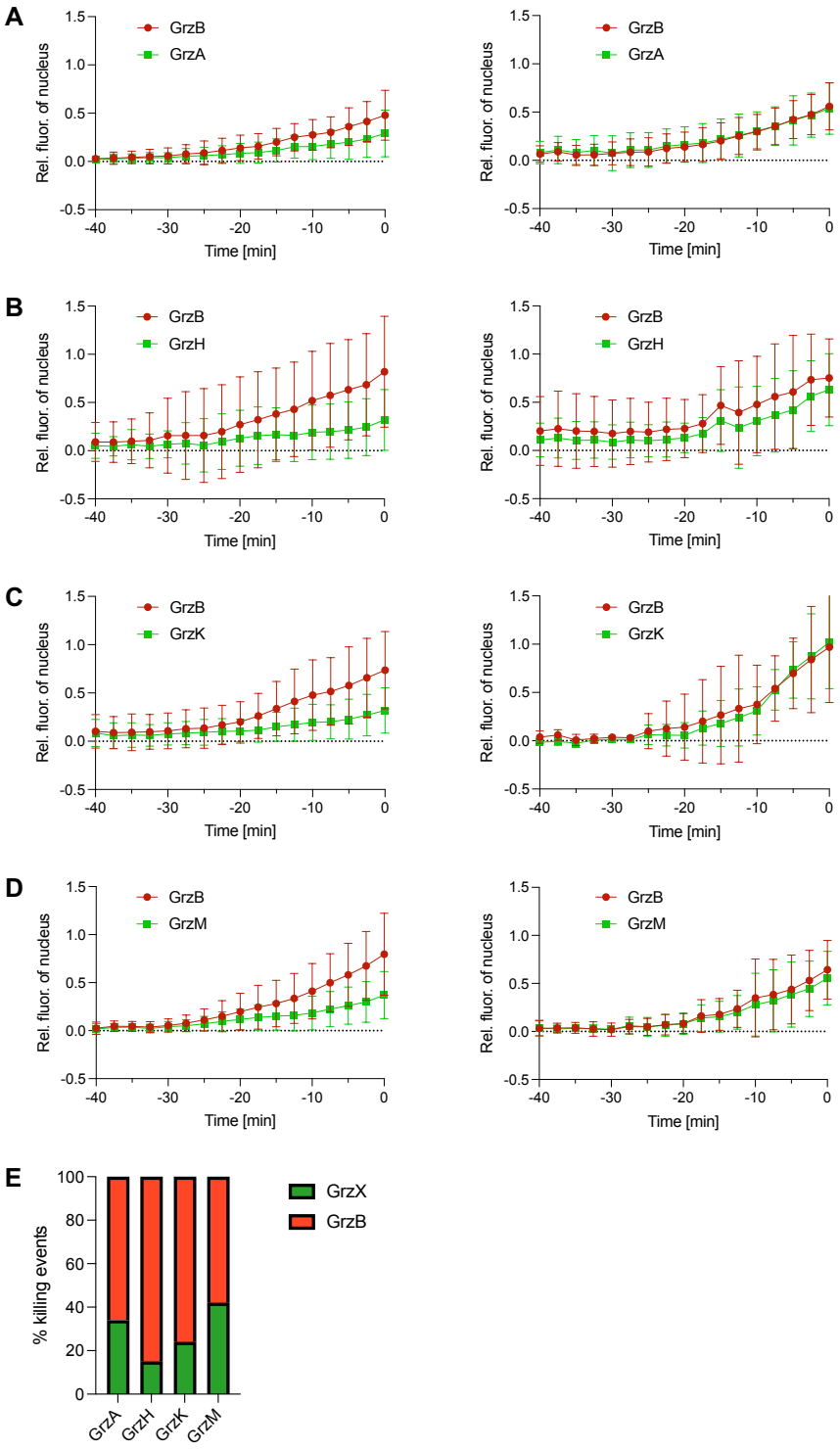

Figure 21: Live cell imaging of resting NK cells in co-culture with HeLa CD48 granzyme reporter cells (E:T 1:1). (n = 4 – 5 donors, 43 – 52 cells) **A** Effector cells incubated with HeLa CD48 NES-GrzA-mGFP-T2A-NES-GrzB-mCherry (GrzA-GrzB) reporter cells, **B** with GrzH-GrzB reporter cells, **C** with GrzK-GrzB reporter cells or **D** with GrzM-GrzB reporter cells. Killing strategies were found to be dominantly induced by granzyme B (left) or equal granzyme activity was measured (right). In **E** the percentage of the killing strategy of the NK cells is shown. Red bars represent the killing progress of the live cell imaging graphs **A - D** on the left hand, green bars represent the killing progress of the right-hand side.

8.14 Granzyme K expression levels are increased in CD56^{bright} NK cells compared to CD56^{dim} and are negatively correlated with granzyme B

As already described in the literature (Bratke et al., 2005, Bade et al., 2005a) the granzyme K and B content in CD56 dim and bright NK cells differs strongly. These findings were further confirmed by our results, which are shown in **figure 22**. **Figure 22A** represents a flow cytometry staining of GrzB and GrzK in NK cells from whole blood samples. Here, the negative correlation of granzyme B and K expression within the two populations of CD56 dim and bright NK cells can be observed. For a better comparison the individual mean fluorescence intensity (MFI) of the granzyme measurement is presented in **figure 22B**. While GrzB expression is significantly ($P < 0.0001$) higher in CD56^{dim} NK cells than in CD56^{bright} NK cells, the opposite is true for GrzK levels ($P = 0.001$).

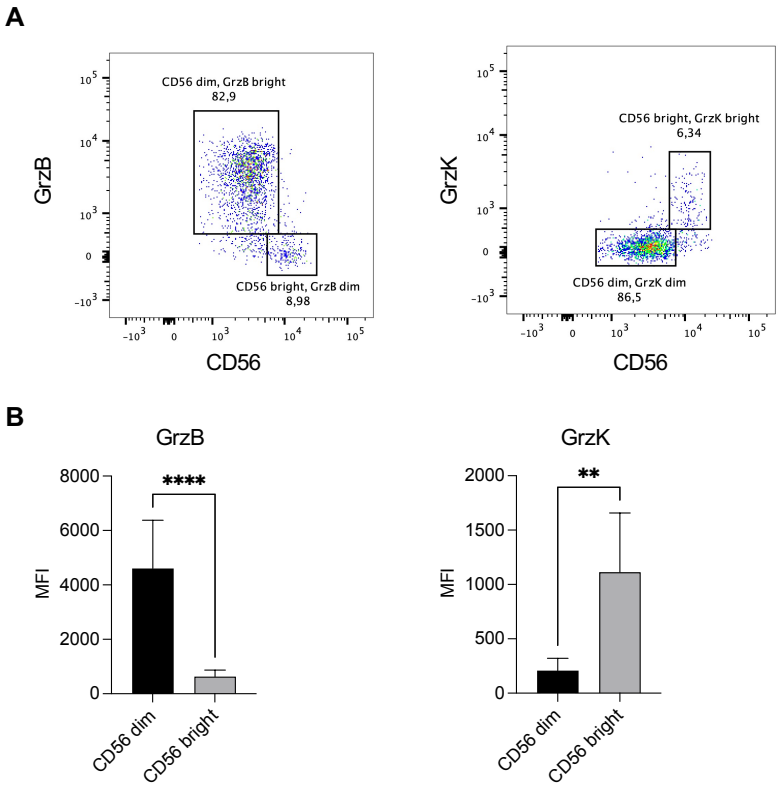

Figure 22: Granzyme B and K content of resting CD56 dim and bright NK cells. **A** Representative flow cytometry dot plots of Granzyme B and K staining. **B** Quantification (n = 8) of the mean fluorescent intensity (MFI) of the Granzyme B and K staining of resting NK cells. Unpaired t test. P values: ** $P \leq 0.01$, **** $P \leq 0.0001$.

8.15 CD56 dim and bright NK cells exhibit comparable killing strategies

To analyze whether a higher granzyme content might be related to an increased use of these granzymes, live cell imaging was performed with sorted CD56 dim or bright NK cells (**figure 23**). In this experiment, exclusively HeLa GrzK-GrzB reporter cells were used as target cells. In the **figures 23A – C** the specified killing strategies of CD56 dim and bright NK cells are shown. On the left-hand side, the killing strategies of the $CD56^{bright}$ NK cells are presented and on the right-hand side the reporter cleavage induced by $CD56^{dim}$ NK cells is shown. In **figure 23A** the GrzB activity is dominant over GrzK activity, indicated by the increasing levels of mCherry signal within the nuclei of the target cells (red line). This observation is true for both CD56 dim and bright NK cell killing events. An equal usage of GrzB and GrzK for HeLa cell killing is demonstrated in **figure 23B**. Besides these events there are killing strategies initiated without any GrzB or GrzK activity (**figure 23C**) and therefore might be executed by other granzymes or death receptor signaling. Furthermore, the involvement of GrzB leads on average to a faster death of target cells than without it (comp. **23A** with **23B & C**). The pie charts in **figure 23D** show the proportions of the three different killing strategies for the individual NK cell population. Although CD56 dim and bright NK cells have such different expression levels of granzyme B and K, the killing strategies are comparable. This might be correlated to possible differences in granzyme release, efficiency in delivery, target cell uptake or reporter cleavage.

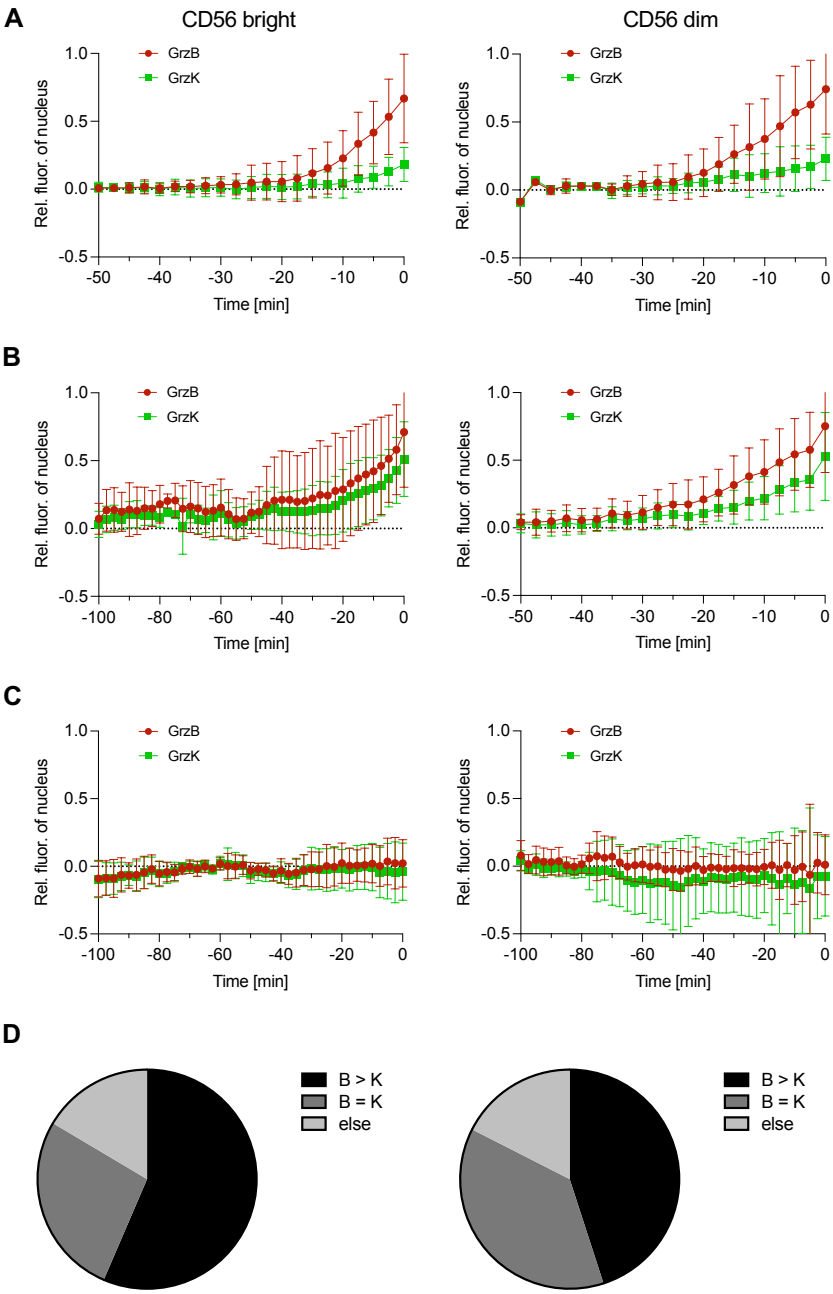

Figure 23: Live cell imaging of CD56 dim and bright NK cells in co-culture with HeLa CD48 NES-GrzK-mGFP-T2A-NES-GrzB-mCherry reporter cells (E:T 2:1). (n = 4 donors, bright: 83 cells total, dim: 40 cells total). **A** Granzyme B dominant killing strategy, **B** killing strategy with comparable Granzyme K and B usage or **C** Granzyme K and B independent killing strategy. **D** Proportional distribution of killing strategies of CD56 bright (left) and CD56 dim (right) NK cells.

8.16 CD56^{bright} NK cells release more granzyme K than CD56^{dim} NK cells

To investigate whether CD56 dim and bright NK cells not only possess but also release different levels of granzyme K and B, ELISA-tests were performed. For this purpose, CD56 dim or bright NK cells were stimulated by ionomycin and PMA, by co-incubation with the target cell line HeLa CD48 or by plate-bound anti-

NKp30. Negative controls were performed by incubating the effector cells in CTL medium alone or with plate-bound MOPC21 (IgG isotype control). Whole cell lysates served as positive control to gather information of the NK cells' potential granzyme content. In **figure 24A** the measurement of released GrzK is presented. For all conditions tested, higher GrzK levels are found for $CD56^{bright}$ NK cells compared to $CD56^{dim}$. Already in the negative controls (Medium or MOPC21), the spontaneous release of GrzK seems to be higher for $CD56^{bright}$ NK cells. A presumably comparable granzyme release was induced by the unspecific stimulation with ionomycin and PMA, but on closer inspection, the GrzK concentration of $CD56^{bright}$ NK cells is significantly increased. This result can be found for all conditions among CD56 dim and bright NK cells, albeit to different extents. The strongest trigger for GrzK release is observed with the combination of ionomycin and PMA followed by the stimulation with HeLa cells. Plate-bound antibodies against the activating receptor NKp30 resulted in the lowest GrzK release. This finding is true for both $CD56^{bright}$ and $CD56^{dim}$ NK cells.

Figure 24B shows the GrzB concentration determination. As expected, the GrzB levels are inverse to GrzK levels for $CD56^{bright}$ NK cells. This time, $CD56^{dim}$ tend to already release more GrzB in control conditions (Medium and MOPC21). The total GrzB content of $CD56^{dim}$ NK cells is significantly higher compared to GrzB levels of $CD56^{bright}$ NK cells, indicated by measured concentrations of the cell lysates. Due to the high variances, the GrzB release among the two NK cell subpopulations is not significantly different upon HeLa cell co-incubation or unspecific stimulation with ionomycin and PMA. The only significantly higher GrzB release of $CD56^{bright}$ compared to $CD56^{dim}$ was triggered by binding with the anti-NKp30 antibody. Compared to medium control, the stimulation with ionomycin/PMA, HeLa cells or anti-NKp30 resulted in similar GrzB release by $CD56^{dim}$ NK cells ($P < 0.0001$). For $CD56^{bright}$ NK cells the stimulation with anti-NKp30 was less efficient and led to lower GrzB levels in the supernatant ($P < 0.01$). This could be explained by the lower expression of natural cytotoxicity receptors on $CD56^{bright}$ NK cells in comparison to $CD56^{dim}$ NK cells, which lead to lower activation signals. However, if one considers the absolute concentration levels of GrzB and GrzK, our hypothesis seems to be confirmed: Although $CD56^{bright}$ NK cells possess and release more GrzK compared to $CD56^{dim}$ NK cells, the GrzB release is still high and might outperform the effects of GrzK.

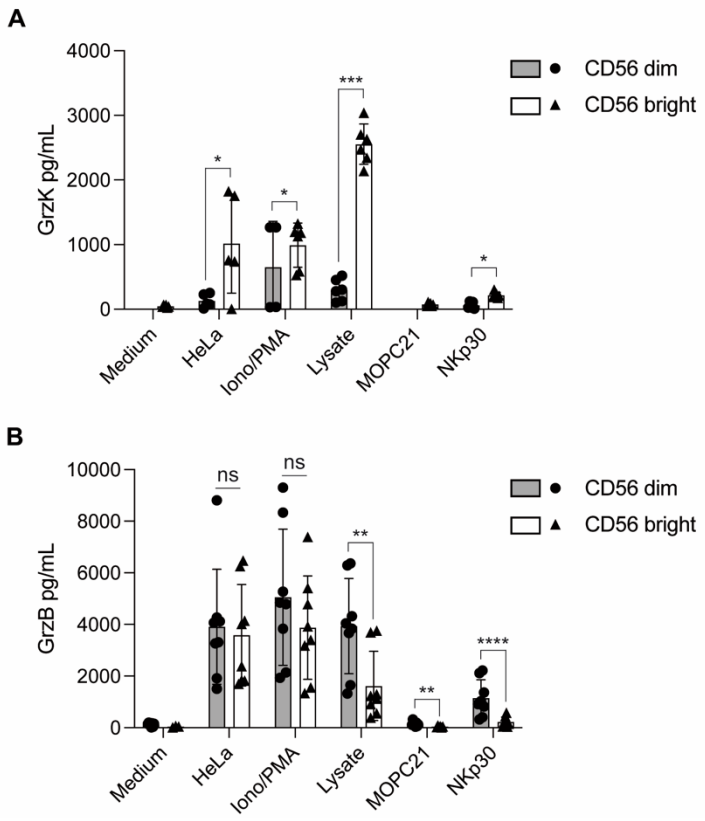

Figure 24: CD56 dim and bright NK cells release different concentrations of granzyme K and B. Granzyme release by NK cells (in pg/mL) into the supernatant upon the stimulation with HeLa CD48 target cells, ionomycin (1 μg/mL) and PMA (10 μM) or plate-bound αNKp30 (2 μg/mL). (Medium and αMOPC21 as negative controls, whole cell lysate as positive control). **A** GrzK concentration of supernatants measured by ELISA method or **B** GrzK concentration of supernatants measured by ELISA method. Statistical analysis was performed with log(Y) data points and one-way ANOVA test (n = 4, duplicates). P values: * P ≤ 0.05, ** P ≤ 0.01, *** P ≤ 0.001, **** P ≤ 0.0001.

8.17 Granzyme K is lost during cultivation

Since CD56^{bright} NK cells represent only a small percentage of resting NK cells, we attempted to culture these cells. Unfortunately, the phenotype of highly expressed GrzK was lost after only one week in our standard NK cell culture (method chapter 7.3), as shown in **figure 25**. In this figure, the granzyme content of CD56 dim and bright NK cells was monitored and compared under the culture conditions for our activated NK cells over three weeks. Resting NK cells exhibited differential GrzK expression immediately after sorting. The GrzK content of CD56^{bright} NK cells was significantly increased compared to CD56^{dim}. After one week, this phenotype had then completely disappeared and no recovery was detected until week three. GrzB was again found to be significantly higher expressed in CD56^{dim} NK cells compared to CD56^{bright} resting NK cells. Changing

phenotypes were also observed for the other granzymes during cultivation. While we noticed the loss of GrzK under these conditions, the granzymes A and B were first increased and then reduced again, in both CD56 dim and bright NK cells. GrzH expression was only slightly decreased and GrzM expression increased in $CD56^{dim}$ NK cells. It should be noted, however, that the initial value of the resting NK cells for the other granzymes A, H and M was not collected and included in the graphs. Therefore, we can only evaluate the development of GrzA, H and M levels during culture, but not the before-and-after effect. CD56 was expressed differently among the two subpopulations, but remained relatively stable over the cultivation timespan.

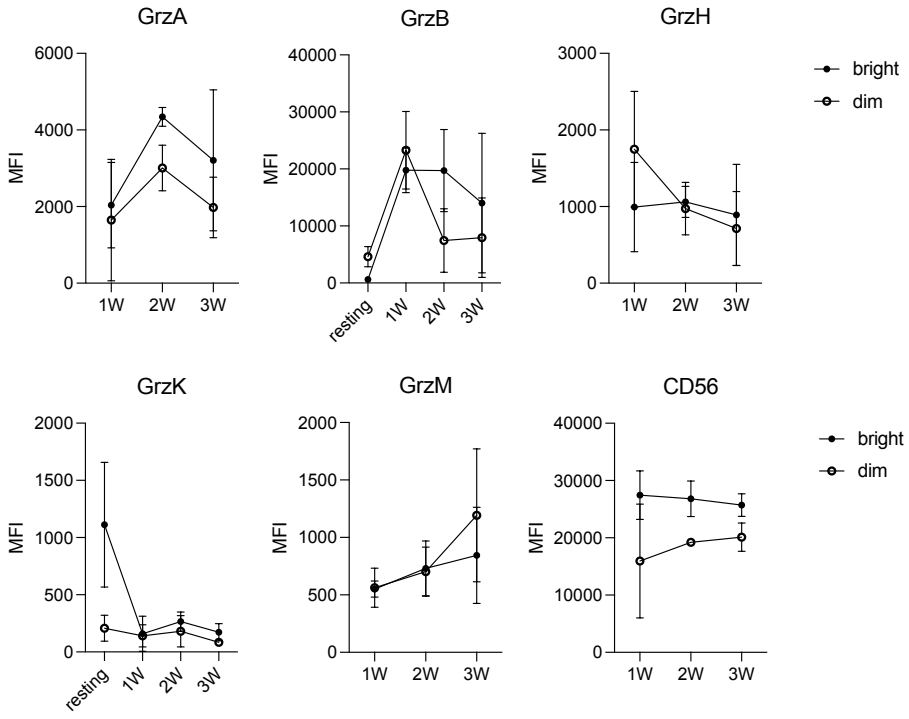

Figure 25: Granzyme content in resting CD56 dim and bright NK cells before and during culture. Development of GrzK and GrzB content was monitored during the culture from the beginning of the NK cell isolation until 3 weeks of culture conditions. The remaining granzymes as well as CD56 were stained only for 3 weeks of culture.

8.18 Activated NK cells change their granzyme content

Since we observed differences in the granzyme content during our NK cell culture conditions, we wanted to compare the granzyme content of resting and activated NK cells. In **figure 26A** the representative flow cytometry stainings for the different granzymes in various primary NK cells (NK cells of freshly isolated PBMC, NK cells of Buffy coats or activated NK cells) are shown. In comparison

to the unstained control (gray histogram), the primary NK cells are all positive for the granzymes A, B, H and M, but few to no signals can be detected for GrzK. Further separation into the subpopulations $CD56^{dim}$ and $CD56^{bright}$ reveals that primary NK cells also express GrzK. GrzB and GrzH are equally expressed among the different cell populations. While GrzA seems to be upregulated upon activation, GrzM is less strongly expressed in activated NK cells than in resting populations of NK cells from freshly isolated PBMC or Buffy coat NK cells. These findings are partly reflected in the quantification in **figure 26B**. While the expression of GrzH and GrzM decreases significantly upon NK cell activation, GrzB is increased. For granzymes A and K, no significant differences can be found between resting and activated NK cells.

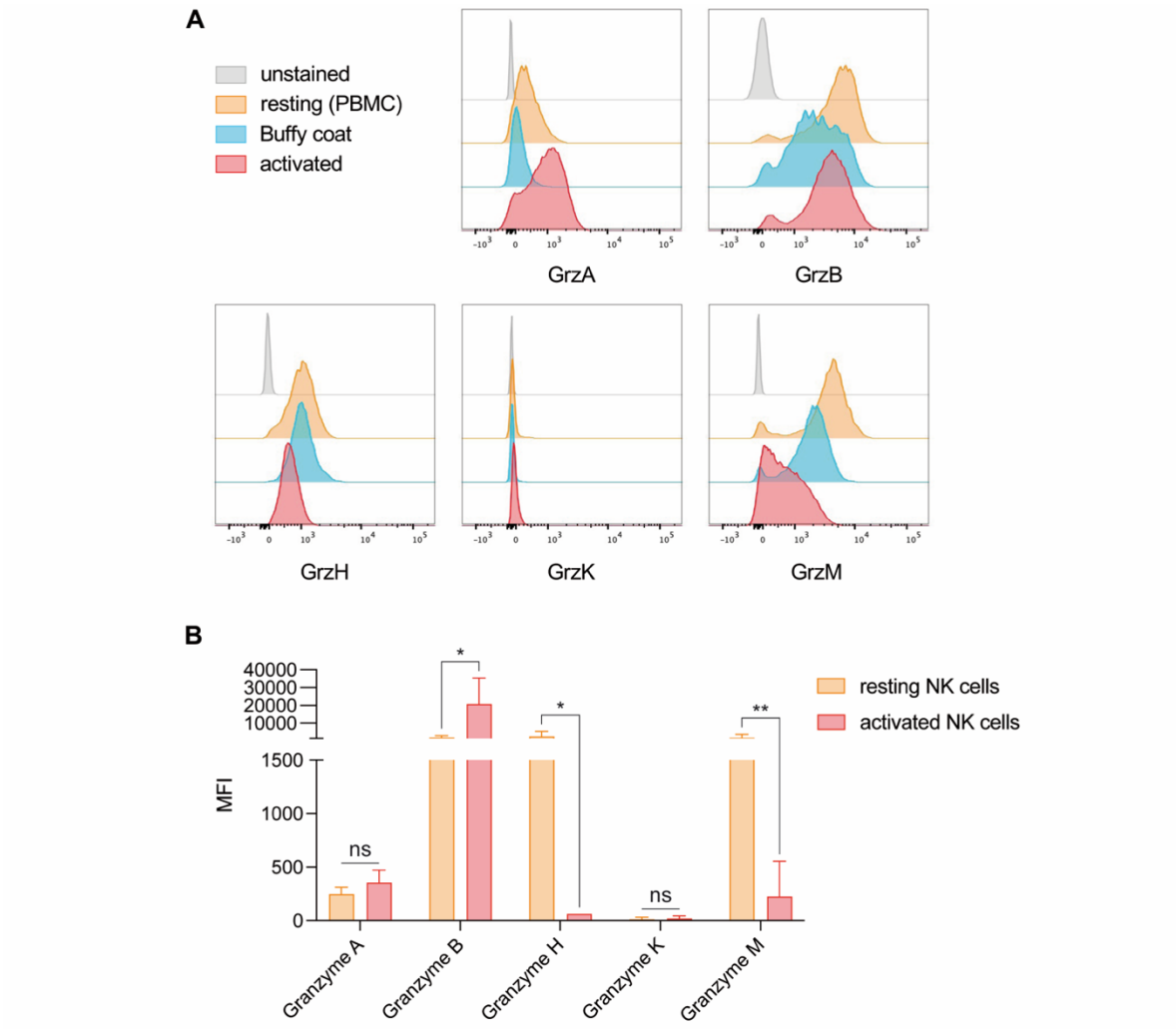

Figure 26: Granzyme content of primary NK cells. A Representative staining of granzymes in primary resting (isolated from fresh PBMC or buffy coats) or activated NK cells. Unstained NK cells (gray), stained NK cells of freshly isolated PBMC (orange), NK cells freshly isolated from buffy coats (blue) and activated NK cells (red). **B** Quantification of the mean fluorescence intensity (MFI) signal of the individual experiments (n = 6). Statistical analysis was performed with log(Y) data points and an ordinary one-way ANOVA test. P values: * $P \leq 0.05$.

8.19 Granzyme expression is influenced by various stimuli

Since the cultivation of NK cells results in a significant change in granzyme expression levels, we wanted to determine what type of stimulus could be responsible for this. Therefore, freshly isolated PBMC were incubated under several conditions of stimulation: with a low dose of IL-15 as control, with an interleukin cocktail of IL-12, IL-15 and IL-18, with universal type I IFN (uIFNα), with Lipopolysaccharide (LPS) or with K562-feeder cells (**figures 27 – 31**). To compare possible differences, we gated on CD56 dim and bright NK cells, respectively. In **figure 27** the results for GrzA are shown. Already under control conditions, GrzA expression levels slightly increase in $CD56^{bright}$ NK cells within 120 h, whereas the expression was stable in $CD56^{dim}$ NK cells. Stable expression by both subpopulations was also observed for the stimulation with uIFNα. A response of GrzA expression upon stimulation with LPS or K562 was not detected earlier than 48 h after supplementation. The interleukin cocktail of IL-12, IL-15 and IL-18 triggered a strong increase of GrzA already after 24 h. In addition, the $CD56^{bright}$ NK cells showed a stronger reaction to the stimulus compared to $CD56^{dim}$ in all of the three conditions.

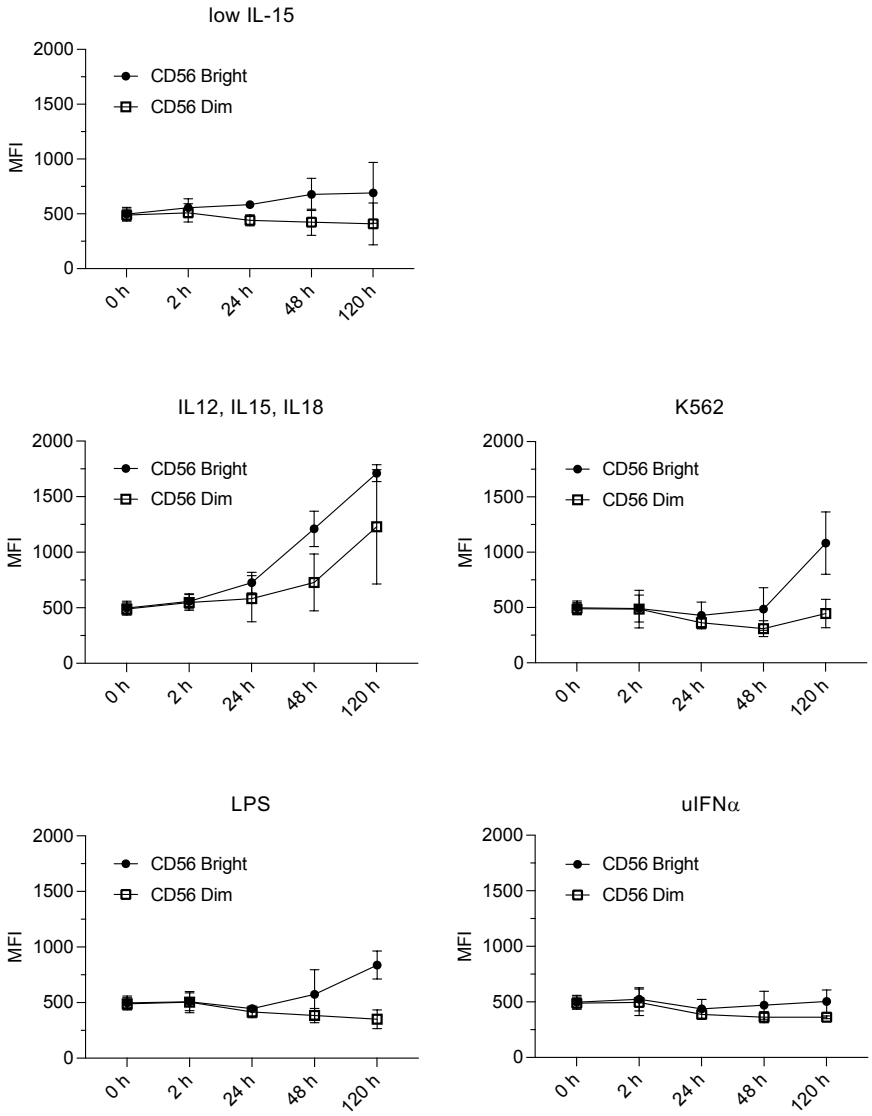

Figure 27: Granzyme A expression levels of CD56 dim and bright NK cells of freshly isolated PBMC incubated with different stimuli. PBMC were stimulated with low levels of IL-15 as negative control (10 IU/mL), an interleukin cocktail of IL-12, IL-15 and IL-18 (1 μg/mL, 50 IU/mL, 5 μg/mL), lipopolysaccharide (LPS) (1 μg/mL), universal type I interferon (uIFNα) (1000 U/mL), irradiated (30 gray) K562-mb15-41BBL feeder cells (K562 feeder) (5 x 10^5, E:T 4:1). The mean fluorescence intensity (MFI) of granzyme A expression of CD56 dim and bright NK cells was monitored over a time span of 120 h.

Figure 28 shows the expression levels of GrzB under the stimulation conditions for 120 hours. Again, stimulation with either low IL-15, LPS, uIFNα or K562-feeder cells triggered only minor changes in the expression levels of GrzB within 120 hours. Our finding that $CD56^{bright}$ NK cells express higher GrzB levels compared to $CD56^{dim}$ NK cells was again confirmed. After 48 hours, the GrzB expression was comparable between the two subpopulations under the low IL-15 and uIFNα conditions, or the GrzB content of $CD56^{bright}$ NK cells even exceeded that of $CD56^{dim}$ after stimulation with LPS or K562-feeder cells. This pattern can be observed for the first 2 hours of interleukin cocktail stimulation, too. Here, the

GrzB expression rises steeply up to 48 hours. At this point the CD56^{bright} NK cells produced more GrzB than the CD56^{dim} NK cells did. After 120 hours of stimulation, the GrzB levels of both subpopulations decrease and equalize again at a similar level.

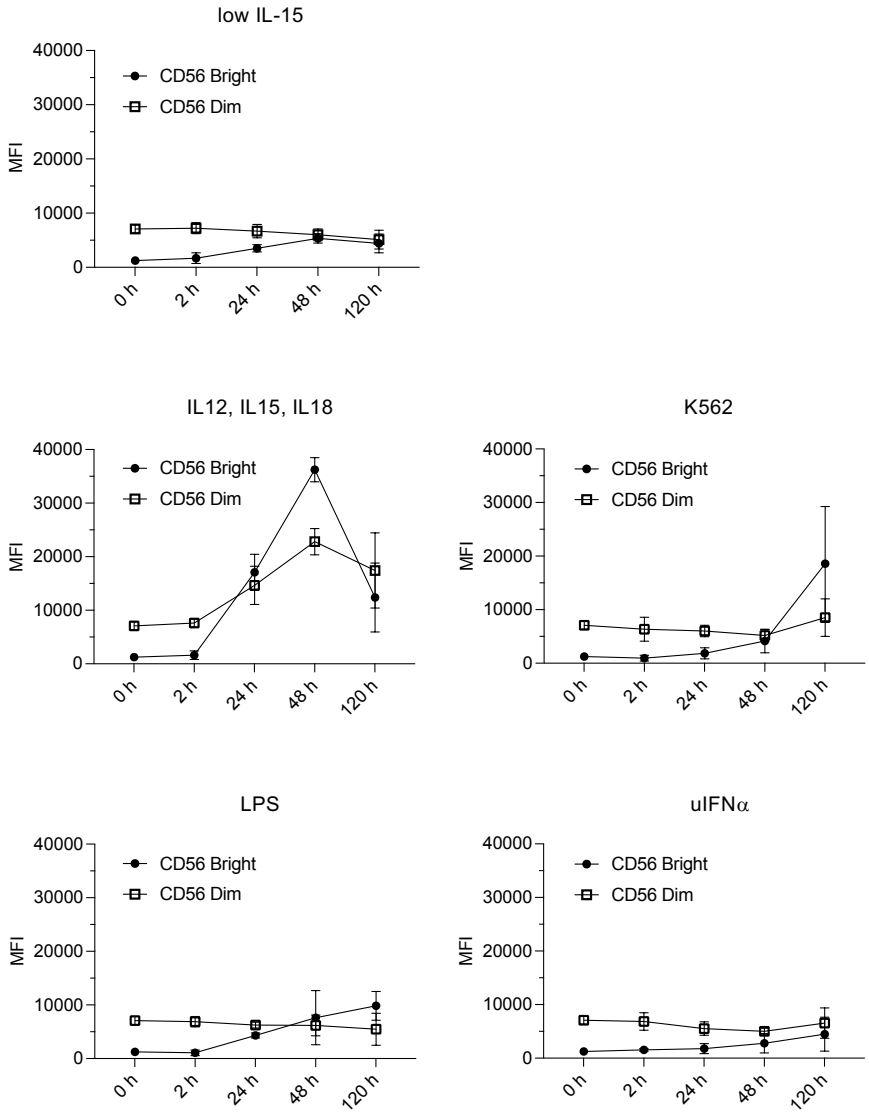

Figure 28: Granzyme B expression levels of CD56 dim and bright NK cells of freshly isolated PBMC incubated with different stimuli. PBMC were stimulated with low levels of IL-15 as negative control (10 IU/mL), an interleukin cocktail of IL-12, IL-15 and IL-18 (1 μg/mL, 50 IU/mL, 5 μg/mL), lipopolysaccharide (LPS) (1 μg/mL), universal type I interferon (uIFNα) (1000 U/mL), irradiated (30 gray) K562-mb15-41BBL feeder cells (K562 feeder) (5 x 10^5, E:T 4:1). The mean fluorescence intensity (MFI) of granzyme B expression of CD56 dim and bright NK cells was monitored over a time span of 120 h.

The results for GrzH are found in **figure 29**, where only minor changes in expression levels can be found for all conditions. As previously described for GrzB, GrzH is higher expressed by resting CD56^{dim} NK cells. After 48 to 120 hours the levels of GrzH are equal in both NK cell subpopulations. In contrast

to all other granzymes, GrzH is not upregulated upon stimulation with the interleukin cocktail.

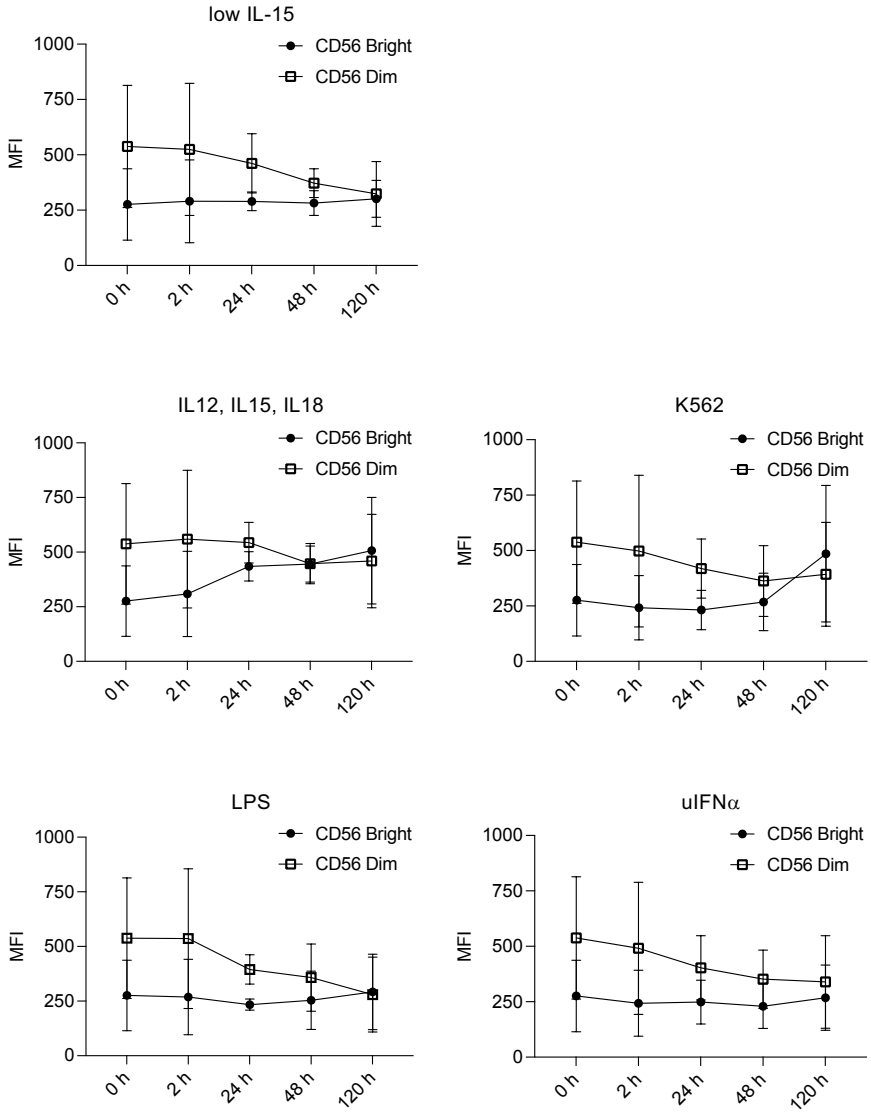

Figure 29: Granzyme H expression levels of CD56 dim and bright NK cells of freshly isolated PBMC incubated with different stimuli. PBMC were stimulated with low levels of IL-15 as negative control (10 IU/mL), an interleukin cocktail of IL-12, IL-15 and IL-18 (1 μg/mL, 50 IU/mL, 5 μg/mL), lipopolysaccharide (LPS) (1 μg/mL), universal type I interferon (uIFNα) (1000 U/mL), irradiated (30 gray) K562-mb15-41BBL feeder cells (K562 feeder) (5 x 10^5, E:T 4:1). The mean fluorescence intensity (MFI) of granzyme H expression of CD56 dim and bright NK cells was monitored over a time span of 120 h.

For GrzK expression levels we discovered almost similar patterns for all the different stimuli conditions used (**figure 30**). $CD56^{bright}$ NK cells exhibit, in contrast to $CD56^{dim}$ NK cells, higher levels of GrzK. During the incubation time span, the GrzK levels of $CD56^{bright}$ NK cells decreased continuously and almost reached the expression levels of $CD56^{dim}$ NK cells after 120 hours. These findings are consistent with the results in **figure 25**, where the difference in GrzK levels

between CD56 bright and dim NK cells disappeared after one week of cell culture conditions.

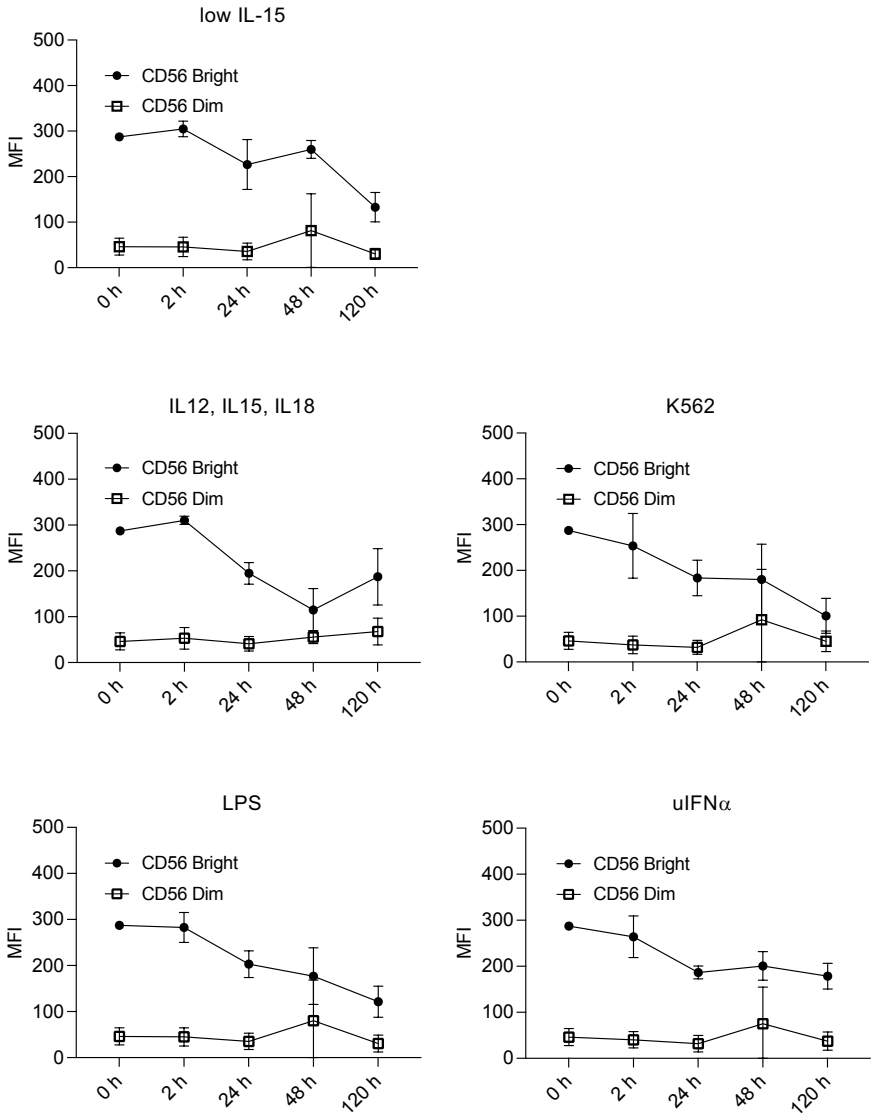

Figure 30: Granzyme K expression levels of CD56 dim and bright NK cells of freshly isolated PBMC incubated with different stimuli. PBMC were stimulated with low levels of IL-15 as negative control (10 IU/mL), an interleukin cocktail of IL-12, IL-15 and IL-18 (1 μg/mL, 50 IU/mL, 5 μg/mL), lipopolysaccharide (LPS) (1 μg/mL), universal type I interferon (uIFNα) (1000 U/mL), irradiated (30 gray) K562-mb15-41BBL feeder cells (K562 feeder) (5 x 10^5, E:T 4:1). The mean fluorescence intensity (MFI) of granzyme K expression of CD56 dim and bright NK cells was monitored over a time span of 120 h.

For GrzM, the expression levels are higher in $CD56^{dim}$ NK cells compared to $CD56^{bright}$ (**figure 31**). For all five conditions tested, GrzM levels in $CD56^{dim}$ NK cells were continuously decreasing, while the levels in $CD56^{bright}$ NK cells remained stable for the incubation time span of 120 hours. Upon stimulation with the interleukin cocktail, LPS and K562-feeder cells, the loss of GrzM was more pronounced than in the control condition with low IL-15 or incubation with uIFNα.

Overall, the different granzyme levels between CD56 dim and bright NK cells continue to equalize during cultivation. The individual stimuli lead to an increase or decrease of different granzymes levels expressed by the two NK cell populations. However, after 120 hours at the latest, the granzyme levels of both NK cell populations are always comparable. These results show that granzyme expression levels change during cultivation of NK cells.

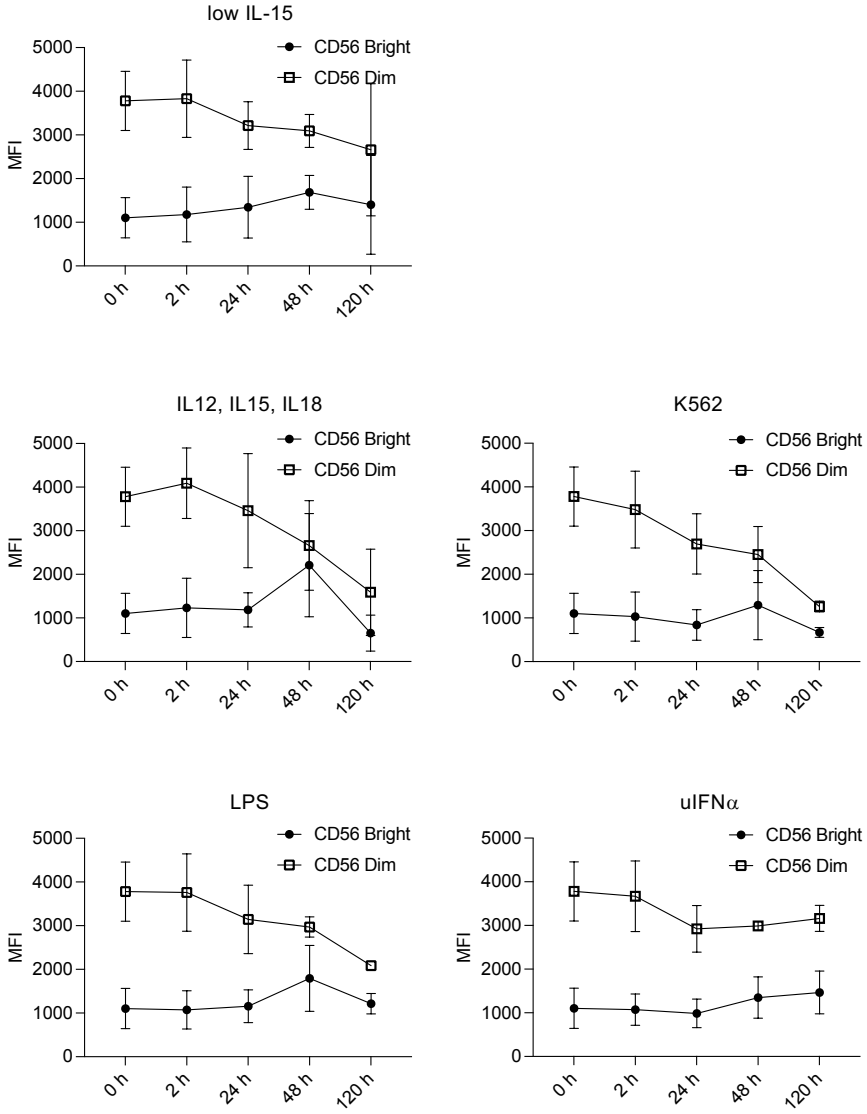

Figure 31: Granzyme M expression levels of CD56 dim and bright NK cells of freshly isolated PBMC incubated with different stimuli. PBMC were stimulated with low levels of IL-15 as negative control (10 IU/mL), an interleukin cocktail of IL-12, IL-15 and IL-18 (1 μg/mL, 50 IU/mL, 5 μg/mL), lipopolysaccharide (LPS) (1 μg/mL), universal type I interferon (uIFNα) (1000 U/mL), irradiated (30 gray) K562-mb15-41BBL feeder cells (K562 feeder) (5 x 10^5, E:T 4:1). The mean fluorescence intensity (MFI) of granzyme M expression of CD56 dim and bright NK cells was monitored over a time span of 120 h.

8.20 Granzyme A greatly supports the cytotoxicity of activated NK cells

To be able to assess which granzymes are used by activated NK cells, we again performed live cell imaging experiments. The results are shown in **figure 32**. The left graphs of **figure 32A – D** represent the killing strategies in which GrzB was dominantly used. In the right graphs killing events were observed that showed equal granzyme activity within the target cells. All GrzB dominant target cell deaths showed comparable courses for every granzyme reporter cleavage, respectively. In the case of simultaneous activity of GrzB and one of the other granzymes, the raw data show a much more dominant activity for GrzA than for the granzymes H, K, or M. Unfortunately, this is difficult to see in the summarized graph (**figure 32A, right**). Furthermore, the killing events with GrzA and GrzB took much longer (around 40 minutes) compared to killing events induced by the usage of GrzB together with granzyme H, K or M (comp. **figure 32A, right** with **figure 32B – D, right**). However, not only the strength of activity, but also the frequency of GrzA activity is higher compared to the other granzymes, which can be observed in **figure 32E**. Comparing the summarized data in **figure 32E** to the results of live cell imaging of resting NK cells (**figure 21E**), GrzB has a lesser influence than GrzA. Activated NK cells use GrzA equally together with GrzB or rather dominantly in 68% of the killing events. Only 32% of the killing events were dominantly triggered by GrzB activity when using the GrzA-GrzB reporter cells in this experiment. Interestingly, GrzA expression does not appear to be significantly increased in activated NK cells compared to resting NK cells (**figure 26**). Also, GrzM is still important for the killing strategy, although at a lower rate (28%) than it is the case for the resting NK cells (GrzM: 42%). Granzyme H and K activity was detected in just 12% and 15% of killings, respectively. The altered killing strategy of activated NK cells suggests that both altered expression of granzymes and surface molecules could have an impact.

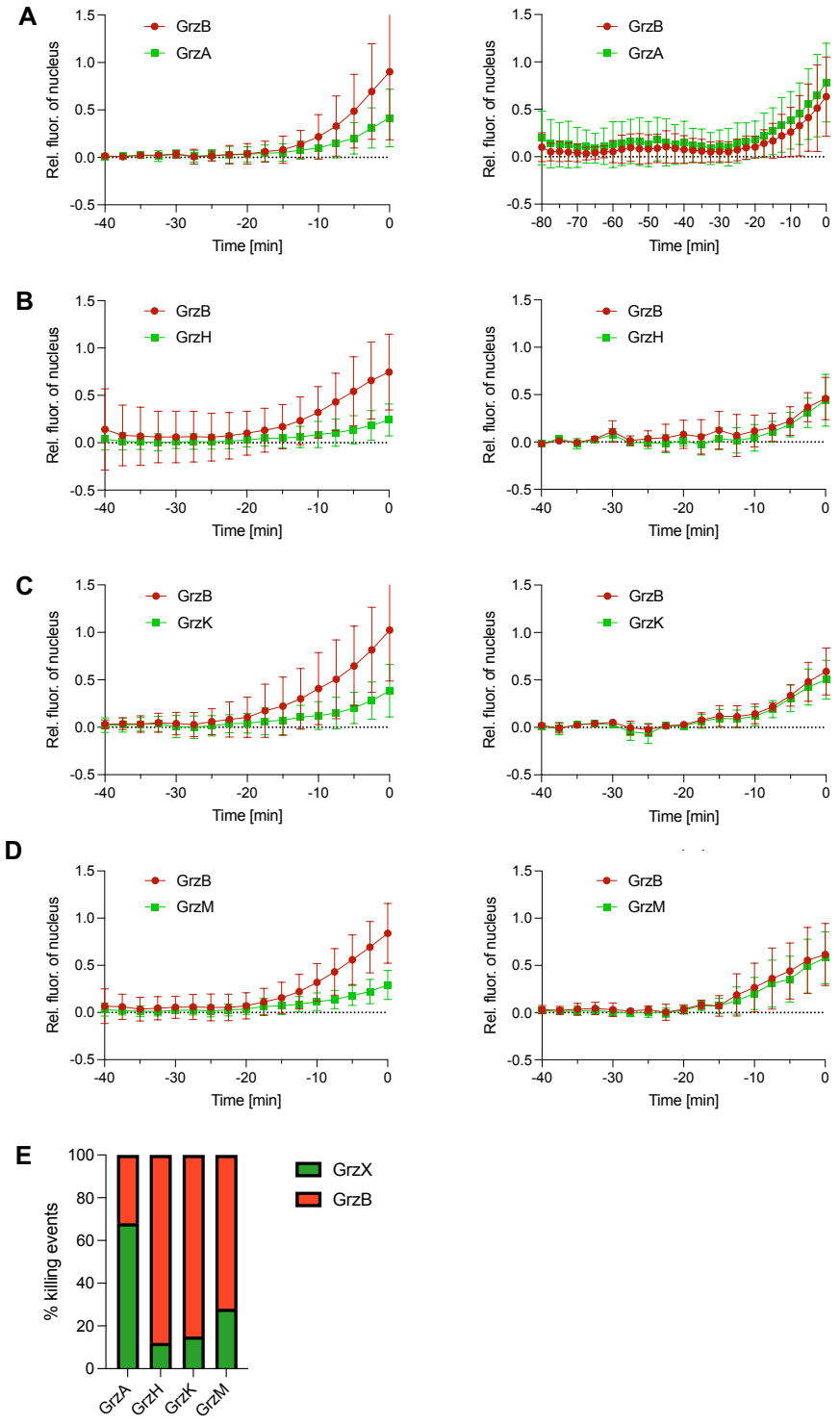

Figure 32: Live cell imaging of activated NK cells in co-culture with HeLa CD48 granzyme reporter cells (E:T 1:1). (n = 4 – 5 donors, 49 – 56 cells) **A** Effector cells incubated with HeLa CD48 NES-GrzA-mGFP-T2A-NES-GrzB-mCherry (GrzA-GrzB) reporter cells, **B** with GrzH-GrzB reporter cells, **C** with GrzK-GrzB reporter cells or **D** with GrzM-GrzB reporter cells. In **E** the percentage of the killing strategy of the NK cells is shown. Red bars represent the killing progress of the live cell imaging graphs A - D on the left hand, green bars represent the killing progress of the right-hand side.

8.21 Uncleavable reporters reveal background noise of granzyme reporters for activated NK cells

To analyze the actual signal of the reporter cleavage without background noise, activated NK cells were co-incubated with uncleavable HeLa reporter cells. The uncleavable reporters are the same as already used to discover NK92 background signal. The NES-AAAAA-GFP-T2A-NES-GrzB-mCherry (AAAAA-GrzB) can still be cleaved by GrzB, but granzymes A, H, K and M are no longer able to do so, while the NES-GrzA-GFP-T2A-NES-AAAAFGR-mCherry (GrzA-AAAAFGR) is uncleavable for GrzB. In **figure 33A** the reporter cleavage within HeLa AAAAA-GrzB reporter cells is shown. GrzB activity can still be detected, but the signal for GFP reporter cleavage can also be found in the nuclei of the target cells. A background signal due to target cell shrinkage upon cell death can thus also be found for killing by activated NK cells. The cleavage of GrzA-AAAAFGR reporter by granzyme activity of activated NK cells is comparable to the result of NK92, too (compare **figure 15**). Here, GrzB is no longer able to cleave the peptide coupled to mCherry, but signals slightly above baseline are still visible. GrzA activity is still observed and as expected overall lower compared to GrzB reporter cleavage (comp. **figure 33A** GrzA with GrzB cleavage). In **figure 33B** the quantification of the granzyme activity compared to the uncleavable reporters, normalized to the GrzB activity, is shown. The signal intensity of GrzB specific cleavage was set to 100%. The GFP signals of the other reporters and mCherry signal of GrzA-AAAAFGR were calculated in correlation to the GrzB signal. It was found that the uncleavable GFP reporter (AAAAA) accounted for 21% and the uncleavable mCherry reporter (AAAAFGR) accounted for 19% of the corresponding GrzB signal, comparable to the results with NK92 cells. Activated NK cells trigger a true signal of reporter cleavage in HeLa target cells through the use of granzyme A, K and M followed by GrzH.

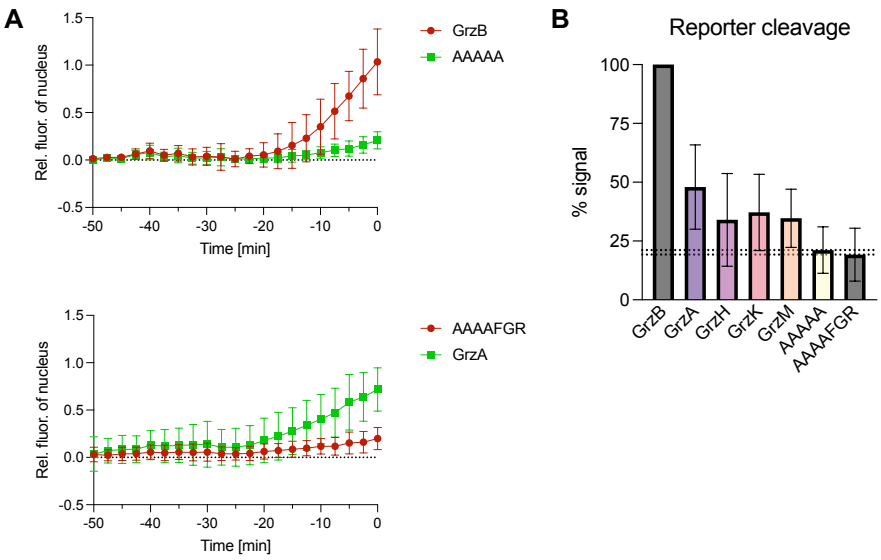

Figure 33: Live cell imaging of activated NK cells co-cultured (E:T 1:1) with HeLa CD48 uncleavable reporter cells. A Relative fluorescence of the nucleus of HeLa CD48 NES-AAAAA-mGFP-T2A-NES-GrzB-mCherry reporter cells (top) or of HeLa CD48 NES-GrzA-mGFP-T2A-NES-AAAFGR-mCherry reporter cells (bottom). **B** Normalization of endpoint measurements (timepoint 0) of the fluorescent signal upon reporter cleavage for all granzyme and uncleavable reporters in percentage, relative to the signal of GrzB.

8.22 Western blotting partially underlines live cell imaging results

To further confirm our results from the live cell imaging experiments, a Western blot was performed (**figure 34**). For this purpose, the HeLa reporter cells were incubated with activated NK cells under the same conditions as in the live cell imaging experiments. The lysates were loaded as depicted in the figure and immunostained with either an anti-GFP (top) or anti-mCherry antibody (bottom). The first two lanes are loaded with GrzA-GrzB reporter. Here, a cleavage product can be recognized for the anti-GFP as well as for the anti-mCherry staining, as a result of granzyme A and B activity. No cleavage products were found for both the granzyme H and K reporters when incubated with effector cells for anti-GFP detection. In contrast, GrzB activity was again observed. These results partially reflect the findings of our microscopy data. GrzH and GrzK were found in microscopy analysis, although not particularly pronounced. Since these findings were determined at the level of a single cell, reporter cleavage could be insufficient to be detected in a bulk assay. The last two lanes were loaded with GrzM-GrzB HeLa reporter cells incubated without or with effector cells. Identically to GrzA, a reporter cleavage product was detected with the anti-GFP antibody, suggesting that GrzM was active in these target cells. Since a GrzB reporter

cleavage product was also found for the GrzM-GrzB reporter, this band can be understood as a positive control for this experiment.

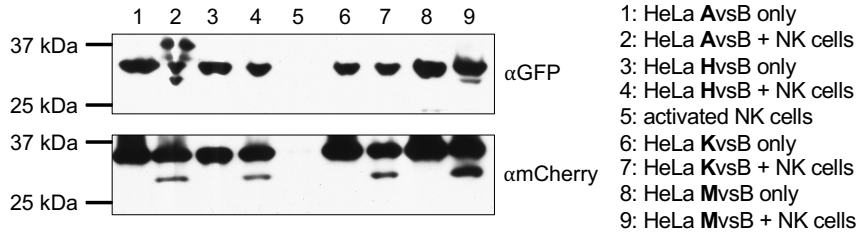

Figure 34: Confirmation of live cell imaging experiments of activated NK cells with HeLa reporter cells by Western blotting. Western blot of HeLa reporter cells in co-culture with activated NK cells (E:T 2:1). HeLa reporter cells were incubated with effector cells for 4 h, harvested and lysed. Reporter cleavage triggered by the effector cells was detected by an anti-GFP or anti-mCherry antibody.

8.23 Granzyme inhibition with DCI results in baseline fluorescence levels during live cell imaging

Since attempts to knock out granzymes in primary NK cells failed, we used the inhibitor DCI to confirm our reporter specificity in life cell imaging experiments for activated NK cells. Activated NK cells were pre-incubated with the pan-protease inhibitor DCI for 30 minutes and then added to the HeLa reporter cell lines. The results are shown in **figure 35**. As expected, for granzyme H, K and M reporter cells only baseline levels of nuclear fluorescence were detected. For the GrzA-GrzB reporter, the measurements deviate more from the baseline values and have a higher variance overall. The killing events in **figure 35** were thus expected to be induced by death receptor signaling and once again proofed the reporter specificity for granzymes.

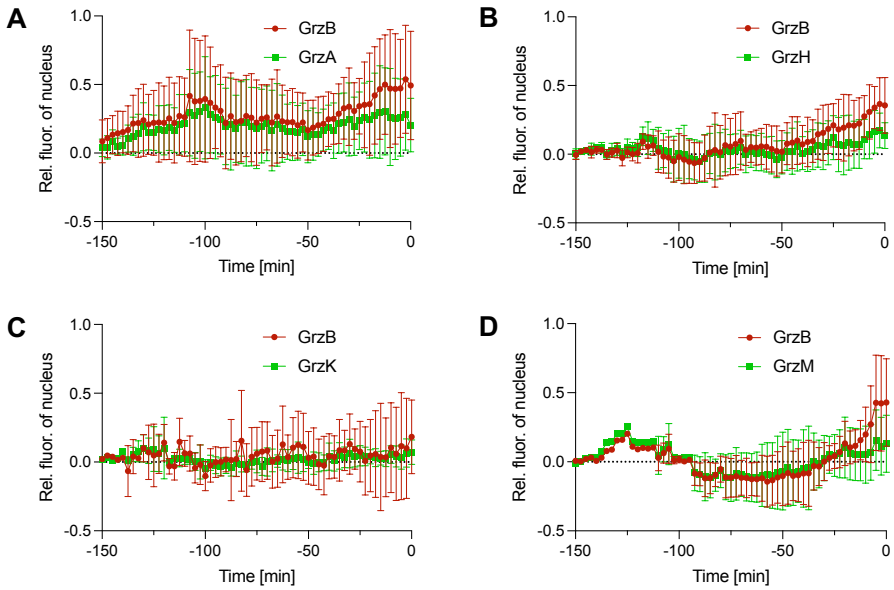

Figure 35: Live cell imaging of activated NK cells in co-culture with HeLa CD48 granzyme reporter cells (E:T 1:1) and additional DCI incubation. Activated NK cells incubated with HeLa CD48 **A** NES-GrzA-mGFP-T2A-NES-GrzB-mCherry (GrzA-GrzB) reporter cells, **B** with GrzH-GrzB reporter cells, **C** with GrzK-GrzB reporter cells or **D** with GrzM-GrzB reporter cells. The co-incubation of effector and target cells was performed after a pre-incubation of effector cells with 3,4-Dichloroisocoumarin (DCI, 25 μM).

8.24 Granzyme H might not be released with the other granzymes

Activated NK cells express high levels of granzyme A and B, which they make use of. While the granzymes H, K and M are less expressed, GrzM still has a higher impact on target cell killing than H and K. To clarify whether the granzymes are not only expressed, but released upon degranulation, granule release kinetic experiments were performed (**figure 36**). With this experiment, we wanted to exclude the possibility that GrzH activity was rarely detected within target cells because it is simply not released. Activated NK cells were incubated with HeLa target cells and degranulation and thus the release of granzymes was monitored over a time span of 24 hours. To observe the potential loss of granzymes, the expression level of degranulating NK cells ($CD107a^+$) was compared to non-degranulating ($CD107a^-$) NK cells. In the upper left graph, the percentages of $CD107a^-$ and $CD107a^+$ NK cells are shown as curves over time. First degranulating cells were observed after 1 hour and their number increased until 8 hours. From here on, the CD107a staining remained stable until 24 hours after the start of the experiment. For the granzymes A, B, K and M, as well as for perforin, a clear loss in $CD107a^+$ NK cells can be noticed compared to $CD107a^-$

cells. Their release was already detected after 15 to 30 minutes and continued to decrease over time. Up to 24 hours, the reservoirs for GrzA and GrzM were still empty and not refilled, in contrast to GrzB storage. Here, the reservoir seems to be refilled already after 6 hours and further exceeded the levels of non-degranulating NK cells. After 24 hours, GrzB expression was again similar in $CD107a^-$ and $CD107a^+$ NK cells, whereas the complete refillment of perforin seems to take longer. The courses of GrzH showed a slightly different picture, where no differences in granzyme levels could be detected between degranulating and non-degranulating NK cells. Instead, an overall slight decrease of GrzH can be observed, which differs greatly from the release pattern of the other granzymes. This finding could already explain, why GrzH activity was only rarely monitored in target cells of activated NK cells.

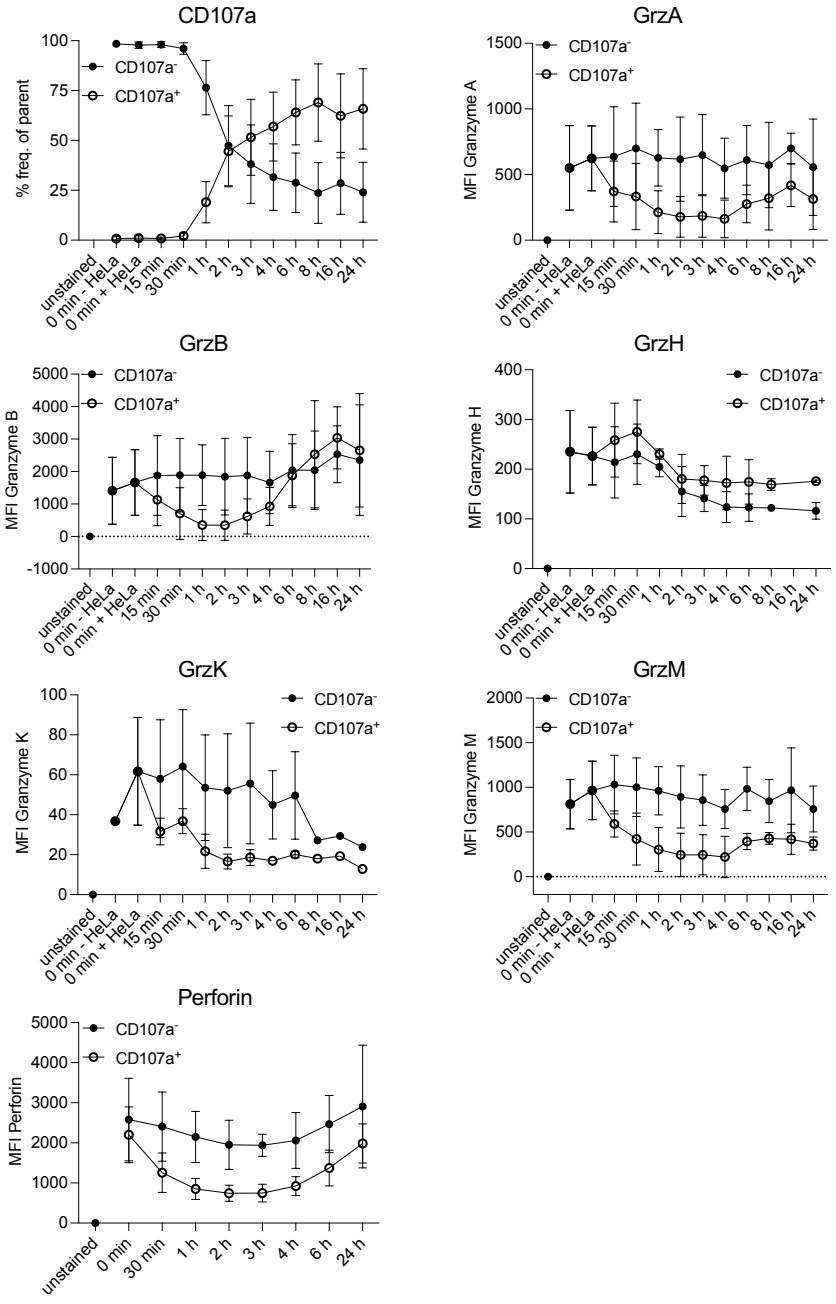

Figure 36: Granzyme content release of activated NK cells during co-incubation with HeLa CD48 target cells (E:T 1:2). Mean fluorescence intensity of individual granzymes and perforin as well as percentages of CD107a positive and negative cells was monitored during the co-incubation of activated NK cells with HeLa cells within 24 h.

To investigate whether the GrzB refillment was accurate, we repeated the experiment with additional incubation of the NK cells with the protein translation inhibitor cycloheximide (CHX). **Figure 37** shows the results for the percentage of $CD107a^-$ and $CD107a^+$ NK cells and for all granzymes. Since GrzB restorage occurred after 6 hours, the endpoint for this kinetic was set accordingly to this time point. The upper left graph again shows the percentage of $CD107a^-$ and $CD107a^+$ NK cells. In this experiment, the intersection of the two curves occurred

later than in the experiment without CHX incubation, while a comparable picture can be described for the granzyme release. GrzA, GrzM and GrzK are still depleted in degranulating NK cells and for GrzH a relatively stable expression in both CD107a$^-$ and CD107a$^+$ NK cells can be detected. In case of GrzB, a refillment or expression overshoot was no longer observed. This result suggests that the recognition of GrzB loss and its regulation for recovery occurs independently of the other granzymes. Although the other granzymes have also been secreted and these cells are obviously deficient, the NK cells' first step is to replenish GrzB. This rapid replenishment also suggests that GrzB is the most important granzyme for NK cell cytotoxicity.

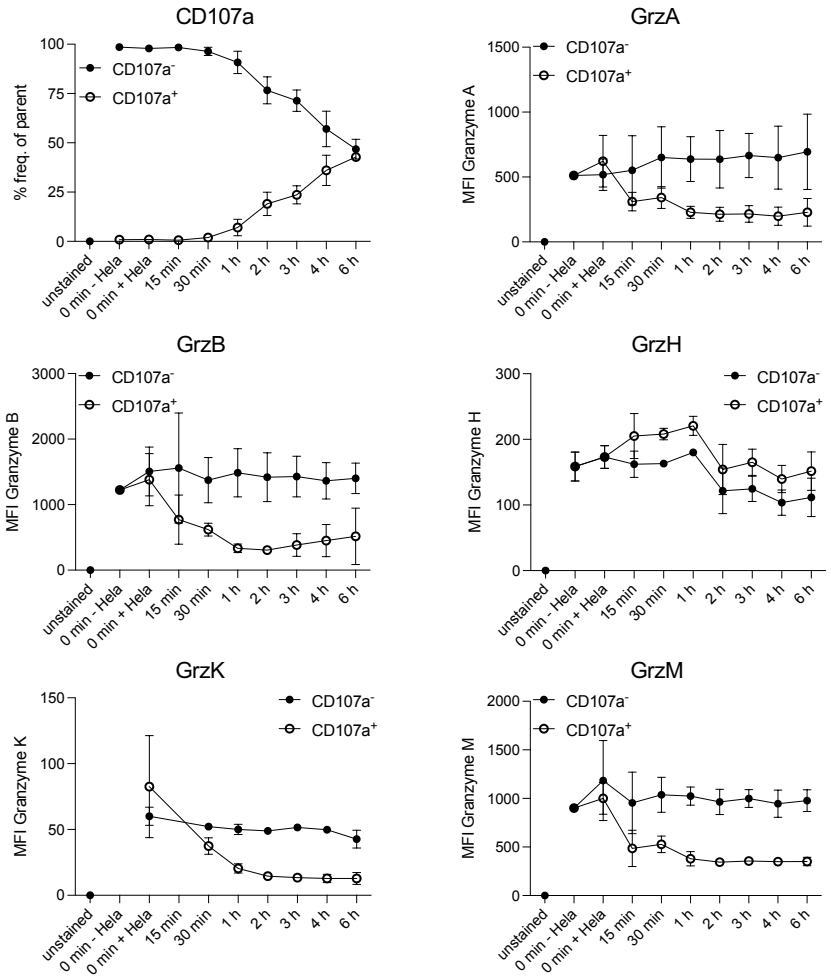

Figure 37: Granzyme content release of activated NK cells during co-incubation with HeLa CD48 target cells (E:T 1:2) with additional CHX incubation. NK cells were pre-incubated with the protein translation inhibitor cycloheximide (CHX). Mean fluorescent intensity of the individual granzymes as well as percentages of CD107a positive and negative cells was monitored during the co-incubation of activated NK cells with HeLa cells within 24 h.

9 Discussion

9.1 Fluorescent localization reporters

Natural killer cells play important roles in the early defense against several pathogens and protect us from aberrant cells. Their activation is tightly regulated, but fast and efficient when it comes to the detection of target cells. NK cells have the choice between two different pathways to exert their cytotoxicity, the death receptor-mediated and the granule-mediated pathway. The latter was the focus of this thesis. Lytic granules are secretory vesicles that contain several cytotoxic proteins such as the serin proteases granzymes as well as perforin and granulysin. While GrzB is well described in literature, the other human granzymes A, H, K and M have long been of only secondary interest to researchers. In this thesis we have therefore been interested in the functionality of these granzymes. We wondered why NK cells possess five different granzymes. Do these granzymes have their own task or are they supporters of GrzB? We also wanted to figure out what strategy the NK cells follow when the main player GrzB is depleted. Are NK cells still able to perform cytotoxicity and if so, to what extent? Are the other granzymes used at all by NK cells to kill target cells? To answer these questions, we created fluorescent reporters to monitor granzyme activity within target cells. Compared to other specific protease biosensors based on fluorophore quenching (Packard et al., 2007), FRET imaging (Choi and Mitchison, 2013) or luciferase-dependent bioluminescence (Li et al., 2014, Vrazo et al., 2015, Kanno et al., 2007) our reporter allows parallel monitoring of the activity of two proteases within a single target cell. An advantage of the direct comparison of two granzymes is the possibility to draw conclusions about the potency of the different granzymes and to investigate a possible temporal order of granzyme activity. To facilitate true direct comparability of the activity of two granzymes, the individual reporters are encoded on a single plasmid and are equimolarly expressed in target cells under the control of a single promoter, given by the genetic coupling via a T2A sequence. In previous studies, protease activities were measured in parallel by transfecting two plasmids, each encoding one reporter (Liesche et al., 2018). This may result in inaccuracies in both the absolute amounts of the respective plasmids taken up by the cells and the

possible different expression levels of the individual constructs. Furthermore, the expression of reporters by target cells is also more advantageous in terms of comparability between target cells and temporal measurement compared to cell-permeable substrates used in some studies (Packard et al., 2007). Our reporters, in which cleavage leads to a redistribution of fluorescent proteins, are ideal for monitoring granzyme activity in individual cells over time using microscopy. Thus, a statement can be made about the kinetics and temporal order, which is unclear in bulk assays, so that important physiological details can be lost. On the other hand, systems using an on-off-system allow statistical bulk analysis via flow cytometry, whereas our system is more time-consuming due to the detailed analysis of individual cells.

The cleavage sites that function as bait for the different granzymes were identified by positional scanning combinatorial libraries or analysing their substrates (Mahrus and Craik, 2005, Guo et al., 2010). Since GrzB is the best-described granzyme, its target sequences are also well studied. Therefore, several peptide sequences have been extracted and confirmed to be cleaved by GrzB. For example, the peptide sequences RIED'S and VGPD'FGR were found in the substrates BID and DNA-PKc, respectively (Choi and Mitchison, 2013, Backes et al., 2005, Casciola-Rosen et al., 2007). These cleavage sites were already used in several studies, including the ones mentioned above, to create GrzB reporters. Liesche et al. created single fluorescent reporters comparing these two GrzB cleavage sites. Compared to the RIED'S reporter, the GrzB activity measured with the VGPD'FGR reporter was more distinguishable from caspase 8 activity, whereupon the peptide sequence VGPD'FGR was chosen to design our reporters (Liesche et al., 2018). Furthermore, this group already tested the cleavage sites of GrzA, H, K and M, which rely on the findings of Mahrus et al.: RIED'S for GrzB, IGNR'S for GrzA, PTSY'G for GrzH, YRFK'G for GrzK and KVPL'AA for GrzM. Thus, we used these sequences for GrzA, H, K and M to create our reporters. Also, research groups including Mahrus et al. were able to design specific inhibitors for all granzymes except for GrzH (Guo et al., 2010, Wu et al., 2009, Mahrus and Craik, 2005, Mahrus et al., 2004). With these inhibitors the specificity of the peptide sequences for the individual granzyme was verified again. Therefore, it was important for us to prove the functionality of these individual cleavage sites in our reporters.

Unfortunately, only the target reporter cell incubation with recombinant GrzA and GrzB led to conclusive results via Western blot analysis (**figure 7**), while the other three granzymes did not show a definitive outcome (data not shown). One possible explanation could be the different sources of the recombinant granzymes. While the granzymes A and B were produced and isolated from the human NK cell lines NK92 or YT, GrzH, K and M were purified from *E. coli* or mouse myeloma cells (NS0). Since the glycosylation status of granzymes might be relevant for their activity (Sattar et al., 2003), the origin of the respective recombinant granzyme could influence the outcome of *in vitro* experiments based on host cell specific posttranslational modifications. Due to the fact that we were able to deliver GrzB but not GrzA into the target reporter cells by electroporation, we cannot exclude that the recombinant granzymes H, K and M were also unable to enter the target cells and therefore no activity was measured. Whole cell lysates of target reporter cells, produced by nitrogen cavitation, allowed both recombinant GrzA and GrzB to fulfil their task. This observation might be explained by the fact that GrzA is a homodimer and twice as large as GrzB, and therefore was not able to enter the target cell by electroporation due to its size. Furthermore, the other granzymes used in nitrogen cavitation experiments could be inhibited by the cellular content, including organelle fractions, of the target cells. Thus, the lysis of cell organelles such as the endoplasmic reticulum could lead to a pH shift that could be unfavourable for the granzyme activity as their optimal pH is around 7 (Griffiths and Isaaz, 1993). Also, granzyme inhibition by masking target sequences or alternative targeting cannot be excluded.

Although over 70% of the cells express the reporter, the individual cells appear to produce less of the GrzK-GrzB reporter than the other reporter cells. This could explain why the cleavage product is not visible in our Western blot, as the signal is too weak to detect. Fortunately, the heterogeneity in reporter expression levels is not important in microscopy, since the ratio between nuclear and cytosolic fluorescence is calculated for each individual target cell. Using NK92 granzyme KOs, we were able to confirm reporter specificity for GrzA and GrzB, as the fluorescence measurement was at baseline levels when we incubated the NK92 GrzB KO or GrzA&B KO with the GrzA-GrzB HeLa reporter cells in **figure 14**. From the data presented in **figures 8 and 14** we can conclude that the granzyme reporters for GrzA and GrzB are very specific for the respective granzyme activity,

and also do not lead to any cleavage of the granzyme reporters for GrzH, GrzK and GrzM. In activated NK cells, we found GrzH, K and M activity in microscopy experiments (**figure 32**). Inhibition of granzymes with the serin protease inhibitor DCI again resulted in baseline fluorescence levels for all reporters (**figure 35**), which confirmed specific granzyme activity. However, DCI was previously found to not inhibit GrzM effectively (Rukamp et al., 2004). This is contrary to our experimental results and cannot be conclusively clarified. In addition, we investigated whether weak fluorescence signals triggered by other granzymes than GrzB were true signals or background signal. False positive signals could be the result of target cell shrinkage upon cell death. For the granzymes A, H, K and M, the measured signals increased around 5 minutes before target cell death (**figures 13, 21, 23A and 32 left graphs**). Experiments with uncleavable reporters revealed the background signal by the effect just described (**figure 15B and 33B**). Results for the individual effector cells are discussed in more detail in the next two chapters.

In summary, the cleavage sites for granzymes were identified by positional scanning of combinatorial libraries or analysing their substrates (Mahrus and Craik, 2005, Guo et al., 2010). In our experiments, the specificity of the cleavage sites for GrzA and GrzB was confirmed by Western blot experiments, but the proof of specificity for the cleavage sites of the granzymes H, K and M was not possible. Experiments with DCI pre-treatment of effector cells resulted in baseline levels of all granzyme reporters, which suggests that the reporters are granzyme specific. Granzymes cleave several different substrates and therefore recognize a variety of cleavage sites. This does not mean that less preferred cleavage sites are wrong or less important. Some of them are more suitable for our purposes of reporter design as they are cleaved more efficiently. Under physiological conditions, a better outcome additionally depends on the relevance of the granzyme substrate. The cleavage of a critical or a bystander substrate could result in the activation of different apoptotic pathways, the number of follow-up substrates or interaction partners. The accessibility and subcellular localization of the native substrates also plays a major role.

9.2 NK92

Since NK cells and therefore granzymes become more and more important in tumor immunotherapy (Klingemann et al., 2016), we started to characterize the killing strategy of NK92 cells. NK92 cells are highly cytotoxic against tumor cells and can be more easily propagated and genetically manipulated compared to primary NK cells. We wanted to test whether NK92 will be still able to exhibit cytotoxicity when the main granzyme GrzB, or both GrzA and GrzB, are depleted. The successful use of the CRISPR/Cas9 method to knock out these granzymes in NK92 cells was verified by flow cytometry and is shown in **figure 9**.

Except for slightly different expression levels of the activating NK cell receptors NKp30 and NKp44, all cytotoxic proteins and surface molecules tested were equally expressed among NK92 WT and KO cell lines (**figures 9, 10, 11**). Different expression levels as well as degranulation potentials can be explained by the clonality of the KO cell lines, which unfortunately cannot be avoided. Moreover, the expression levels of activating NK cell receptors could also lead to different degranulation outcome among these cell lines. To curb the problem, several individual clones have been combined to reduce uncommon phenotypes in our Grz KO cell lines.

Since there are only minor changes in the expression levels of activating NK cell receptors but not in the granzyme content or other important cytotoxic proteins, the NK92 WT and granzyme KO cell lines were used in different cytotoxicity assays to investigate their killing strategies. Bulk cytotoxicity assays (**figure 16**) already showed the impairment of NK cell cytotoxicity due to the loss of granzymes, although death receptors mostly compensated for this. The inhibition of death receptors allowed a closer look at the importance of the different granzymes in the killing strategy of NK92 cells. The loss of GrzB had a stronger effect on NK92 cytotoxicity than the loss of GrzA, which is also confirmed by single cell analysis in our microscopy experiments (**figure 14**) and is also in agreement with the literature (Liesche et al., 2018, Mahrus and Craik, 2005). The lower contribution of GrzA can be explained by several aspects. GrzB is expressed by NK92 at a higher level than GrzA (**figure 9**), consequently less GrzA molecules enter the target cell and cleave the reporter. However, we can only make a statement about the overall level of granzyme expression in the NK

cell, but not about the content of individual granules. Since NK92 cells use only about 10% of their granules in each attack (Gwalani and Orange, 2018), it remains unclear if the granzyme content in granules is variable or whether NK cells are able to select granules that have a specific granzyme content. Furthermore, lower expression levels of GrzA could contribute to the observation that killing by GrzA takes much longer compared to GrzB (**figure 14A and B**). Moreover, the substrate conversion rate by GrzA or delivery of GrzA into the target cell could further contribute to this theory. As mentioned earlier, the cleavage efficiency of the peptide sequences used could also be different for the compared granzymes, since we do not know for all of them whether they originate from critical or bystander substrates (Andrade et al., 1998, Plasman et al., 2011). Finally, the mere fact that GrzA is a homodimer could make a big difference. Compared to the other granzymes, GrzA is the only one that forms a homodimer and is therefore twice as large (Joeckel and Bird, 2014b). This could already be a disadvantage on the way to the substrate, but could also affect the cleavage of the reporter, as access to the active site of GrzA might be restricted in the dimeric state (Bell et al., 2003).

Contrary to our expectations, target cells killed by GrzA (NK92 GrzB KO) did not exhibit a shifted ratio of types of cell death. The target cells showed a comparable ratio of membrane blebbing (apoptosis) and membrane leakage (necrosis or other forms of cell death) as in GrzB-mediated cell deaths. It is already known from the literature that GrzA can induce pyroptosis by gasdermin B (GSDMB), which is a form of proinflammatory cell death (Zhou et al., 2020). In our microscopy experiments, we did not verify whether membrane leakage could be pyroptosis. HeLa cells do weakly express the GSDMB isoform GSDML1 (Sun et al., 2008), but this pathway does not seem to be favoured in our experiments, as we could not detect a higher ratio of target cell deaths with membrane leakage triggered by GrzA compared to GrzB.

The fact that NK92 kill HeLa cells exclusively by using GrzA and GrzB is also shown in another cytotoxicity assay (**figure 17**). Interestingly, the studies of Liesche et al. revealed activity of GrzB, A, H and K but not M in HeLa reporter cells treated with NK92-C1 effector cells (Liesche et al., 2018). Furthermore, the chromium-release results in **figure 17** clearly show that granzymes mediate

target cell specific cytotoxicity. While NK92 cannot induce cytotoxicity in HeLa or 721.221 cells after depletion of the main granzymes A and B and additional inhibition of death receptors, Jurkat cells were still killed. This finding was very surprising, since the degranulation of NK92 triggered by Jurkat cells was very low compared to the other target cells (**figure 12**). This could be explained by the possible secretion of membrane-less complexes of cytotoxic molecules (supramolecular attack particles (SMAP)) by NK cells and is dependent on the diversity of receptor engagement (Ambrose et al., 2020). Like NK92 WT, NK92 GrzA&B KO cells were still able to kill the target cells without using death receptors (**figure 17**). It was therefore suggested that the granzymes H, K and M could play a role here. For example, GrzH was found to be internalized by Jurkat cells into endosome-like vesicles (Edwards et al., 1999). However, we do not know whether Jurkat cells express granzyme substrates that are not available in HeLa and 721.221. Also, a possible influence of the phenotype of the target cells on the NK cell-specific release of granzymes is not yet known, but a heterogeneous secretion of vesicles, SMAPs and cytotoxic molecules triggered by different plate-bound ligands has already been described in human NK cells (Ambrose et al., 2020). Furthermore, Gross et al. showed that the expression of Hsp70 on target cells triggers both the expression and release of GrzB by NK cells. Furthermore, GrzB is taken up into $Hsp70^{+}$ target cells in a perforin-independent manner (Gross et al., 2003). By the additional incubation with DCI (**figure 19B**) we could exclude the contribution of perforin and granulysin to the killing of Jurkat cells. Furthermore, cysteine proteases could contribute to the lysis of Jurkat, as some isocumarins, the class of inhibitors DCI is part of, were able to inhibit these enzymes, too (Powers et al., 2002). Similar results were found in granzyme KO mice. Here, despite their GrzA and GrzB double KO, the T or NK cells were able to induce cell death of lymphoma target cells with or without Fas expression (Simon et al., 1997). Like us, this study concluded that the influence of other (unknown) proteases cannot be ruled out. Interestingly, the target cells in our study are like Jurkat cells: lymphoma cells that seem to be sensitive to some other proteases. Therefore, it was surprising that 721.221, which are also lymphoma cells but B cells, show the same cytotoxic “pattern” as HeLa target cells in our experiments and not a comparable “pattern” to Jurkat cells (**figure 17**). Unfortunately, experiments with Jurkat reporter cells could not

unravel whether the killing of these cells were triggered by one of the remaining granzymes H, K or M or a (unknown) serine protease. Effects that we could observe with the NK92 WT were hardly recognizable when the NK92 GrzA&B KO cells were used as effector cells (**figure19D**). Therefore, another approach could be the co-incubation of lysates from both the target reporter cells and the effector cells. The endogenous granzymes might be able to cleave the reporters. However, it would be difficult to determine which granzyme or other protease is responsible for cleaving the reporters. Knockouts of the granzymes H, K and M in NK92 GrzA&B KO cells might give further clues as to whether it is one of these granzymes.

Taken together, GrzB plays a more important role in the cytotoxicity of NK92 cells than GrzA. In our study, we were able to show that the human NK92 cell line relies mainly on GrzB for its killing strategy, and is supported by GrzA. A previous study by Shresta et al. suggested that GrzA could act as a “backup” system for GrzB in mouse CTL, which would be in line with our findings for the human NK92 cell line (Shresta et al., 1999). In fact, the loss of GrzB in NK92 cells is compensated by GrzA. In contrast to GrzB, GrzA-mediated killing takes longer. The reasons for this can be very diverse, but are not yet clarified. Since GrzB is able to induce both caspase-dependent and -independent pathways, the caspase-independent GrzA pathway is therefore thought to provide a failsafe mechanism in case that the apoptosis-initiating caspase pathway is blocked by target cell properties (Shresta et al., 1999, Beresford et al., 1999).

9.3 Primary NK cells

NK92 cells kill their HeLa target cells exclusively via GrzB with the support of GrzA. Loss of GrzB in NK92 leads to a GrzA-based killing strategy without the influence of any other granzyme. A comparable preference of GrzB has previously been described in the literature for primary NK and T cells. Our microscopy experiments additionally revealed the use the granzymes H, K and M (**figure 21 and 32**). Surprisingly, GrzA appears to play a greater role in activated NK cell-induced cytotoxicity than expected, as GrzA dominated or was equally active as GrzB in 68% of target cell kills. Furthermore, the activity of the granzymes M, K and H was observed (**figure 32)** and the order can therefore be

described as: A/B > M > K > H (**figure 32E**). In resting NK cells, GrzB was also dominantly active in the target cells, while the preference for the other granzymes shifted towards GrzM activity (B > M > A > K > H) (**figure 21E**). For both resting and activated NK cells, dominant killing strategies of GrzB were more or less supported by the other granzymes. Strong activity of the granzymes H, K and M were observed exclusively together with GrzB (**figures 21 and 32**). Interestingly, the differences in the relative expression levels of the individual granzymes do not necessarily reflect the activity of the granzymes in the target cells (**figure 26**). For example, GrzA is shown to be expressed to comparable levels by resting and activated NK cells, but it appears to be used to different extents and frequencies in their killing strategy. Furthermore, GrzH is expressed significantly higher by resting NK cells than by activated ones, but GrzH activity is found rarely in target cells of both effectors. In contrast, the expression levels of GrzM do show a correlation with its activity in target cells. Resting NK cells triggered more GrzM activity than activated target cells and also express more GrzM. However, we found these very heterogeneous granzyme expression levels in primary NK cells by analyzing them in bulk (**figure 20**), but the granzyme content of a single NK cell killing a target cell in our microscopy experiment remains unclear due to technical limitations. Therefore, a target cell death triggered by equal activity of GrzB and GrzM **(figure 21D**, right) might be triggered by a NK cell that also equally expressed these two granzymes, while a GrzB dominant killing was executed by a NK cell with high GrzB content and lower expression levels of other granzymes (**figure 20**). Contrary to our expectations, the distinct granzyme levels in $CD56^{dim}$ and $CD56^{bright}$ did not result in different killing strategies triggered by the two subpopulations. Although $CD56^{bright}$ NK cells express significantly more GrzK than their $CD56^{dim}$ counterparts (**figure 22**), the killing strategy seems to be similar in microscopy experiments (**figure 23**).

Accordingly, we wondered whether the release of granzymes by NK cells could be correlated with granzyme activity in target cells rather than with their expression levels. Indeed, $CD56^{bright}$ NK cells secrete more GrzK than $CD56^{dim}$ (**figure 24A**), but a higher release did not result in higher reporter cleavage within the target cells. One hypothesis could be that the quantitative release of GrzB by $CD56^{bright}$ NK cells is still too high (**figure 24B**) to be competed by GrzK, or GrzB is qualitatively more efficient in delivery, entry into target cells or reporter

cleavage. The first hypothesis is supported by the fact that both GrzA and GrzK are required in micro molar amounts, while GrzB is already sufficient in nanomolar amounts to induce apoptosis (Joeckel and Bird, 2014a). Another explanation could be that GrzK plays a less important role in killing target cells. NK cells have a large supply of GrzK mRNA (Przetak et al., 1995), which is presumably waiting for the right stimulus to induce protein expression. Interestingly, GrzK content is strongly reduced when NK cells become active, supporting the theory that GrzK is less important for target cell killing, but rather has immunomodulatory functions (**figure 25**) (Bade et al., 2005b, Bouwman et al., 2021, Sharma et al., 2016). In addition, the surface expression of activating receptors on the NK cell or of ligands on the target cells could lead to different signal transduction resulting in the release of a varying granzyme content. A varying reaction of two NK cell subpopulations was already observed in our experiments. Here, $CD56^{dim}$ NK cells respond more strongly to the stimulation with anti-NKp30, possibly because they express more NCR compared to $CD56^{bright}$, whereas the unspecific stimulation with ionomycin and PMA resulted in comparable granzyme release among CD56 dim and bright NK cells. The generally weaker stimulation with anti-NKp30 could be due to the fact that the synergy of different activating receptors is required for sufficient stimulation of resting NK cells (Bryceson et al., 2006, Marcus et al., 2014). Interestingly, heterogeneous secretion of vesicles and cytotoxic molecules triggered by different ligands has already been observed in human NK cells (Ambrose et al., 2020).

However, the question arose why we were unable to proliferate the GrzK-rich NK cell population under our cell culture conditions. Therefore, we wondered which factors could influence the expression of granzymes during activating cell culture conditions. The upregulation of granzymes A and B, but also of perforin, has been attributed to stimulation with IL-2, IL-15 and IL-21 in several studies (Kim et al., 2010, Liu et al., 1989, Janas et al., 2005, Frederiksen et al., 2008, Jewett and Bonavida, 1996) and can be observed for our activated NK cells, triggered by exactly these interleukins used in our protocol. For this reason, PBMC were incubated with different stimuli. All stimuli tested appear to promote loss of GrzK in $CD56^{bright}$ NK cells but had no effect on $CD56^{dim}$ NK cells. We therefore concluded that GrzK loss occurs as soon as the NK cells become activated

(**figure 30**). As $CD56^{bright}$ NK cells are the more immature NK cells and adapt their content more and more to the $CD56^{dim}$ NK cells during culture further supports the theory that GrzK rather has immunomodulatory functions than it is important for target cell killing. Interestingly, as GrzK was found to potentiate lipopolysaccharide (LPS) induced cytokine release from monocytes (Wensink et al., 2014, Wensink et al., 2016), we suggested a possible positive feedback loop on the expression of other granzymes. This effect could be mediated by the production of pro-inflammatory cytokines by immune cells that trigger the upregulation of granzymes in CTLs or NK cells. GrzK could therefore enhance the indirect influence of LPS via other immune cells onto NK cells, which in turn leads to the expression of GrzB and is thus an indirect supporter. This theory is supported by our finding that $CD56^{bright}$ NK cells show higher GrzB expression than $CD56^{dim}$ cells after about 48 hours (**figure 28**).

Release of granzymes by activated NK cells revealed that, with the exception of GrzH, all granzymes were released upon degranulation (**figure 36**). NK cells that did degranulate ($CD107a^{+}$) exhibited reduced levels of the granzymes A, B, K and M as well as perforin already 15 to 30 minutes after co-incubation with target cells compared to NK cells that did not degranulate ($CD107a^{-}$). Moreover, the kinetics of granzyme release led us suggest that GrzH could be stored within other granules that are released at a later time point or only react to certain stimuli such as virus infected target cells. Because of its ability to cleave virus-related proteins, GrzH might be thought to protect the host cell from viral infection and therefore does not need to be released. Furthermore, GrzH is able to cleave the 100K adenovirus protein, which is an inhibitor of GrzB (Andrade et al., 2001, Andrade et al., 2007). This support of GrzB by GrzH could therefore be important in fighting virus-infected cells and thus tumor cells might not be the correct stimulus to trigger GrzH activity. We were therefore interested in the influence of uIFNα, which could mimic viral infection, as Type I IFN subtypes are secreted by peripheral blood leukocytes to protect against viral infections (Nyman et al., 1998, Szubin et al., 2008). In our experiments (**figure 29**), GrzH expression levels of resting NK cells did not respond to the incubation with uIFNα. Whether these assumptions are true under physiological conditions has not been targeted in our study or in the literature yet, but could explain why only little GrzH activity was observed in tumor target cells. Nevertheless, these experiments were performed

as bulk assays, too and do not allow conclusions for single cells. Whether all granzymes are stored and released from the same or separate lytic granules, was not targeted in this project and to our knowledge has not yet been adequately researched. Additionally, the age, activation level, maturation, priming status or education of a NK cell could influence the outcome of granule release and granzyme expression.

In summary, resting and activated primary NK cells show different granzyme expression levels and also use them differently. A higher expression of a certain granzyme does not seem to automatically correlate with a higher activity within the NK cells' target cell. Since we tested the NK cell killing strategy at the level of a single cell, but the granzyme content was measured in bulk, we cannot prove whether this assumption is true. As granzyme expression in primary NK cells appears to be very heterogeneous, a distinct phenotype in granzyme expression of different subpopulations could correlate with the granzyme-mediated killing-strategy they adopt. Moreover, as mentioned before, both the NK cell phenotype and the target cell phenotype could play a role. The possible correlation between ligand expression and granzyme release is still poorly understood. The entry of the granzyme into the different target cells as well as the substrate availability need to be understood to conclude on granzyme specific killing strategies. To further improve the NK cell immunotherapy, basic research is important to understand the cytotoxicity of NK cells to better equip effector cells to a given type of disease-specific target cell. Specific stimulation to generate a particular granzyme phenotype of NK cells could be tailored to the target cell, leading to a better outcome.

10 References

1984. IUPAC-IUB Joint Commission on Biochemical Nomenclature (JCBN). Nomenclature and symbolism for amino acids and peptides. Recommendations 1983. *Biochem J,* 219**,** 345-73.

ADRAIN, C., MURPHY, B. M. & MARTIN, S. J. 2005. Molecular ordering of the caspase activation cascade initiated by the cytotoxic T lymphocyte/natural killer (CTL/NK) protease granzyme B. *J Biol Chem,* 280**,** 4663-73.

AL-LAMKI, Z., WALI, Y. A., WASIFUDDIN, S. M., ZACHARIAH, M., AL-MJENI, R., LI, C., MURALITHARAN, S., AL-KHARUSI, K., GUNARATNE, P., PETERSON, L., GIBBS, R., GINGRAS, M. C. & MARGOLIN, J. F. 2005. Identification of prognosis markers in pediatric high-risk acute lymphoblastic leukemia. *Pediatr Hematol Oncol,* 22**,** 629-43.

ALBECK, J. G., BURKE, J. M., ALDRIDGE, B. B., ZHANG, M., LAUFFENBURGER, D. A. & SORGER, P. K. 2008. Quantitative analysis of pathways controlling extrinsic apoptosis in single cells. *Mol Cell,* 30**,** 11-25.

ALIMONTI, J. B., SHI, L., BAIJAL, P. K. & GREENBERG, A. H. 2001. Granzyme B induces BID-mediated cytochrome c release and mitochondrial permeability transition. *J Biol Chem,* 276**,** 6974-82.

AMBROSE, A. R., HAZIME, K. S., WORBOYS, J. D., NIEMBRO-VIVANCO, O. & DAVIS, D. M. 2020. Synaptic secretion from human natural killer cells is diverse and includes supramolecular attack particles. *Proc Natl Acad Sci U S A,* 117**,** 23717-23720.

ANDRADE, F., BULL, H. G., THORNBERRY, N. A., KETNER, G. W., CASCIOLA-ROSEN, L. A. & ROSEN, A. 2001. Adenovirus L4-100K assembly protein is a granzyme B substrate that potently inhibits granzyme B-mediated cell death. *Immunity,* 14**,** 751-61.

ANDRADE, F., FELLOWS, E., JENNE, D. E., ROSEN, A. & YOUNG, C. S. 2007. Granzyme H destroys the function of critical adenoviral proteins required for viral DNA replication and granzyme B inhibition. *EMBO J,* 26**,** 2148-57.

ANDRADE, F., ROY, S., NICHOLSON, D., THORNBERRY, N., ROSEN, A. & CASCIOLA-ROSEN, L. 1998. Granzyme B directly and efficiently cleaves several downstream caspase substrates: implications for CTL-induced apoptosis. *Immunity,* 8**,** 451-60.

ANTIA, R., SCHLEGEL, R. A. & WILLIAMSON, P. 1992. Binding of perforin to membranes is sensitive to lipid spacing and not headgroup. *Immunol Lett,* 32**,** 153-7.

ATKINSON, E. A., BARRY, M., DARMON, A. J., SHOSTAK, I., TURNER, P. C., MOYER, R. W. & BLEACKLEY, R. C. 1998. Cytotoxic T lymphocyte-assisted suicide. Caspase 3 activation is primarily the result of the direct action of granzyme B. *J Biol Chem,* 273**,** 21261-6.

BABICHUK, C. K. & BLEACKLEY, R. C. 1997. Mutational analysis of the murine granzyme B gene promoter in primary T cells and a T cell clone. *J Biol Chem,* 272**,** 18564-71.

BABICHUK, C. K., DUGGAN, B. L. & BLEACKLEY, R. C. 1996. In vivo regulation of murine granzyme B gene transcription in activated primary T cells. *J Biol Chem,* 271**,** 16485-93.

BACKES, C., KUENTZER, J., LENHOF, H. P., COMTESSE, N. & MEESE, E. 2005. GraBCas: a bioinformatics tool for score-based prediction of Caspase- and Granzyme B-cleavage sites in protein sequences. *Nucleic Acids Res,* 33**,** W208-13.

BADE, B., BOETTCHER, H. E., LOHRMANN, J., HINK-SCHAUER, C., BRATKE, K., JENNE, D. E., VIRCHOW, J. C., JR. & LUTTMANN, W. 2005a. Differential expression of the granzymes A, K and M and perforin in human peripheral blood lymphocytes. *Int Immunol,* 17**,** 1419-28.

BADE, B., LOHRMANN, J., TEN BRINKE, A., WOLBINK, A. M., WOLBINK, G. J., TEN BERGE, I. J., VIRCHOW, J. C., JR., LUTTMANN, W. & HACK, C. E. 2005b. Detection of soluble human granzyme K in vitro and in vivo. *Eur J Immunol,* 35**,** 2940-8.

BALAJI, K. N., SCHASCHKE, N., MACHLEIDT, W., CATALFAMO, M. & HENKART, P. A. 2002. Surface cathepsin B protects cytotoxic lymphocytes from self-destruction after degranulation. *J Exp Med,* 196**,** 493-503.

BANERJEA, A., AHMED, S., HANDS, R. E., HUANG, F., HAN, X., SHAW, P. M., FEAKINS, R., BUSTIN, S. A. & DORUDI, S. 2004. Colorectal cancers with microsatellite instability display mRNA expression signatures characteristic of increased immunogenicity. *Mol Cancer,* 3**,** 21.

BARNHART, B. C., ALAPPAT, E. C. & PETER, M. E. 2003. The CD95 type I/type II model. *Semin Immunol,* 15**,** 185-93.

BARRY, M., HEIBEIN, J. A., PINKOSKI, M. J., LEE, S. F., MOYER, R. W., GREEN, D. R. & BLEACKLEY, R. C. 2000. Granzyme B short-circuits the need for caspase 8 activity during granule-mediated cytotoxic T-lymphocyte killing by directly cleaving Bid. *Mol Cell Biol,* 20**,** 3781-94.

BEAL, A. M., ANIKEEVA, N., VARMA, R., CAMERON, T. O., NORRIS, P. J., DUSTIN, M. L. & SYKULEV, Y. 2008. Protein kinase C theta regulates stability of the peripheral adhesion ring junction and contributes to the sensitivity of target cell lysis by CTL. *J Immunol,* 181**,** 4815-24.

BEAUDOUIN, J., LIESCHE, C., ASCHENBRENNER, S., HORNER, M. & EILS, R. 2013. Caspase-8 cleaves its substrates from the plasma membrane upon CD95-induced apoptosis. *Cell Death Differ,* 20**,** 599-610.

BELL, J. K., GOETZ, D. H., MAHRUS, S., HARRIS, J. L., FLETTERICK, R. J. & CRAIK, C. S. 2003. The oligomeric structure of human granzyme A is a determinant of its extended substrate specificity. *Nat Struct Biol,* 10**,** 527-34.

BERESFORD, P. J., XIA, Z., GREENBERG, A. H. & LIEBERMAN, J. 1999. Granzyme A loading induces rapid cytolysis and a novel form of DNA damage independently of caspase activation. *Immunity,* 10**,** 585-94.

BERESFORD, P. J., ZHANG, D., OH, D. Y., FAN, Z., GREER, E. L., RUSSO, M. L., JAJU, M. & LIEBERMAN, J. 2001. Granzyme A activates an endoplasmic reticulum-associated caspase-independent nuclease to induce single-stranded DNA nicks. *J Biol Chem,* 276**,** 43285-93.

BIRD, C. H., SUN, J., UNG, K., KARAMBALIS, D., WHISSTOCK, J. C., TRAPANI, J. A. & BIRD, P. I. 2005. Cationic sites on granzyme B contribute to cytotoxicity by promoting its uptake into target cells. *Mol Cell Biol,* 25**,** 7854-67.

BIRD, C. H., SUTTON, V. R., SUN, J., HIRST, C. E., NOVAK, A., KUMAR, S., TRAPANI, J. A. & BIRD, P. I. 1998. Selective regulation of apoptosis: the cytotoxic lymphocyte serpin proteinase inhibitor 9 protects against granzyme B-mediated apoptosis without perturbing the Fas cell death pathway. *Mol Cell Biol,* 18**,** 6387-98.

BLADERGROEN, B. A., STRIK, M. C., BOVENSCHEN, N., VAN BERKUM, O., SCHEFFER, G. L., MEIJER, C. J., HACK, C. E. & KUMMER, J. A. 2001. The granzyme B inhibitor, protease inhibitor 9, is mainly expressed by dendritic cells and at immune-privileged sites. *J Immunol,* 166**,** 3218-25.

BLADERGROEN, B. A., STRIK, M. C., WOLBINK, A. M., WOUTERS, D., BROEKHUIZEN, R., KUMMER, J. A. & HACK, C. E. 2005. The granzyme B inhibitor proteinase inhibitor 9 (PI9) is expressed by human mast cells. *Eur J Immunol,* 35**,** 1175-83.

BLAKELY, A., GORMAN, K., OSTERGAARD, H., SVOBODA, K., LIU, C. C., YOUNG, J. D. & CLARK, W. R. 1987. Resistance of cloned cytotoxic T lymphocytes to cell-mediated cytotoxicity. *J Exp Med,* 166**,** 1070-83.

BLINK, E. J., JIANSHENG, Z., HU, W., CALANNI, S. T., TRAPANI, J. A., BIRD, P. I. & JANS, D. A. 2005. Interaction of the nuclear localizing cytolytic granule serine protease granzyme B with importin alpha or beta: modulation by the serpin inhibitor PI-9. *J Cell Biochem,* 95**,** 598-610.

BLOTT, E. J. & GRIFFITHS, G. M. 2002. Secretory lysosomes. *Nat Rev Mol Cell Biol,* 3**,** 122-31.

BOIVIN, W. A., COOPER, D. M., HIEBERT, P. R. & GRANVILLE, D. J. 2009. Intracellular versus extracellular granzyme B in immunity and disease: challenging the dogma. *Lab Invest,* 89**,** 1195-220.

BORREGO, F., ULBRECHT, M., WEISS, E. H., COLIGAN, J. E. & BROOKS, A. G. 1998. Recognition of human histocompatibility leukocyte antigen (HLA)-E complexed with HLA class I signal sequence-derived peptides by CD94/NKG2 confers protection from natural killer cell-mediated lysis. *J Exp Med,* 187**,** 813-8.

BOTS, M. & MEDEMA, J. P. 2006. Granzymes at a glance. *J Cell Sci,* 119**,** 5011-4.

BOTTINO, C., CASTRICONI, R., PENDE, D., RIVERA, P., NANNI, M., CARNEMOLLA, B., CANTONI, C., GRASSI, J., MARCENARO, S., REYMOND, N., VITALE, M., MORETTA, L., LOPEZ, M. & MORETTA, A. 2003. Identification of PVR (CD155) and Nectin-2 (CD112) as cell surface ligands for the human DNAM-1 (CD226) activating molecule. *J Exp Med,* 198**,** 557-67.

BOUWMAN, A. C., VAN DAALEN, K. R., CRNKO, S., TEN BROEKE, T. & BOVENSCHEN, N. 2021. Intracellular and Extracellular Roles of Granzyme K. *Front Immunol,* 12**,** 677707.

BOVENSCHEN, N., QUADIR, R., VAN DEN BERG, A. L., BRENKMAN, A. B., VANDENBERGHE, I., DEVREESE, B., JOORE, J. & KUMMER, J. A. 2009. Granzyme K displays highly restricted substrate specificity that only partially overlaps with granzyme A. *J Biol Chem,* 284**,** 3504-12.

BRANDT, C. S., BARATIN, M., YI, E. C., KENNEDY, J., GAO, Z., FOX, B., HALDEMAN, B., OSTRANDER, C. D., KAIFU, T., CHABANNON, C., MORETTA, A., WEST, R., XU, W., VIVIER, E. & LEVIN, S. D. 2009. The B7 family member B7-H6 is a tumor cell ligand for the activating natural killer cell receptor NKp30 in humans. *J Exp Med,* 206**,** 1495-503.

BRATKE, K., KUEPPER, M., BADE, B., VIRCHOW, J. C., JR. & LUTTMANN, W. 2005. Differential expression of human granzymes A, B, and K in natural killer cells and during CD8+ T cell differentiation in peripheral blood. *Eur J Immunol,* 35**,** 2608-16.

BRODIN, P., KARRE, K. & HOGLUND, P. 2009. NK cell education: not an on-off switch but a tunable rheostat. *Trends Immunol,* 30**,** 143-9.

BROWNE, K. A., BLINK, E., SUTTON, V. R., FROELICH, C. J., JANS, D. A. & TRAPANI, J. A. 1999. Cytosolic delivery of granzyme B by bacterial toxins: evidence that endosomal disruption, in addition to transmembrane pore formation, is an important function of perforin. *Mol Cell Biol,* 19**,** 8604-15.

BRYCESON, Y. T., LJUNGGREN, H. G. & LONG, E. O. 2009. Minimal requirement for induction of natural cytotoxicity and intersection of activation signals by inhibitory receptors. *Blood,* 114**,** 2657-66.

BRYCESON, Y. T., MARCH, M. E., LJUNGGREN, H. G. & LONG, E. O. 2006. Synergy among receptors on resting NK cells for the activation of natural cytotoxicity and cytokine secretion. *Blood,* 107**,** 159-66.

BURKHARDT, J. K., HESTER, S., LAPHAM, C. K. & ARGON, Y. 1990. The lytic granules of natural killer cells are dual-function organelles combining secretory and pre-lysosomal compartments. *J Cell Biol,* 111**,** 2327-40.

BURSHTYN, D. N., SHIN, J., STEBBINS, C. & LONG, E. O. 2000. Adhesion to target cells is disrupted by the killer cell inhibitory receptor. *Curr Biol,* 10**,** 777-80.

BUZZA, M. S., HIRST, C. E., BIRD, C. H., HOSKING, P., MCKENDRICK, J. & BIRD, P. I. 2001. The granzyme B inhibitor, PI-9, is present in endothelial and mesothelial cells, suggesting that it protects bystander cells during immune responses. *Cell Immunol,* 210**,** 21-9.

BUZZA, M. S., HOSKING, P. & BIRD, P. I. 2006. The granzyme B inhibitor, PI-9, is differentially expressed during placental development and up-regulated in hydatidiform moles. *Placenta,* 27**,** 62-9.

BUZZA, M. S., ZAMURS, L., SUN, J., BIRD, C. H., SMITH, A. I., TRAPANI, J. A., FROELICH, C. J., NICE, E. C. & BIRD, P. I. 2005. Extracellular matrix remodeling by human granzyme B via cleavage of vitronectin, fibronectin, and laminin. *J Biol Chem,* 280**,** 23549-58.

CASCIOLA-ROSEN, L., GARCIA-CALVO, M., BULL, H. G., BECKER, J. W., HINES, T., THORNBERRY, N. A. & ROSEN, A. 2007. Mouse and human granzyme B have distinct tetrapeptide specificities and abilities to recruit the bid pathway. *J Biol Chem,* 282**,** 4545-4552.

CHAMPSAUR, M. & LANIER, L. L. 2010. Effect of NKG2D ligand expression on host immune responses. *Immunol Rev,* 235**,** 267-85.

CHOI, P. J. & MITCHISON, T. J. 2013. Imaging burst kinetics and spatial coordination during serial killing by single natural killer cells. *Proc Natl Acad Sci U S A,* 110**,** 6488-93.

CHOWDHURY, D., BERESFORD, P. J., ZHU, P., ZHANG, D., SUNG, J. S., DEMPLE, B., PERRINO, F. W. & LIEBERMAN, J. 2006. The exonuclease TREX1 is in the SET complex and acts in concert with NM23-H1 to degrade DNA during granzyme A-mediated cell death. *Mol Cell,* 23**,** 133-42.

CHOWDHURY, D. & LIEBERMAN, J. 2008. Death by a thousand cuts: granzyme pathways of programmed cell death. *Annu Rev Immunol,* 26**,** 389-420.

CHOY, J. C., HUNG, V. H., HUNTER, A. L., CHEUNG, P. K., MOTYKA, B., GOPING, I. S., SAWCHUK, T., BLEACKLEY, R. C., PODOR, T. J., MCMANUS, B. M. & GRANVILLE, D. J. 2004. Granzyme B induces smooth muscle cell apoptosis in the absence of perforin: involvement of extracellular matrix degradation. *Arterioscler Thromb Vasc Biol,* 24**,** 2245-50.

CLAUS, M., MEINKE, S., BHAT, R. & WATZL, C. 2008. Regulation of NK cell activity by 2B4, NTB-A and CRACC. *Front Biosci,* 13**,** 956-65.

COHNEN, A., CHIANG, S. C., STOJANOVIC, A., SCHMIDT, H., CLAUS, M., SAFTIG, P., JANSSEN, O., CERWENKA, A., BRYCESON, Y. T. & WATZL, C. 2013. Surface CD107a/LAMP-1 protects natural killer cells from degranulation-associated damage. *Blood,* 122**,** 1411-8.

COLONNA, M., NAVARRO, F., BELLON, T., LLANO, M., GARCIA, P., SAMARIDIS, J., ANGMAN, L., CELLA, M. & LOPEZ-BOTET, M. 1997. A common inhibitory receptor for major histocompatibility complex class I molecules on human lymphoid and myelomonocytic cells. *J Exp Med,* 186**,** 1809-18.

CULLEN, S. P., ADRAIN, C., LUTHI, A. U., DURIEZ, P. J. & MARTIN, S. J. 2007. Human and murine granzyme B exhibit divergent substrate preferences. *J Cell Biol,* 176**,** 435-44.

DAVIS, D. M. & DUSTIN, M. L. 2004. What is the importance of the immunological synapse? *Trends Immunol,* 25**,** 323-7.

DE KONING, P. J., KUMMER, J. A., DE POOT, S. A., QUADIR, R., BROEKHUIZEN, R., MCGETTRICK, A. F., HIGGINS, W. J., DEVREESE, B., WORRALL, D. M. & BOVENSCHEN, N. 2011.

Intracellular serine protease inhibitor SERPINB4 inhibits granzyme M-induced cell death. *PLoS One,* 6**,** e22645.

DE SAINT BASILE, G., MENASCHE, G. & FISCHER, A. 2010. Molecular mechanisms of biogenesis and exocytosis of cytotoxic granules. *Nat Rev Immunol,* 10**,** 568-79.

DE WIT, H., WALTER, A. M., MILOSEVIC, I., GULYAS-KOVACS, A., RIEDEL, D., SORENSEN, J. B. & VERHAGE, M. 2009. Synaptotagmin-1 docks secretory vesicles to syntaxin-1/SNAP-25 acceptor complexes. *Cell,* 138**,** 935-46.

EDWARDS, K. M., KAM, C. M., POWERS, J. C. & TRAPANI, J. A. 1999. The human cytotoxic T cell granule serine protease granzyme H has chymotrypsin-like (chymase) activity and is taken up into cytoplasmic vesicles reminiscent of granzyme B-containing endosomes. *J Biol Chem,* 274**,** 30468-73.

ERIKSSON, M., LEITZ, G., FALLMAN, E., AXNER, O., RYAN, J. C., NAKAMURA, M. C. & SENTMAN, C. L. 1999. Inhibitory receptors alter natural killer cell interactions with target cells yet allow simultaneous killing of susceptible targets. *J Exp Med,* 190**,** 1005-12.

EWEN, C. L., KANE, K. P. & BLEACKLEY, R. C. 2012. A quarter century of granzymes. *Cell Death Differ,* 19**,** 28-35.

FAN, Z., BERESFORD, P. J., OH, D. Y., ZHANG, D. & LIEBERMAN, J. 2003. Tumor suppressor NM23-H1 is a granzyme A-activated DNase during CTL-mediated apoptosis, and the nucleosome assembly protein SET is its inhibitor. *Cell,* 112**,** 659-72.

FELDMANN, J., CALLEBAUT, I., RAPOSO, G., CERTAIN, S., BACQ, D., DUMONT, C., LAMBERT, N., OUACHEE-CHARDIN, M., CHEDEVILLE, G., TAMARY, H., MINARD-COLIN, V., VILMER, E., BLANCHE, S., LE DEIST, F., FISCHER, A. & DE SAINT BASILE, G. 2003. Munc13-4 is essential for cytolytic granules fusion and is mutated in a form of familial hemophagocytic lymphohistiocytosis (FHL3). *Cell,* 115**,** 461-73.

FELLOWS, E., GIL-PARRADO, S., JENNE, D. E. & KURSCHUS, F. C. 2007. Natural killer cell-derived human granzyme H induces an alternative, caspase-independent cell-death program. *Blood,* 110**,** 544-52.

FERNANDEZ, N. C., TREINER, E., VANCE, R. E., JAMIESON, A. M., LEMIEUX, S. & RAULET, D. H. 2005. A subset of natural killer cells achieves self-tolerance without expressing inhibitory receptors specific for self-MHC molecules. *Blood,* 105**,** 4416-23.

FISCHER, U., JANICKE, R. U. & SCHULZE-OSTHOFF, K. 2003. Many cuts to ruin: a comprehensive update of caspase substrates. *Cell Death Differ,* 10**,** 76-100.

FREDERIKSEN, K. S., LUNDSGAARD, D., FREEMAN, J. A., HUGHES, S. D., HOLM, T. L., SKRUMSAGER, B. K., PETRI, A., HANSEN, L. T., MCARTHUR, G. A., DAVIS, I. D. & SKAK, K. 2008. IL-21 induces in vivo immune activation of NK cells and CD8(+) T cells in patients with metastatic melanoma and renal cell carcinoma. *Cancer Immunol Immunother,* 57**,** 1439-49.

FREGEAU, C. J. & BLEACKLEY, R. C. 1991. Transcription of two cytotoxic cell protease genes is under the control of different regulatory elements. *Nucleic Acids Res,* 19**,** 5583-90.

FROELICH, C. J., ORTH, K., TURBOV, J., SETH, P., GOTTLIEB, R., BABIOR, B., SHAH, G. M., BLEACKLEY, R. C., DIXIT, V. M. & HANNA, W. 1996. New paradigm for lymphocyte granule-mediated cytotoxicity. Target cells bind and internalize granzyme B, but an endosomolytic agent is necessary for cytosolic delivery and subsequent apoptosis. *J Biol Chem,* 271**,** 29073-9.

FROELICH, C. J., ZHANG, X., TURBOV, J., HUDIG, D., WINKLER, U. & HANNA, W. L. 1993. Human granzyme B degrades aggrecan proteoglycan in matrix synthesized by chondrocytes. *J Immunol,* 151**,** 7161-71.

GAHRING, L., CARLSON, N. G., MEYER, E. L. & ROGERS, S. W. 2001. Granzyme B proteolysis of a neuronal glutamate receptor generates an autoantigen and is modulated by glycosylation. *J Immunol,* 166**,** 1433-8.

GANOR, Y., TEICHBERG, V. I. & LEVITE, M. 2007. TCR activation eliminates glutamate receptor GluR3 from the cell surface of normal human T cells, via an autocrine/paracrine granzyme B-mediated proteolytic cleavage. *J Immunol,* 178**,** 683-92.

GOODRIDGE, J. P., JACOBS, B., SAETERSMOEN, M. L., CLEMENT, D., HAMMER, Q., CLANCY, T., SKARPEN, E., BRECH, A., LANDSKRON, J., GRIMM, C., PFEFFERLE, A., MEZA-ZEPEDA, L., LORENZ, S., WIIGER, M. T., LOUCH, W. E., ASK, E. H., LIU, L. L., OEI, V. Y. S., KJALLQUIST, U., LINNARSSON, S., PATEL, S., TASKEN, K., STENMARK, H. & MALMBERG, K. J. 2019. Remodeling of secretory lysosomes during education tunes functional potential in NK cells. *Nat Commun,* 10**,** 514.

GOPING, I. S., BARRY, M., LISTON, P., SAWCHUK, T., CONSTANTINESCU, G., MICHALAK, K. M., SHOSTAK, I., ROBERTS, D. L., HUNTER, A. M., KORNELUK, R. & BLEACKLEY, R. C. 2003. Granzyme B-induced apoptosis requires both direct caspase activation and relief of caspase inhibition. *Immunity,* 18**,** 355-65.

GRAVESTEIN, L. A. & BORST, J. 1998. Tumor necrosis factor receptor family members in the immune system. *Semin Immunol,* 10**,** 423-34.

GRIFFITHS, G. M. & ISAAZ, S. 1993. Granzymes A and B are targeted to the lytic granules of lymphocytes by the mannose-6-phosphate receptor. *J Cell Biol,* 120**,** 885-96.

GROSS, C., KOELCH, W., DEMAIO, A., ARISPE, N. & MULTHOFF, G. 2003. Cell surface-bound heat shock protein 70 (Hsp70) mediates perforin-independent apoptosis by specific binding and uptake of granzyme B. *J Biol Chem,* 278**,** 41173-81.

GROSSMAN, W. J., VERBSKY, J. W., TOLLEFSEN, B. L., KEMPER, C., ATKINSON, J. P. & LEY, T. J. 2004. Differential expression of granzymes A and B in human cytotoxic lymphocyte subsets and T regulatory cells. *Blood,* 104**,** 2840-8.

GRUJIC, M., BRAGA, T., LUKINIUS, A., ELORANTA, M. L., KNIGHT, S. D., PEJLER, G. & ABRINK, M. 2005. Serglycin-deficient cytotoxic T lymphocytes display defective secretory granule maturation and granzyme B storage. *J Biol Chem,* 280**,** 33411-8.

GUO, Y., CHEN, J., SHI, L. & FAN, Z. 2010. Valosin-containing protein cleavage by granzyme K accelerates an endoplasmic reticulum stress leading to caspase-independent cytotoxicity of target tumor cells. *J Immunol,* 185**,** 5348-59.

GUO, Y., CHEN, J., ZHAO, T. & FAN, Z. 2008. Granzyme K degrades the redox/DNA repair enzyme Ape1 to trigger oxidative stress of target cells leading to cytotoxicity. *Mol Immunol,* 45**,** 2225-35.

GWALANI, L. A. & ORANGE, J. S. 2018. Single Degranulations in NK Cells Can Mediate Target Cell Killing. *J Immunol,* 200**,** 3231-3243.

HADDAD, P., WARGNIER, A., BOURGE, J. F., SASPORTES, M. & PAUL, P. 1993. A promoter element of the human serine esterase granzyme B gene controls specific transcription in activated T cells. *Eur J Immunol,* 23**,** 625-9.

HEIBEIN, J. A., BARRY, M., MOTYKA, B. & BLEACKLEY, R. C. 1999. Granzyme B-induced loss of mitochondrial inner membrane potential (Delta Psi m) and cytochrome c release are caspase independent. *J Immunol,* 163**,** 4683-93.

HEIBEIN, J. A., GOPING, I. S., BARRY, M., PINKOSKI, M. J., SHORE, G. C., GREEN, D. R. & BLEACKLEY, R. C. 2000. Granzyme B-mediated cytochrome c release is regulated by the Bcl-2 family members bid and Bax. *J Exp Med,* 192**,** 1391-402.

HELD, W., MACDONALD, H. R., WEISSMAN, I. L., HESS, M. W. & MUELLER, C. 1990. Genes encoding tumor necrosis factor alpha and granzyme A are expressed during development of autoimmune diabetes. *Proc Natl Acad Sci U S A,* 87**,** 2239-43.

HERBERMAN, R. B., NUNN, M. E. & LAVRIN, D. H. 1975. Natural cytotoxic reactivity of mouse lymphoid cells against syngeneic acid allogeneic tumors. I. Distribution of reactivity and specificity. *Int J Cancer,* 16**,** 216-29.

HERNANDEZ-PIGEON, H., JEAN, C., CHARRUYER, A., HAURE, M. J., BAUDOUIN, C., CHARVERON, M., QUILLET-MARY, A. & LAURENT, G. 2007. UVA induces granzyme B in human keratinocytes through MIF: implication in extracellular matrix remodeling. *J Biol Chem,* 282**,** 8157-64.

HIRST, C. E., BUZZA, M. S., BIRD, C. H., WARREN, H. S., CAMERON, P. U., ZHANG, M., ASHTON-RICKARDT, P. G. & BIRD, P. I. 2003. The intracellular granzyme B inhibitor, proteinase inhibitor 9, is up-regulated during accessory cell maturation and effector cell degranulation, and its overexpression enhances CTL potency. *J Immunol,* 170**,** 805-15.

HIRST, C. E., BUZZA, M. S., SUTTON, V. R., TRAPANI, J. A., LOVELAND, K. L. & BIRD, P. I. 2001. Perforin-independent expression of granzyme B and proteinase inhibitor 9 in human testis and placenta suggests a role for granzyme B-mediated proteolysis in reproduction. *Mol Hum Reprod,* 7**,** 1133-42.

HOCHEGGER, K., ELLER, P., HUBER, J. M., BERNHARD, D., MAYER, G., ZLABINGER, G. J. & ROSENKRANZ, A. R. 2007. Expression of granzyme A in human polymorphonuclear neutrophils. *Immunology,* 121**,** 166-73.

HOFFMANN, S. C., COHNEN, A., LUDWIG, T. & WATZL, C. 2011. 2B4 engagement mediates rapid LFA-1 and actin-dependent NK cell adhesion to tumor cells as measured by single cell force spectroscopy. *J Immunol,* 186**,** 2757-64.

HOLLESTELLE, M. J., LAI, K. W., VAN DEUREN, M., LENTING, P. J., DE GROOT, P. G., SPRONG, T. & BOVENSCHEN, N. 2011. Cleavage of von Willebrand factor by granzyme M destroys its factor VIII binding capacity. *PLoS One,* 6**,** e24216.

HORIUCHI, K., SAITO, S., SASAKI, R., TOMATSU, T. & TOYAMA, Y. 2003. Expression of granzyme B in human articular chondrocytes. *J Rheumatol,* 30**,** 1799-810.

HUA, G., ZHANG, Q. & FAN, Z. 2007. Heat shock protein 75 (TRAP1) antagonizes reactive oxygen species generation and protects cells from granzyme M-mediated apoptosis. *J Biol Chem,* 282**,** 20553-60.

HUNTINGTON, J. A., READ, R. J. & CARRELL, R. W. 2000. Structure of a serpin-protease complex shows inhibition by deformation. *Nature,* 407**,** 923-6.

IRMLER, M., HERTIG, S., MACDONALD, H. R., SADOUL, R., BECHERER, J. D., PROUDFOOT, A., SOLARI, R. & TSCHOPP, J. 1995. Granzyme A is an interleukin 1 beta-converting enzyme. *J Exp Med,* 181**,** 1917-22.

JAMES, A. M., HSU, H. T., DONGRE, P., UZEL, G., MACE, E. M., BANERJEE, P. P. & ORANGE, J. S. 2013. Rapid activation receptor- or IL-2-induced lytic granule convergence in human natural killer cells requires Src, but not downstream signaling. *Blood,* 121**,** 2627-37.

JANAS, M. L., GROVES, P., KIENZLE, N. & KELSO, A. 2005. IL-2 regulates perforin and granzyme gene expression in CD8+ T cells independently of its effects on survival and proliferation. *J Immunol,* 175**,** 8003-10.

JANS, D. A., BRIGGS, L. J., JANS, P., FROELICH, C. J., PARASIVAM, G., KUMAR, S., SUTTON, V. R. & TRAPANI, J. A. 1998. Nuclear targeting of the serine protease granzyme A (fragmentin-1). *J Cell Sci,* 111 (Pt 17)**,** 2645-54.

JANS, D. A., JANS, P., BRIGGS, L. J., SUTTON, V. & TRAPANI, J. A. 1996. Nuclear transport of granzyme B (fragmentin-2). Dependence of perforin in vivo and cytosolic factors in vitro. *J Biol Chem,* 271**,** 30781-9.

JENNE, D. E. & TSCHOPP, J. 1988. Granzymes, a family of serine proteases released from granules of cytolytic T lymphocytes upon T cell receptor stimulation. *Immunol Rev,* 103**,** 53-71.

JEWETT, A. & BONAVIDA, B. 1996. Target-induced inactivation and cell death by apoptosis in a subset of human NK cells. *J Immunol,* 156**,** 907-15.

JOECKEL, L. T. & BIRD, P. I. 2014a. Are all granzymes cytotoxic in vivo? *Biol Chem,* 395**,** 181-202.

JOECKEL, L. T. & BIRD, P. I. 2014b. Blessing or curse? Proteomics in granzyme research. *Proteomics Clin Appl,* 8**,** 351-81.

JOHNSEN, A. C., HAUX, J., STEINKJER, B., NONSTAD, U., EGEBERG, K., SUNDAN, A., ASHKENAZI, A. & ESPEVIK, T. 1999. Regulation of APO-2 ligand/trail expression in NK cells-involvement in NK cell-mediated cytotoxicity. *Cytokine,* 11**,** 664-72.

JOST, S. & ALTFELD, M. 2013. Control of human viral infections by natural killer cells. *Annu Rev Immunol,* 31**,** 163-94.

KAISERMAN, D. & BIRD, P. I. 2010. Control of granzymes by serpins. *Cell Death Differ,* 17**,** 586-95.

KANNO, A., YAMANAKA, Y., HIRANO, H., UMEZAWA, Y. & OZAWA, T. 2007. Cyclic luciferase for real-time sensing of caspase-3 activities in living mammals. *Angew Chem Int Ed Engl,* 46**,** 7595-9.

KARRE, K. 2008. Natural killer cell recognition of missing self. *Nat Immunol,* 9**,** 477-80.

KARRE, K., LJUNGGREN, H. G., PIONTEK, G. & KIESSLING, R. 1986. Selective rejection of H-2-deficient lymphoma variants suggests alternative immune defence strategy. *Nature,* 319**,** 675-8.

KEEFE, D., SHI, L., FESKE, S., MASSOL, R., NAVARRO, F., KIRCHHAUSEN, T. & LIEBERMAN, J. 2005. Perforin triggers a plasma membrane-repair response that facilitates CTL induction of apoptosis. *Immunity,* 23**,** 249-62.

KELLY, J. M., WATERHOUSE, N. J., CRETNEY, E., BROWNE, K. A., ELLIS, S., TRAPANI, J. A. & SMYTH, M. J. 2004. Granzyme M mediates a novel form of perforin-dependent cell death. *J Biol Chem,* 279**,** 22236-42.

KHAZEN, R., MULLER, S., GAUDENZIO, N., ESPINOSA, E., PUISSEGUR, M. P. & VALITUTTI, S. 2016. Melanoma cell lysosome secretory burst neutralizes the CTL-mediated cytotoxicity at the lytic synapse. *Nat Commun,* 7**,** 10823.

KIESSLING, R., KLEIN, E. & WIGZELL, H. 1975. "Natural" killer cells in the mouse. I. Cytotoxic cells with specificity for mouse Moloney leukemia cells. Specificity and distribution according to genotype. *Eur J Immunol,* 5**,** 112-7.

KIM, H. S., DAS, A., GROSS, C. C., BRYCESON, Y. T. & LONG, E. O. 2010. Synergistic signals for natural cytotoxicity are required to overcome inhibition by c-Cbl ubiquitin ligase. *Immunity,* 32**,** 175-86.

KIM, S., POURSINE-LAURENT, J., TRUSCOTT, S. M., LYBARGER, L., SONG, Y. J., YANG, L., FRENCH, A. R., SUNWOO, J. B., LEMIEUX, S., HANSEN, T. H. & YOKOYAMA, W. M. 2005. Licensing of natural killer cells by host major histocompatibility complex class I molecules. *Nature,* 436**,** 709-13.

KLINGEMANN, H., BOISSEL, L. & TONEGUZZO, F. 2016. Natural Killer Cells for Immunotherapy - Advantages of the NK-92 Cell Line over Blood NK Cells. *Front Immunol,* 7**,** 91.

KRZEWSKI, K. & COLIGAN, J. E. 2012. Human NK cell lytic granules and regulation of their exocytosis. *Front Immunol,* 3**,** 335.

KRZEWSKI, K., GIL-KRZEWSKA, A., NGUYEN, V., PERUZZI, G. & COLIGAN, J. E. 2013. LAMP1/CD107a is required for efficient perforin delivery to lytic granules and NK-cell cytotoxicity. *Blood,* 121**,** 4672-83.

KUMMER, J. A., KAMP, A. M., CITARELLA, F., HORREVOETS, A. J. & HACK, C. E. 1996. Expression of human recombinant granzyme A zymogen and its activation by the cysteine proteinase cathepsin C. *J Biol Chem,* 271**,** 9281-6.

KURSCHUS, F. C., BRUNO, R., FELLOWS, E., FALK, C. S. & JENNE, D. E. 2005. Membrane receptors are not required to deliver granzyme B during killer cell attack. *Blood,* 105**,** 2049-58.

KURSCHUS, F. C., FELLOWS, E., STEGMANN, E. & JENNE, D. E. 2008. Granzyme B delivery via perforin is restricted by size, but not by heparan sulfate-dependent endocytosis. *Proc Natl Acad Sci U S A,* 105**,** 13799-804.

LANIER, L. L. 2008. Up on the tightrope: natural killer cell activation and inhibition. *Nat Immunol,* 9**,** 495-502.

LAW, R. H., LUKOYANOVA, N., VOSKOBOINIK, I., CARADOC-DAVIES, T. T., BARAN, K., DUNSTONE, M. A., D'ANGELO, M. E., ORLOVA, E. V., COULIBALY, F., VERSCHOOR, S., BROWNE, K. A., CICCONE, A., KUIPER, M. J., BIRD, P. I., TRAPANI, J. A., SAIBIL, H. R. & WHISSTOCK, J. C. 2010. The structural basis for membrane binding and pore formation by lymphocyte perforin. *Nature,* 468**,** 447-51.

LAW, R. H., ZHANG, Q., MCGOWAN, S., BUCKLE, A. M., SILVERMAN, G. A., WONG, W., ROSADO, C. J., LANGENDORF, C. G., PIKE, R. N., BIRD, P. I. & WHISSTOCK, J. C. 2006. An overview of the serpin superfamily. *Genome Biol,* 7**,** 216.

LEUNG, C., HODEL, A. W., BRENNAN, A. J., LUKOYANOVA, N., TRAN, S., HOUSE, C. M., KONDOS, S. C., WHISSTOCK, J. C., DUNSTONE, M. A., TRAPANI, J. A., VOSKOBOINIK, I., SAIBIL, H. R. & HOOGENBOOM, B. W. 2017. Real-time visualization of perforin nanopore assembly. *Nat Nanotechnol,* 12**,** 467-473.

LI, J., FIGUEIRA, S. K., VRAZO, A. C., BINKOWSKI, B. F., BUTLER, B. L., TABATA, Y., FILIPOVICH, A., JORDAN, M. B. & RISMA, K. A. 2014. Real-time detection of CTL function reveals distinct patterns of caspase activation mediated by Fas versus granzyme B. *J Immunol,* 193**,** 519-28.

LIEBERMAN, J. 2003. The ABCs of granule-mediated cytotoxicity: new weapons in the arsenal. *Nat Rev Immunol,* 3**,** 361-70.

LIESCHE, C., SAUER, P., PRAGER, I., URLAUB, D., CLAUS, M., EILS, R., BEAUDOUIN, J. & WATZL, C. 2018. Single-Fluorescent Protein Reporters Allow Parallel Quantification of Natural Killer Cell-Mediated Granzyme and Caspase Activities in Single Target Cells. *Front Immunol,* 9**,** 1840.

LIU, C. C., RAFII, S., GRANELLI-PIPERNO, A., TRAPANI, J. A. & YOUNG, J. D. 1989. Perforin and serine esterase gene expression in stimulated human T cells. Kinetics, mitogen requirements, and effects of cyclosporin A. *J Exp Med,* 170**,** 2105-18.

LIU, Z., CHEN, O., WALL, J. B. J., ZHENG, M., ZHOU, Y., WANG, L., VASEGHI, H. R., QIAN, L. & LIU, J. 2017. Systematic comparison of 2A peptides for cloning multi-genes in a polycistronic vector. *Sci Rep,* 7**,** 2193.

LJUNGGREN, H. G. & MALMBERG, K. J. 2007. Prospects for the use of NK cells in immunotherapy of human cancer. *Nat Rev Immunol,* 7**,** 329-39.

LOEB, C. R., HARRIS, J. L. & CRAIK, C. S. 2006. Granzyme B proteolyzes receptors important to proliferation and survival, tipping the balance toward apoptosis. *J Biol Chem,* 281**,** 28326-35.

LONG, E. O. 2008. Negative signaling by inhibitory receptors: the NK cell paradigm. *Immunol Rev,* 224**,** 70-84.

LOPEZ, J. A., JENKINS, M. R., RUDD-SCHMIDT, J. A., BRENNAN, A. J., DANNE, J. C., MANNERING, S. I., TRAPANI, J. A. & VOSKOBOINIK, I. 2013a. Rapid and unidirectional perforin pore delivery at the cytotoxic immune synapse. *J Immunol,* 191**,** 2328-34.

LOPEZ, J. A., SUSANTO, O., JENKINS, M. R., LUKOYANOVA, N., SUTTON, V. R., LAW, R. H., JOHNSTON, A., BIRD, C. H., BIRD, P. I., WHISSTOCK, J. C., TRAPANI, J. A., SAIBIL, H. R. & VOSKOBOINIK, I. 2013b. Perforin forms transient pores on the target cell plasma membrane to facilitate rapid access of granzymes during killer cell attack. *Blood,* 121**,** 2659-68.

LOSASSO, V., SCHIFFER, S., BARTH, S. & CARLONI, P. 2012. Design of human granzyme B variants resistant to serpin B9. *Proteins,* 80**,** 2514-22.

LU, H., HOU, Q., ZHAO, T., ZHANG, H., ZHANG, Q., WU, L. & FAN, Z. 2006. Granzyme M directly cleaves inhibitor of caspase-activated DNase (CAD) to unleash CAD leading to DNA fragmentation. *J Immunol,* 177**,** 1171-8.

LUCAS, M., SCHACHTERLE, W., OBERLE, K., AICHELE, P. & DIEFENBACH, A. 2007. Dendritic cells prime natural killer cells by trans-presenting interleukin 15. *Immunity,* 26**,** 503-17.

MACDONALD, G., SHI, L., VANDE VELDE, C., LIEBERMAN, J. & GREENBERG, A. H. 1999. Mitochondria-dependent and -independent regulation of Granzyme B-induced apoptosis. *J Exp Med,* 189**,** 131-44.

MACE, E. M., DONGRE, P., HSU, H. T., SINHA, P., JAMES, A. M., MANN, S. S., FORBES, L. R., WATKIN, L. B. & ORANGE, J. S. 2014. Cell biological steps and checkpoints in accessing NK cell cytotoxicity. *Immunol Cell Biol,* 92**,** 245-55.

MAHRUS, S. & CRAIK, C. S. 2005. Selective chemical functional probes of granzymes A and B reveal granzyme B is a major effector of natural killer cell-mediated lysis of target cells. *Chem Biol,* 12**,** 567-77.

MAHRUS, S., KISIEL, W. & CRAIK, C. S. 2004. Granzyme M is a regulatory protease that inactivates proteinase inhibitor 9, an endogenous inhibitor of granzyme B. *J Biol Chem,* 279**,** 54275-82.

MARCUS, A., GOWEN, B. G., THOMPSON, T. W., IANNELLO, A., ARDOLINO, M., DENG, W., WANG, L., SHIFRIN, N. & RAULET, D. H. 2014. Recognition of tumors by the innate immune system and natural killer cells. *Adv Immunol,* 122**,** 91-128.

MARTIN, P., WALLICH, R., PARDO, J., MULLBACHER, A., MUNDER, M., MODOLELL, M. & SIMON, M. M. 2005. Quiescent and activated mouse granulocytes do not express granzyme A and B or perforin: similarities or differences with human polymorphonuclear leukocytes? *Blood,* 106**,** 2871-8.

MARTIN, S. J., AMARANTE-MENDES, G. P., SHI, L., CHUANG, T. H., CASIANO, C. A., O'BRIEN, G. A., FITZGERALD, P., TAN, E. M., BOKOCH, G. M., GREENBERG, A. H. & GREEN, D. R. 1996. The cytotoxic cell protease granzyme B initiates apoptosis in a cell-free system by proteolytic processing and activation of the ICE/CED-3 family protease, CPP32, via a novel two-step mechanism. *EMBO J,* 15**,** 2407-16.

MARTINVALET, D., DYKXHOORN, D. M., FERRINI, R. & LIEBERMAN, J. 2008. Granzyme A cleaves a mitochondrial complex I protein to initiate caspase-independent cell death. *Cell,* 133**,** 681-92.

MARTINVALET, D., ZHU, P. & LIEBERMAN, J. 2005. Granzyme A induces caspase-independent mitochondrial damage, a required first step for apoptosis. *Immunity,* 22**,** 355-70.

MEDEMA, J. P., TOES, R. E., SCAFFIDI, C., ZHENG, T. S., FLAVELL, R. A., MELIEF, C. J., PETER, M. E., OFFRINGA, R. & KRAMMER, P. H. 1997. Cleavage of FLICE (caspase-8) by granzyme B during cytotoxic T lymphocyte-induced apoptosis. *Eur J Immunol,* 27**,** 3492-8.

MENAGER, M. M., MENASCHE, G., ROMAO, M., KNAPNOUGEL, P., HO, C. H., GARFA, M., RAPOSO, G., FELDMANN, J., FISCHER, A. & DE SAINT BASILE, G. 2007. Secretory cytotoxic granule maturation and exocytosis require the effector protein hMunc13-4. *Nat Immunol,* 8**,** 257-67.

MENTLIK, A. N., SANBORN, K. B., HOLZBAUR, E. L. & ORANGE, J. S. 2010. Rapid lytic granule convergence to the MTOC in natural killer cells is dependent on dynein but not cytolytic commitment. *Mol Biol Cell,* 21**,** 2241-56.

METKAR, S. S. & FROELICH, C. J. 2004. Human neutrophils lack granzyme A, granzyme B, and perforin. *Blood,* 104**,** 905-6; author reply 907-8.

MOTYKA, B., KORBUTT, G., PINKOSKI, M. J., HEIBEIN, J. A., CAPUTO, A., HOBMAN, M., BARRY, M., SHOSTAK, I., SAWCHUK, T., HOLMES, C. F., GAULDIE, J. & BLEACKLEY, R. C. 2000. Mannose 6-phosphate/insulin-like growth factor II receptor is a death receptor for granzyme B during cytotoxic T cell-induced apoptosis. *Cell,* 103**,** 491-500.

MURIS, J. J., YLSTRA, B., CILLESSEN, S. A., OSSENKOPPELE, G. J., KLUIN-NELEMANS, J. C., EIJK, P. P., NOTA, B., TIJSSEN, M., DE BOER, W. P., VAN DE WIEL, M., VAN DEN IJSSEL, P. R., JANSEN, P., DE BRUIN, P. C., VAN KRIEKEN, J. H., MEIJER, G. A., MEIJER, C. J. & OUDEJANS, J. J. 2007. Profiling of apoptosis genes allows for clinical stratification of primary nodal diffuse large B-cell lymphomas. *Br J Haematol,* 136**,** 38-47.

NAGLER, A., LANIER, L. L., CWIRLA, S. & PHILLIPS, J. H. 1989. Comparative studies of human FcRIII-positive and negative natural killer cells. *J Immunol,* 143**,** 3183-91.

NAPOLI, A. M., FAST, L. D., GARDINER, F., NEVOLA, M. & MACHAN, J. T. 2012. Increased granzyme levels in cytotoxic T lymphocytes are associated with disease severity in emergency department patients with severe sepsis. *Shock,* 37**,** 257-62.

NORA BRUNING, V. B., CARSTEN WATZL 2022. Analyzing the activity of proteases such as granzyme B and caspase-8 inside living cells using fluorescence localization reporters. *In:* DEPARTMENT OF IMMUNOLOGY, L. R. C. O. W. E. A. H. F. A. T. D. I., DORTMUND, GERMANY (ed.).

NYMAN, T. A., TOLO, H., PARKKINEN, J. & KALKKINEN, N. 1998. Identification of nine interferon-alpha subtypes produced by Sendai virus-induced human peripheral blood leucocytes. *Biochem J,* 329 (Pt 2)**,** 295-302.

ORANGE, J. S. 2008. Formation and function of the lytic NK-cell immunological synapse. *Nat Rev Immunol,* 8**,** 713-25.

PACKARD, B. Z., TELFORD, W. G., KOMORIYA, A. & HENKART, P. A. 2007. Granzyme B activity in target cells detects attack by cytotoxic lymphocytes. *J Immunol,* 179**,** 3812-20.

PEGRAM, H. J., ANDREWS, D. M., SMYTH, M. J., DARCY, P. K. & KERSHAW, M. H. 2011. Activating and inhibitory receptors of natural killer cells. *Immunol Cell Biol,* 89**,** 216-24.

PEREIRA-LEAL, J. B. & SEABRA, M. C. 2001. Evolution of the Rab family of small GTP-binding proteins. *J Mol Biol,* 313**,** 889-901.

PETER, M. E. & KRAMMER, P. H. 2003. The CD95(APO-1/Fas) DISC and beyond. *Cell Death Differ,* 10**,** 26-35.

PETERS, P. J., BORST, J., OORSCHOT, V., FUKUDA, M., KRAHENBUHL, O., TSCHOPP, J., SLOT, J. W. & GEUZE, H. J. 1991. Cytotoxic T lymphocyte granules are secretory lysosomes, containing both perforin and granzymes. *J Exp Med,* 173**,** 1099-109.

PINKOSKI, M. J., WATERHOUSE, N. J., HEIBEIN, J. A., WOLF, B. B., KUWANA, T., GOLDSTEIN, J. C., NEWMEYER, D. D., BLEACKLEY, R. C. & GREEN, D. R. 2001. Granzyme B-mediated apoptosis proceeds predominantly through a Bcl-2-inhibitable mitochondrial pathway. *J Biol Chem,* 276**,** 12060-7.

PLASMAN, K., VAN DAMME, P., KAISERMAN, D., IMPENS, F., DEMEYER, K., HELSENS, K., GOETHALS, M., BIRD, P. I., VANDEKERCKHOVE, J. & GEVAERT, K. 2011. Probing the efficiency of proteolytic events by positional proteomics. *Mol Cell Proteomics,* 10**,** M110 003301.

POLI, A., MICHEL, T., THERESINE, M., ANDRES, E., HENTGES, F. & ZIMMER, J. 2009. CD56bright natural killer (NK) cells: an important NK cell subset. *Immunology,* 126**,** 458-65.

POWERS, J. C., ASGIAN, J. L., EKICI, O. D. & JAMES, K. E. 2002. Irreversible inhibitors of serine, cysteine, and threonine proteases. *Chem Rev,* 102**,** 4639-750.

PRAGER, I. 2020. *Regulation of natural killer cell cytotoxic pathways during serial killing activity.* PhD Dissertation, TU Dortmund.

PRAGER, I. & WATZL, C. 2019. Mechanisms of natural killer cell-mediated cellular cytotoxicity. *J Leukoc Biol,* 105**,** 1319-1329.

PRZETAK, M. M., YOAST, S. & SCHMIDT, B. F. 1995. Cloning of cDNA for human granzyme 3. *FEBS Lett,* 364**,** 268-71.

QUAN, L. T., TEWARI, M., O'ROURKE, K., DIXIT, V., SNIPAS, S. J., POIRIER, G. G., RAY, C., PICKUP, D. J. & SALVESEN, G. S. 1996. Proteolytic activation of the cell death protease Yama/CPP32 by granzyme B. *Proc Natl Acad Sci U S A,* 93**,** 1972-6.

RAJA, S. M., METKAR, S. S., HONING, S., WANG, B., RUSSIN, W. A., PIPALIA, N. H., MENAA, C., BELTING, M., CAO, X., DRESSEL, R. & FROELICH, C. J. 2005. A novel mechanism for protein delivery: granzyme B undergoes electrostatic exchange from serglycin to target cells. *J Biol Chem,* 280**,** 20752-61.

RAULET, D. H. & VANCE, R. E. 2006. Self-tolerance of natural killer cells. *Nat Rev Immunol,* 6**,** 520-31.

RAZVI, N. Z., KHURSHID, R. & NAGRA, S. A. 2008. To study the significance of apoptotic enzyme granzyme H in breast cancer patients. *J Ayub Med Coll Abbottabad,* 20**,** 84-6.

RISSOAN, M. C., DUHEN, T., BRIDON, J. M., BENDRISS-VERMARE, N., PERONNE, C., DE SAINT VIS, B., BRIERE, F. & BATES, E. E. 2002. Subtractive hybridization reveals the expression of immunoglobulin-like transcript 7, Eph-B1, granzyme B, and 3 novel transcripts in human plasmacytoid dendritic cells. *Blood,* 100**,** 3295-303.

RIZO, J. & SUDHOF, T. C. 2002. Snares and Munc18 in synaptic vesicle fusion. *Nat Rev Neurosci,* 3**,** 641-53.

ROMERO, V., FELLOWS, E., JENNE, D. E. & ANDRADE, F. 2009. Cleavage of La protein by granzyme H induces cytoplasmic translocation and interferes with La-mediated HCV-IRES translational activity. *Cell Death Differ,* 16**,** 340-8.

RONDAY, H. K., VAN DER LAAN, W. H., TAK, P. P., DE ROOS, J. A., BANK, R. A., TEKOPPELE, J. M., FROELICH, C. J., HACK, C. E., HOGENDOORN, P. C., BREEDVELD, F. C. & VERHEIJEN, J. H. 2001. Human granzyme B mediates cartilage proteoglycan degradation and is expressed at the invasive front of the synovium in rheumatoid arthritis. *Rheumatology (Oxford),* 40**,** 55-61.

RUKAMP, B. J., KAM, C. M., NATARAJAN, S., BOLTON, B. W., SMYTH, M. J., KELLY, J. M. & POWERS, J. C. 2004. Subsite specificities of granzyme M: a study of inhibitors and newly synthesized thiobenzyl ester substrates. *Arch Biochem Biophys,* 422**,** 9-22.

RUSSELL, J. H. & LEY, T. J. 2002. Lymphocyte-mediated cytotoxicity. *Annu Rev Immunol,* 20**,** 323-70.

SATTAR, R., ALI, S. A. & ABBASI, A. 2003. Bioinformatics of granzymes: sequence comparison and structural studies on granzyme family by homology modeling. *Biochem Biophys Res Commun,* 308**,** 726-35.

SEDELIES, K. A., SAYERS, T. J., EDWARDS, K. M., CHEN, W., PELLICCI, D. G., GODFREY, D. I. & TRAPANI, J. A. 2004. Discordant regulation of granzyme H and granzyme B expression in human lymphocytes. *J Biol Chem,* 279**,** 26581-7.

SHARIF-ASKARI, E., ALAM, A., RHEAUME, E., BERESFORD, P. J., SCOTTO, C., SHARMA, K., LEE, D., DEWOLF, W. E., NUTTALL, M. E., LIEBERMAN, J. & SEKALY, R. P. 2001. Direct cleavage of the human DNA fragmentation factor-45 by granzyme B induces caspase-activated DNase release and DNA fragmentation. *EMBO J,* 20**,** 3101-13.

SHARMA, M., MERKULOVA, Y., RAITHATHA, S., PARKINSON, L. G., SHEN, Y., COOPER, D. & GRANVILLE, D. J. 2016. Extracellular granzyme K mediates endothelial activation through the cleavage of protease-activated receptor-1. *FEBS J,* 283**,** 1734-47.

SHEN, J., TARESTE, D. C., PAUMET, F., ROTHMAN, J. E. & MELIA, T. J. 2007. Selective activation of cognate SNAREpins by Sec1/Munc18 proteins. *Cell,* 128**,** 183-95.

SHI, L., KEEFE, D., DURAND, E., FENG, H., ZHANG, D. & LIEBERMAN, J. 2005. Granzyme B binds to target cells mostly by charge and must be added at the same time as perforin to trigger apoptosis. *J Immunol,* 174**,** 5456-61.

SHI, X. & JARVIS, D. L. 2007. Protein N-glycosylation in the baculovirus-insect cell system. *Curr Drug Targets,* 8**,** 1116-25.

SHRESTA, S., GRAUBERT, T. A., THOMAS, D. A., RAPTIS, S. Z. & LEY, T. J. 1999. Granzyme A initiates an alternative pathway for granule-mediated apoptosis. *Immunity,* 10**,** 595-605.

SILVERMAN, G. A., BIRD, P. I., CARRELL, R. W., CHURCH, F. C., COUGHLIN, P. B., GETTINS, P. G., IRVING, J. A., LOMAS, D. A., LUKE, C. J., MOYER, R. W., PEMBERTON, P. A., REMOLD-O'DONNELL, E., SALVESEN, G. S., TRAVIS, J. & WHISSTOCK, J. C. 2001. The serpins are an expanding superfamily of structurally similar but functionally diverse proteins. Evolution, mechanism of inhibition, novel functions, and a revised nomenclature. *J Biol Chem,* 276**,** 33293-6.

SIMON, M. M., HAUSMANN, M., TRAN, T., EBNET, K., TSCHOPP, J., THAHLA, R. & MULLBACHER, A. 1997. In vitro- and ex vivo-derived cytolytic leukocytes from granzyme A x B double knockout mice are defective in granule-mediated apoptosis but not lysis of target cells. *J Exp Med,* 186**,** 1781-6.

SIMONE, C. B. & HENKART, P. 1980. Permeability changes induced in erthrocyte ghost targets by antibody-dependent cytotoxic effector cells: evidence for membrane pores. *J Immunol,* 124**,** 954-63.

SMITH, K. J., HAMZA, S. & SKELTON, H. 2004. Topical imidazoquinoline therapy of cutaneous squamous cell carcinoma polarizes lymphoid and monocyte/macrophage populations to a Th1 and M1 cytokine pattern. *Clin Exp Dermatol,* 29**,** 505-12.

SMYTH, M. J., BROWNE, K. A., KINNEAR, B. F., TRAPANI, J. A. & WARREN, H. S. 1995. Distinct granzyme expression in human CD3- CD56+ large granular- and CD3- CD56+ small high density-lymphocytes displaying non-MHC-restricted cytolytic activity. *J Leukoc Biol,* 57**,** 88-93.

SMYTH, M. J., SAYERS, T. J., WILTROUT, T., POWERS, J. C. & TRAPANI, J. A. 1993. Met-ase: cloning and distinct chromosomal location of a serine protease preferentially expressed in human natural killer cells. *J Immunol,* 151**,** 6195-205.

SOUZA-FONSECA-GUIMARAES, F., KRASNOVA, Y., PUTOCZKI, T., MILES, K., MACDONALD, K. P., TOWN, L., SHI, W., GOBE, G. C., MCDADE, L., MIELKE, L. A., TYE, H., MASTERS, S. L., BELZ, G. T., HUNTINGTON, N. D., RADFORD-SMITH, G. & SMYTH, M. J. 2016. Granzyme M has a critical role in providing innate immune protection in ulcerative colitis. *Cell Death Dis,* 7**,** e2302.

SOWER, L. E., FROELICH, C. J., ALLEGRETTO, N., ROSE, P. M., HANNA, W. D. & KLIMPEL, G. R. 1996a. Extracellular activities of human granzyme A. Monocyte activation by granzyme A versus alpha-thrombin. *J Immunol,* 156**,** 2585-90.

SOWER, L. E., KLIMPEL, G. R., HANNA, W. & FROELICH, C. J. 1996b. Extracellular activities of human granzymes. I. Granzyme A induces IL6 and IL8 production in fibroblast and epithelial cell lines. *Cell Immunol,* 171**,** 159-63.

SPAENY-DEKKING, E. H., HANNA, W. L., WOLBINK, A. M., WEVER, P. C., KUMMER, J. A., SWAAK, A. J., MIDDELDORP, J. M., HUISMAN, H. G., FROELICH, C. J. & HACK, C. E. 1998. Extracellular granzymes A and B in humans: detection of native species during CTL responses in vitro and in vivo. *J Immunol,* 160**,** 3610-6.

SPAENY-DEKKING, E. H., KAMP, A. M., FROELICH, C. J. & HACK, C. E. 2000. Extracellular granzyme A, complexed to proteoglycans, is protected against inactivation by protease inhibitors. *Blood,* 95**,** 1465-72.

STENNICKE, H. R., JURGENSMEIER, J. M., SHIN, H., DEVERAUX, Q., WOLF, B. B., YANG, X., ZHOU, Q., ELLERBY, H. M., ELLERBY, L. M., BREDESEN, D., GREEN, D. R., REED, J. C., FROELICH, C. J. & SALVESEN, G. S. 1998. Pro-caspase-3 is a major physiologic target of caspase-8. *J Biol Chem,* 273**,** 27084-90.

STINCHCOMBE, J. C., MAJOROVITS, E., BOSSI, G., FULLER, S. & GRIFFITHS, G. M. 2006. Centrosome polarization delivers secretory granules to the immunological synapse. *Nature,* 443**,** 462-5.

STINCHCOMBE, J. C., PAGE, L. J. & GRIFFITHS, G. M. 2000. Secretory lysosome biogenesis in cytotoxic T lymphocytes from normal and Chediak Higashi syndrome patients. *Traffic,* 1**,** 435-44.

STRASSER, A., JOST, P. J. & NAGATA, S. 2009. The many roles of FAS receptor signaling in the immune system. *Immunity,* 30**,** 180-92.

STRIK, M. C., DE KONING, P. J., KLEIJMEER, M. J., BLADERGROEN, B. A., WOLBINK, A. M., GRIFFITH, J. M., WOUTERS, D., FUKUOKA, Y., SCHWARTZ, L. B., HACK, C. E., VAN HAM, S. M. & KUMMER, J. A. 2007. Human mast cells produce and release the cytotoxic lymphocyte associated protease granzyme B upon activation. *Mol Immunol,* 44**,** 3462-72.

SUN, J., BIRD, C. H., SUTTON, V., MCDONALD, L., COUGHLIN, P. B., DE JONG, T. A., TRAPANI, J. A. & BIRD, P. I. 1996. A cytosolic granzyme B inhibitor related to the viral apoptotic regulator cytokine response modifier A is present in cytotoxic lymphocytes. *J Biol Chem,* 271**,** 27802-9.

SUN, J., WHISSTOCK, J. C., HARRIOTT, P., WALKER, B., NOVAK, A., THOMPSON, P. E., SMITH, A. I. & BIRD, P. I. 2001. Importance of the P4' residue in human granzyme B inhibitors and substrates revealed by scanning mutagenesis of the proteinase inhibitor 9 reactive center loop. *J Biol Chem,* 276**,** 15177-84.

SUN, Q., YANG, J., XING, G., SUN, Q., ZHANG, L. & HE, F. 2008. Expression of GSDML Associates with Tumor Progression in Uterine Cervix Cancer. *Transl Oncol,* 1**,** 73-83.

SUSANTO, O., TRAPANI, J. A. & BRASACCHIO, D. 2012. Controversies in granzyme biology. *Tissue Antigens,* 80**,** 477-87.

SUTTON, V. R., DAVIS, J. E., CANCILLA, M., JOHNSTONE, R. W., RUEFLI, A. A., SEDELIES, K., BROWNE, K. A. & TRAPANI, J. A. 2000. Initiation of apoptosis by granzyme B requires direct cleavage of bid, but not direct granzyme B-mediated caspase activation. *J Exp Med,* 192**,** 1403-14.

SZUBIN, R., CHANG, W. L., GREASBY, T., BECKETT, L. & BAUMGARTH, N. 2008. Rigid interferon-alpha subtype responses of human plasmacytoid dendritic cells. *J Interferon Cytokine Res,* 28**,** 749-63.

TAJER, P., PIKE-OVERZET, K., ARIAS, S., HAVENGA, M. & STAAL, F. J. T. 2019. Ex Vivo Expansion of Hematopoietic Stem Cells for Therapeutic Purposes: Lessons from Development and the Niche. *Cells,* 8.

TANG, H., LI, C., WANG, L., ZHANG, H. & FAN, Z. 2012. Granzyme H of cytotoxic lymphocytes is required for clearance of the hepatitis B virus through cleavage of the hepatitis B virus X protein. *J Immunol,* 188**,** 824-31.

TAREK, N., LE LUDUEC, J. B., GALLAGHER, M. M., ZHENG, J., VENSTROM, J. M., CHAMBERLAIN, E., MODAK, S., HELLER, G., DUPONT, B., CHEUNG, N. K. & HSU, K. C. 2012. Unlicensed NK cells target neuroblastoma following anti-GD2 antibody treatment. *J Clin Invest,* 122**,** 3260-70.

TEO, F. H., DE OLIVEIRA, R. T., MAMONI, R. L., FERREIRA, M. C., NADRUZ, W., JR., COELHO, O. R., FERNANDES JDE, L. & BLOTTA, M. H. 2013. Characterization of CD4+CD28null T cells in patients with coronary artery disease and individuals with risk factors for atherosclerosis. *Cell Immunol,* 281**,** 11-9.

TERME, M., ULLRICH, E., DELAHAYE, N. F., CHAPUT, N. & ZITVOGEL, L. 2008. Natural killer cell-directed therapies: moving from unexpected results to successful strategies. *Nat Immunol,* 9**,** 486-94.

THIERY, J., KEEFE, D., SAFFARIAN, S., MARTINVALET, D., WALCH, M., BOUCROT, E., KIRCHHAUSEN, T. & LIEBERMAN, J. 2010. Perforin activates clathrin- and dynamin-dependent endocytosis, which is required for plasma membrane repair and delivery of granzyme B for granzyme-mediated apoptosis. *Blood,* 115**,** 1582-93.

THOMAS, D. A., DU, C., XU, M., WANG, X. & LEY, T. J. 2000. DFF45/ICAD can be directly processed by granzyme B during the induction of apoptosis. *Immunity,* 12**,** 621-32.

THOMAS, D. A., SCORRANO, L., PUTCHA, G. V., KORSMEYER, S. J. & LEY, T. J. 2001. Granzyme B can cause mitochondrial depolarization and cell death in the absence of BID, BAX, and BAK. *Proc Natl Acad Sci U S A,* 98**,** 14985-90.

THORNBERRY, N. A., RANO, T. A., PETERSON, E. P., RASPER, D. M., TIMKEY, T., GARCIA-CALVO, M., HOUTZAGER, V. M., NORDSTROM, P. A., ROY, S., VAILLANCOURT, J. P., CHAPMAN, K. T. & NICHOLSON, D. W. 1997. A combinatorial approach defines specificities of members of the caspase family and granzyme B. Functional relationships established for key mediators of apoptosis. *J Biol Chem,* 272**,** 17907-11.

TRINCHIERI, G. 1989. Biology of natural killer cells. *Adv Immunol,* 47**,** 187-376.

TSCHOPP, C. M., SPIEGL, N., DIDICHENKO, S., LUTMANN, W., JULIUS, P., VIRCHOW, J. C., HACK, C. E. & DAHINDEN, C. A. 2006. Granzyme B, a novel mediator of allergic inflammation: its induction and release in blood basophils and human asthma. *Blood,* 108**,** 2290-9.

TSUBOTA, K., SAITO, I. & MIYASAKA, N. 1994. Expression of granzyme A and perforin in lacrimal gland of Sjogren's syndrome. *Adv Exp Med Biol,* 350**,** 637-40.

VALIANTE, N. M., UHRBERG, M., SHILLING, H. G., LIENERT-WEIDENBACH, K., ARNETT, K. L., D'ANDREA, A., PHILLIPS, J. H., LANIER, L. L. & PARHAM, P. 1997. Functionally and structurally distinct NK cell receptor repertoires in the peripheral blood of two human donors. *Immunity,* 7**,** 739-51.

VAN DAMME, P., MAURER-STROH, S., PLASMAN, K., VAN DURME, J., COLAERT, N., TIMMERMAN, E., DE BOCK, P. J., GOETHALS, M., ROUSSEAU, F., SCHYMKOWITZ, J., VANDEKERCKHOVE, J. & GEVAERT, K. 2009. Analysis of protein processing by N-terminal proteomics reveals novel species-specific substrate determinants of granzyme B orthologs. *Mol Cell Proteomics,* 8**,** 258-72.

VAN DE CRAEN, M., VAN DEN BRANDE, I., DECLERCQ, W., IRMLER, M., BEYAERT, R., TSCHOPP, J., FIERS, W. & VANDENABEELE, P. 1997. Cleavage of caspase family members by granzyme B: a comparative study in vitro. *Eur J Immunol,* 27**,** 1296-9.

VAN DOMSELAAR, R., DE POOT, S. A., REMMERSWAAL, E. B., LAI, K. W., TEN BERGE, I. J. & BOVENSCHEN, N. 2013. Granzyme M targets host cell hnRNP K that is essential for human cytomegalovirus replication. *Cell Death Differ,* 20**,** 419-29.

VIVIER, E., TOMASELLO, E., BARATIN, M., WALZER, T. & UGOLINI, S. 2008. Functions of natural killer cells. *Nat Immunol,* 9**,** 503-10.

VOSKOBOINIK, I., THIA, M. C., FLETCHER, J., CICCONE, A., BROWNE, K., SMYTH, M. J. & TRAPANI, J. A. 2005. Calcium-dependent plasma membrane binding and cell lysis by perforin are mediated through its C2 domain: A critical role for aspartate residues 429, 435, 483, and 485 but not 491. *J Biol Chem,* 280**,** 8426-34.

VRAZO, A. C., HONTZ, A. E., FIGUEIRA, S. K., BUTLER, B. L., FERRELL, J. M., BINKOWSKI, B. F., LI, J. & RISMA, K. A. 2015. Live cell evaluation of granzyme delivery and death receptor signaling in tumor cells targeted by human natural killer cells. *Blood,* 126**,** e1-e10.

WAGNER, C., IKING-KONERT, C., DENEFLEH, B., STEGMAIER, S., HUG, F. & HANSCH, G. M. 2004. Granzyme B and perforin: constitutive expression in human polymorphonuclear neutrophils. *Blood,* 103**,** 1099-104.

WAGTMANN, N., BIASSONI, R., CANTONI, C., VERDIANI, S., MALNATI, M. S., VITALE, M., BOTTINO, C., MORETTA, L., MORETTA, A. & LONG, E. O. 1995. Molecular clones of the p58 NK cell receptor reveal immunoglobulin-related molecules with diversity in both the extra- and intracellular domains. *Immunity,* 2**,** 439-49.

WALZER, T., JAEGER, S., CHAIX, J. & VIVIER, E. 2007. Natural killer cells: from CD3(-)NKp46(+) to post-genomics meta-analyses. *Curr Opin Immunol,* 19**,** 365-72.

WANG, G. Q., WIECKOWSKI, E., GOLDSTEIN, L. A., GASTMAN, B. R., RABINOVITZ, A., GAMBOTTO, A., LI, S., FANG, B., YIN, X. M. & RABINOWICH, H. 2001. Resistance to granzyme B-mediated cytochrome c release in Bak-deficient cells. *J Exp Med,* 194**,** 1325-37.

WARGNIER, A., LEGROS-MAIDA, S., BOSSELUT, R., BOURGE, J. F., LAFAURIE, C., GHYSDAEL, C. J., SASPORTES, M. & PAUL, P. 1995. Identification of human granzyme B promoter regulatory elements interacting with activated T-cell-specific proteins: implication of Ikaros and CBF binding sites in promoter activation. *Proc Natl Acad Sci U S A,* 92**,** 6930-4.

WATZL, C. 2014. How to trigger a killer: modulation of natural killer cell reactivity on many levels. *Adv Immunol,* 124**,** 137-70.

WATZL, C. & LONG, E. O. 2003. Natural killer cell inhibitory receptors block actin cytoskeleton-dependent recruitment of 2B4 (CD244) to lipid rafts. *J Exp Med,* 197**,** 77-85.

WATZL, C. & LONG, E. O. 2010. Signal transduction during activation and inhibition of natural killer cells. *Curr Protoc Immunol,* Chapter 11**,** Unit 11 9B.

WATZL, C. & URLAUB, D. 2012. Molecular mechanisms of natural killer cell regulation. *Front Biosci (Landmark Ed),* 17**,** 1418-32.

WATZL, C., URLAUB, D., FASBENDER, F. & CLAUS, M. 2014. Natural killer cell regulation - beyond the receptors. *F1000Prime Rep,* 6**,** 87.

WENSINK, A. C., KEMP, V., FERMIE, J., GARCIA LAORDEN, M. I., VAN DER POLL, T., HACK, C. E. & BOVENSCHEN, N. 2014. Granzyme K synergistically potentiates LPS-induced cytokine responses in human monocytes. *Proc Natl Acad Sci U S A,* 111**,** 5974-9.

WENSINK, A. C., KOK, H. M., MEELDIJK, J., FERMIE, J., FROELICH, C. J., HACK, C. E. & BOVENSCHEN, N. 2016. Granzymes A and K differentially potentiate LPS-induced cytokine response. *Cell Death Discov,* 2**,** 16084.

WESTERMANN, J. & PABST, R. 1992. Distribution of lymphocyte subsets and natural killer cells in the human body. *Clin Investig,* 70**,** 539-44.

WILHARM, E., PARRY, M. A., FRIEBEL, R., TSCHESCHE, H., MATSCHINER, G., SOMMERHOFF, C. P. & JENNE, D. E. 1999. Generation of catalytically active granzyme K from Escherichia coli inclusion bodies and identification of efficient granzyme K inhibitors in human plasma. *J Biol Chem,* 274**,** 27331-7.

WILLIAMS, R. L. & URBE, S. 2007. The emerging shape of the ESCRT machinery. *Nat Rev Mol Cell Biol,* 8**,** 355-68.

WU, L., WANG, L., HUA, G., LIU, K., YANG, X., ZHAI, Y., BARTLAM, M., SUN, F. & FAN, Z. 2009. Structural basis for proteolytic specificity of the human apoptosis-inducing granzyme M. *J Immunol,* 183**,** 421-9.

YANG, X., STENNICKE, H. R., WANG, B., GREEN, D. R., JANICKE, R. U., SRINIVASAN, A., SETH, P., SALVESEN, G. S. & FROELICH, C. J. 1998. Granzyme B mimics apical caspases. Description of a unified pathway for trans-activation of executioner caspase-3 and -7. *J Biol Chem,* 273**,** 34278-83.

YOKOYAMA, W. M. & KIM, S. 2006. How do natural killer cells find self to achieve tolerance? *Immunity,* 24**,** 249-57.

ZHANG, D., BERESFORD, P. J., GREENBERG, A. H. & LIEBERMAN, J. 2001a. Granzymes A and B directly cleave lamins and disrupt the nuclear lamina during granule-mediated cytolysis. *Proc Natl Acad Sci U S A,* 98**,** 5746-51.

ZHANG, D., PASTERNACK, M. S., BERESFORD, P. J., WAGNER, L., GREENBERG, A. H. & LIEBERMAN, J. 2001b. Induction of rapid histone degradation by the cytotoxic T lymphocyte protease Granzyme A. *J Biol Chem,* 276**,** 3683-90.

ZHAO, T., ZHANG, H., GUO, Y., ZHANG, Q., HUA, G., LU, H., HOU, Q., LIU, H. & FAN, Z. 2007. Granzyme K cleaves the nucleosome assembly protein SET to induce single-stranded DNA nicks of target cells. *Cell Death Differ,* 14**,** 489-99.

ZHOU, Z., HE, H., WANG, K., SHI, X., WANG, Y., SU, Y., WANG, Y., LI, D., LIU, W., ZHANG, Y., SHEN, L., HAN, W., SHEN, L., DING, J. & SHAO, F. 2020. Granzyme A from cytotoxic lymphocytes cleaves GSDMB to trigger pyroptosis in target cells. *Science,* 368.

ZHU, Y., HUANG, B. & SHI, J. 2016. Fas ligand and lytic granule differentially control cytotoxic dynamics of natural killer cell against cancer target. *Oncotarget,* 7**,** 47163-47172.

11 Abbreviations

AA	amino acid
AP-1	Activator protein 1
Bak	Bcl-2 homologous antagonist killer
Bax	Bcl-2 associated X protein
BID	BH3-only proapoptotic Bcl-2 family member
BSA	bovine serum albumin
BV	brilliant violet
CAD	Caspase-activated DNase
Cas	caspase
CBF	Core-binding factor
CD	cluster of differentiation
CD95L	Fas Ligand, FasL, CD178, APO-1L
CREB	cAMP response element-binding protein
CTL	cytotoxic T lymphocyte
CHX	Cycloheximide
DCI	3,4-Dichloroisocoumarin
DISC	Death-inducing signaling complex
DMSO	dimethyl sulfoxide
DNA-PKc	DNA-dependent protein kinase
DR	death receptor
FACS	fluorescence activated cell sorter
FCM	flow cytometry
FCS	fetal calf serum
FSC	forward scatter
GFP	green fluorescent protein
GrzB	Granzyme B
H	hour(s)
HRP	horseradish peroxidase
ICAD	Inhibitor of caspase-activated DNase
IFN-γ	Interferon-γ
IL	Interleukin
Iono	Ionomycin
IS	immunological synapse
ITIM	immunoreceptor tyrosine-based inhibition motif
kDa	kilo dalton
KIR	Killer-cell immunoglobulin-like receptor
LAMP-1	lysosomal-associated membrane protein 1, CD107a
LSM	lymphocyte separation medium
mAB	monoclonal antibody
MHC	major histocompatibility complex
NCR	Natural cytotoxicity receptor
NES	nuclear export signal
NuMA	Nuclear mitotic apparatus protein
P/S	penicillin/streptomycin
PARP1	Poly(ADP-ribose)-Polymerase 1
PBMC	peripheral blood mononuclear
PBS	phosphate-buffered saline
PE	phycoerythrin
PFA	paraformaldehyde
PVDF	polyvinylidene difluoride

RSB	reducing sample buffer
RT	room temperature
SLAM	Signaling lymphocyte activation molecule
TNF	Tumor necrosis factor
TRAIL	Tumor necrosis factor related apoptosis inducing ligand, TL2, APO2L, CD253, TRAIL, Apo-2L, TNLG6A
TRAILR	TRAIL receptor
uIFNα	Universal Type I IFN
WB	western blot
Z-VAD-FMK	carbobenzoxy-valyl-alanyl-aspartyl-[O-methyl]- fluoromethylketone

12 Appendix

eGFP sequence:

VSKGEELFTGVVPILVELDGDVNGHKFSVSGEGEGDATYGKLTLKFICTTGKL
PVPWPTLVTTLTYGVQCFSRYPDHMKQHDFFKSAMPEGYVQERTIFFKDDGN
YKTRAEVKFEGDTLVNRIELKGIDFKEDGNILGHKLEYNYNSHNVYIMADKQKN
GIKVNFKIRHNIEDGSVQLADHYQQNTPIGDGPVLLPDNHYLSTQSALSKDPNE
KRDHMVLKEFVTAAGITLGMDELYK

mCherry sequence:

VSKGEEDNMAIIKEFMRFKVHMEGSVNGHEFEIEGEGEGRPYEGTQTAKLKV
TKGGPLPFAWDILSPQFMYGSKAYVKHPADIPDYLKLSFPEGFKWERVMNFE
DGGVVTVTQDSSLQDGEFIYKVKLRGTNFPSDGPVMQKKTMGWEASSERMY
PEDGALKGEIKQRLKLKDGGHYDAEVKTTYKAKKPVQLPGAYNVNIKLDITSH
NEDYTIVEQYERAEGRHSTGGMDELYKSGLRSTGSR*

As already described for our reporter constructs in the submitted manuscript (Nora Bruning, 2022)

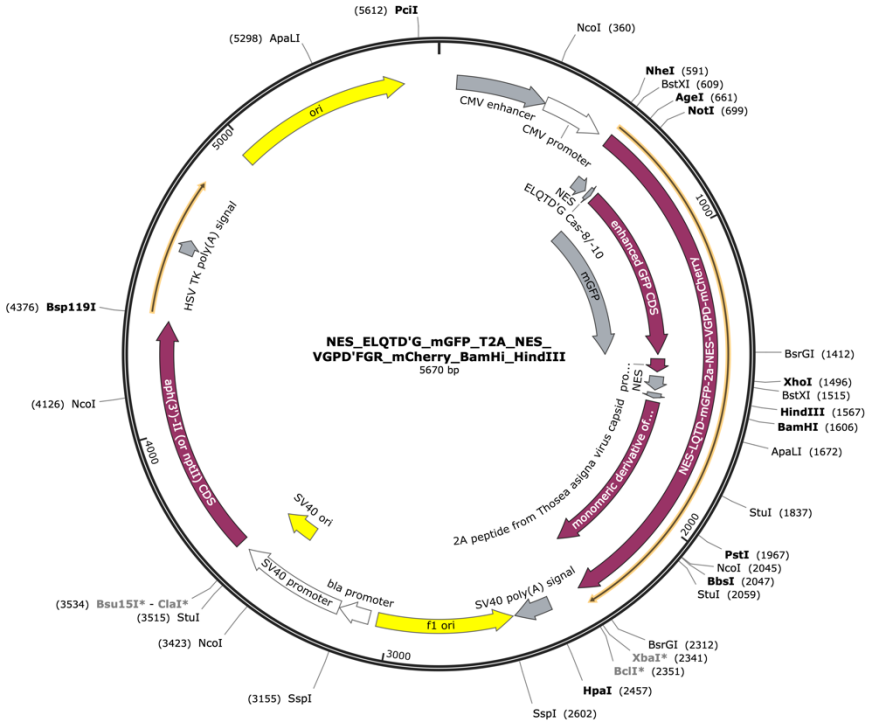

Figure 38: Parent plasmid map. NES-ELQTD'G-mGFP-T2A-NES-VGPD'FGR-mCherry-BamHI-HindIII. The restriction sites for the enzymes BamHI and HindII were added to facilitate the exchange of granzyme cleavage sites.

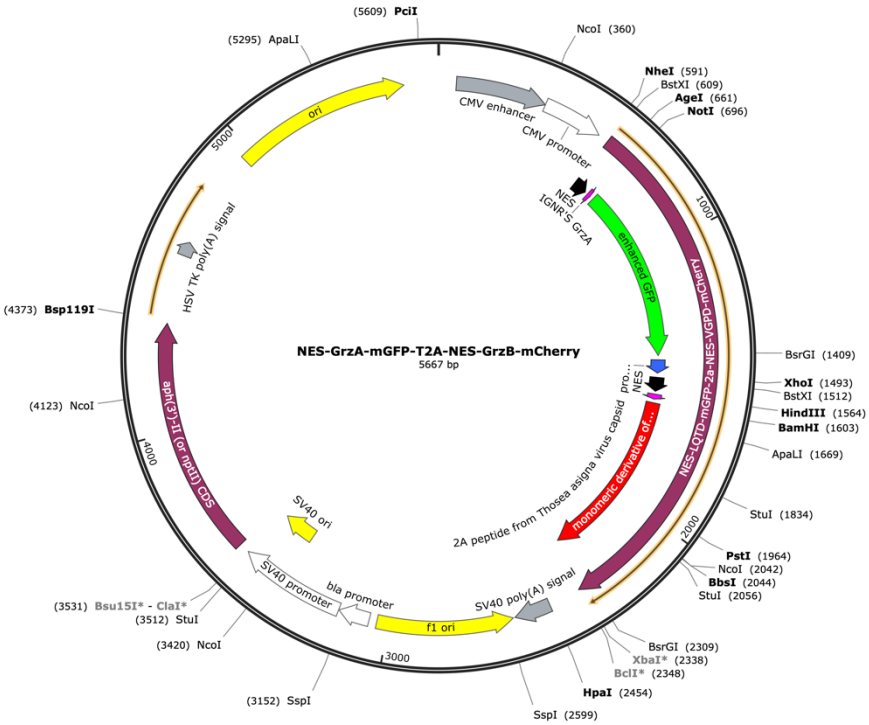

Figure 39: Example for the pEGFP backbone including the granzyme reporter constructs (here GrzA-GrzB). Amino acid sequences of the individual granzyme cleavage sites, the NES domain or T2A sequence are found in the method chapter 7.4 or in the appendix for GFP and mCherry. Nucleotide sequences of the granzyme cleavage sites are found in the chapter 6.10.

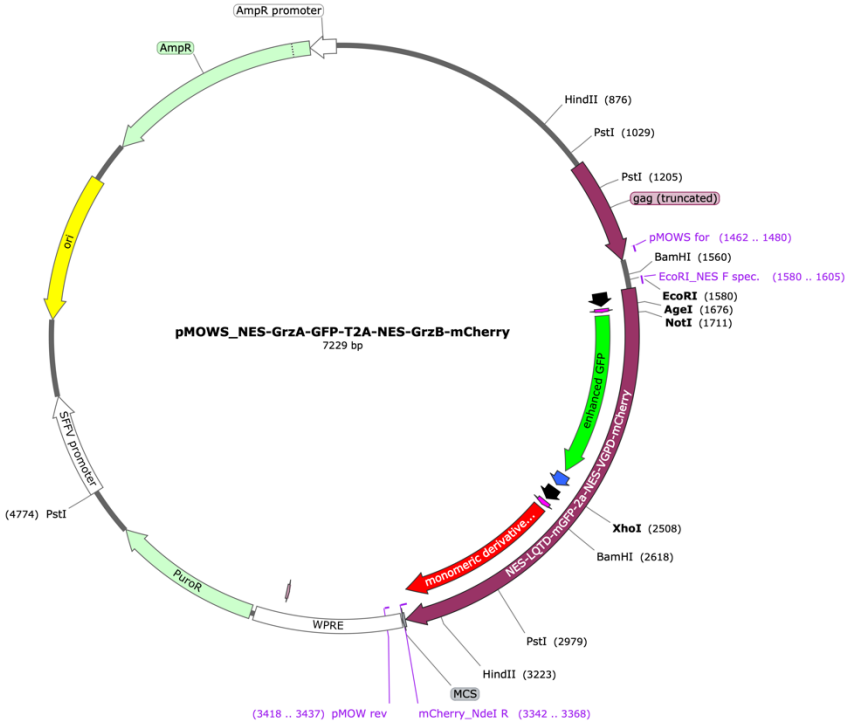

Figure 40: Example for the pMOWS backbone including the granzyme reporter constructs (here GrzA-GrzB). Amino acid sequences of the individual granzyme cleavage sites, the NES domain or T2A are found in the method chapter 7.4 or in the appendix for GFP and mCherry. Nucleotide sequences of the granzyme cleavage sites are found in the chapter 6.10.